USGS
science for a changing world

National Water-Quality Assessment Program
Prepared in cooperation with the Florida Department of Environmental Protection

Estimating Nitrate Concentrations in Groundwater at Selected Wells and Springs in the Surficial Aquifer System and Upper Floridan Aquifer, Dougherty Plain and Marianna Lowlands, Georgia, Florida, and Alabama, 2002–50

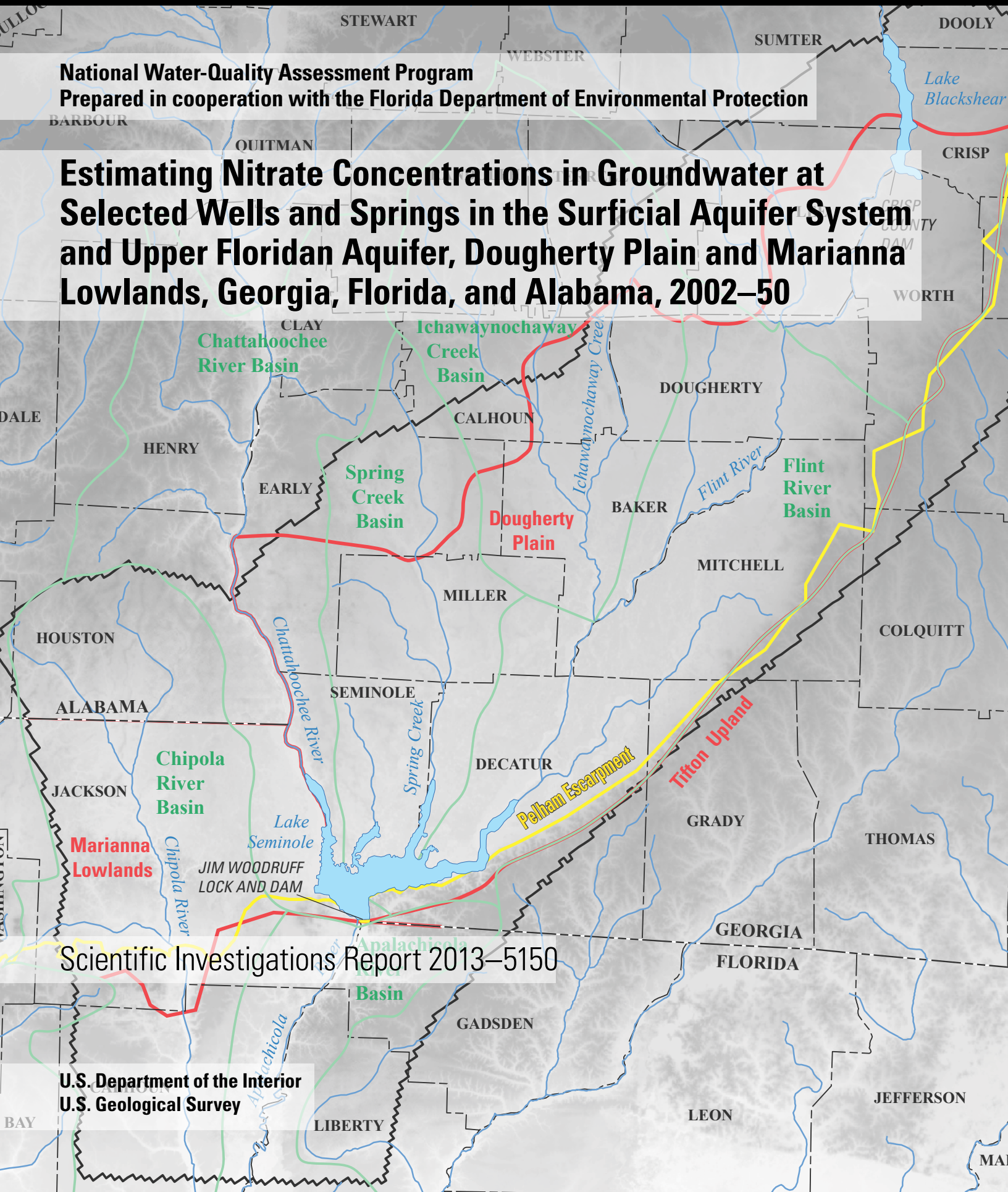

Scientific Investigations Report 2013–5150

U.S. Department of the Interior
U.S. Geological Survey

Estimating Nitrate Concentrations in Groundwater at Selected Wells and Springs in the Surficial Aquifer System and Upper Floridan Aquifer, Dougherty Plain and Marianna Lowlands, Georgia, Florida, and Alabama, 2002–50

By Christy A. Crandall, Brian G. Katz, and Marian P. Berndt

National Water-Quality Assessment Program

Prepared in cooperation with the Florida Department of Environmental Protection

Scientific Investigations Report 2013–5150

U.S. Department of the Interior
U.S. Geological Survey

U.S. Department of the Interior
SALLY JEWELL, Secretary

U.S. Geological Survey
Suzette M. Kimball, Acting Director

U.S. Geological Survey, Reston, Virginia: 2013

Suggested citation:
Crandall, C.A., Katz, B.G., and Berndt, M.P., 2013, Estimating nitrate concentrations in groundwater at selected wells and springs in the surficial aquifer system and Upper Floridan aquifer, Dougherty Plain and Marianna Lowlands, Georgia, Florida, and Alabama, 2002–50: U.S. Geological Survey Scientific Investigations Report 2013–5150, 65 p., http://pubs.usgs.gov/sir/2013/5150/.

Acknowledgments

The authors thank Gary Maddox and Rick Hicks of the Florida Department of Environmental Protection for their support and guidance during this study. The Jackson Blue Spring Working Group provided feedback and a forum for presenting this work.

The authors also thank Wayne Lapham and Michael Woodside of the U.S. Geological Survey (USGS) for their support and guidance. Elliott Jones and Eve Kuniansky of the USGS assisted in converting finite-element model datasets from previous investigations for use in the study. Finally, the authors thank Hal Davis, Connor Haugh, Lynn Torak, and Eve Kuniansky, of the USGS, for their technical reviews of the report.

Contents

Figures

Tables

Conversion Factors and Datums

Inch/Pound to SI

Multiply	By	To obtain
	Length	
inch (in.)	2.54	centimeter (cm)
foot (ft)	0.3048	meter (m)
mile (mi)	1.609	kilometer (km)
	Area	
square mile (mi^2)	2.59	square kilometer (km^2)
	Flow rate	
foot per day (ft/d)	0.3048	meter per day (m/d)
foot per year (ft/yr)	0.3048	meter per year (m/yr)
cubic foot per second (ft^3/s)	0.02832	cubic meter per second (m^3/s)
gallon per minute (gal/min)	0.06309	liter per second (L/s)
gallon per day (gal/d)	0.003785	cubic meter per day (m^3/d)
million gallons per day (Mgal/d)	0.04381	cubic meter per second (m^3/s)
inch per year (in/yr)	25.4	millimeter per year (mm/yr)
	Transmissivity*	
foot squared per day (ft^2/d)	0.0929	meter squared per day (m^2/d)
	Application rate	
pounds per area contributing recharge per year [(lb/area contributing recharge)/yr]	1.121	kilograms per hectare per year [(kg/ha)/yr]

Temperature may be converted as follows:
°C = 5/9 (°F – 32)
°F = (1.8 × °C) + 32

Vertical coordinate information is referenced to the National Geodedic Vertical Datum of 1929 (NGVD 29) or the North American Vertical Datum of 1988 (NAVD 88).

Altitude, as used in this report, refers to distance above the vertical datum.

Horizontal coordinate information is referenced to the North American Datum of 1983 (NAD 83).

*Transmissivity: The standard unit for transmissivity is cubic foot per day per square foot times foot of aquifer thickness [(ft^3/d)/ft^2]ft. In this report, the mathematically reduced form, foot squared per day (ft^2/d), is used for convenience.

Specific conductance is given in microsiemens per centimeter at 25 degrees Celsius (µS/cm at 25 °C).

Concentrations of chemical constituents in water are given either in milligrams per liter (mg/L) or micrograms per liter (µg/L).

Abbreviations

ACFB	Apalachicola–Chattahoochee–Flint River Basin
ACR	area contributing recharge
BMM	Binary mixing model
CFC	chlorofluorocarbons
CLSM	Chipola Local-Scale Model
EMM	Exponential mixing model
EPM	Exponential piston-flow model
^{3}H	Tritium
^{3}He	Helium-3
^{4}He	Helium-4
LPM	Lumped parameter model
MFLSM	Middle Flint Local-Scale Model
mL	milliliter
NAWQA	National Water-Quality Assessment Program
Ne	Neon
NED	National Elevation Dataset
NWFWMD	Northwest Florida Water Management District
PFM	Piston-flow model
SF_6	Sulfur hexafluoride
UFA	Upper Floridan aquifer
USEPA	U.S. Environmental Protection Agency
USGS	U.S. Geological Survey
WY	water year

Estimating Nitrate Concentrations in Groundwater at Selected Wells and Springs in the Surficial Aquifer System and Upper Floridan Aquifer, Dougherty Plain and Marianna Lowlands, Georgia, Florida, and Alabama, 2002–50

By Christy A. Crandall, Brian G. Katz, and Marian P. Berndt

Abstract

Groundwater from the surficial aquifer system and Upper Floridan aquifer in the Dougherty Plain and Marianna Lowlands in southwestern Georgia, northwestern Florida, and southeastern Alabama is affected by elevated nitrate concentrations as a result of the vulnerability of the aquifer, irrigation water-supply development, and intensive agricultural land use. The region relies primarily on groundwater from the Upper Floridan aquifer for drinking-water and irrigation supply. Elevated nitrate concentrations in drinking water are a concern because infants under 6 months of age who drink water containing nitrate concentrations above the U.S. Environmental Protection Agency maximum contaminant level of 10 milligrams per liter as nitrogen can become seriously ill with blue baby syndrome.

In response to concerns about water quality in domestic wells and in springs in the lower Apalachicola–Chattahoochee–Flint River Basin, the Florida Department of Environmental Protection funded a study in cooperation with the U.S. Geological Survey to examine water quality in groundwater and springs that provide base flow to the Chipola River. A three-dimensional, steady-state, regional-scale groundwater-flow model and two local-scale models were used in conjunction with particle tracking to identify travel times and areas contributing recharge to six groundwater sites—three long-term monitor wells (CP-18A, CP-21A, and RF-41) and three springs (Jackson Blue Spring, Baltzell Springs Group, and Sandbag Spring) in the lower Apalachicola–Chattahoochee–Flint River Basin. Estimated nitrate input to groundwater at land surface, based on previous studies of nitrogen fertilizer sales and atmospheric nitrate deposition data, were used in the advective transport models for the period 2002 to 2050. Nitrate concentrations in groundwater samples collected from the six sites during 1993 to 2007 and groundwater age tracer data were used to calibrate the transport aspect of the simulations.

Measured nitrate concentrations (as nitrogen) in wells and springs sampled during the study ranged from 0.37 to 12.73 milligrams per liter. Average apparent ages of groundwater calculated from measurements of chlorofluorocarbon, sulfur hexafluoride, and tritium from wells CP-18A, CP-21A, and RF-41 were about 23, 29, and 32 years, respectively. Average apparent ages of groundwater from Baltzell Springs Group, Sandbag Spring, and Jackson Blue Spring were about 16, 18, and 19 years, respectively. Simulated travel times of particles from the six selected sites ranged from less than 1 day to 511 years; both the minimum and maximum particle travel times were estimated for water from Jackson Blue Spring. Median simulated travel times of particles were about 30, 38, and 62 years for Jackson Blue Spring, Sandbag Spring, and Baltzell Springs Group, respectively. Study results indicated that travel times for approximately 50 percent of the particles from all spring sites were less than 50 years. The median simulated travel times of particles arriving at receptor wells CP-18A, CP-21A, and RF-41 were about 50, 35, and 36 years, respectively. All particle travel times were within the same order of magnitude as the tracer-derived average apparent ages for water, although slightly older than the measured ages. Travel time estimates were substantially greater than the measured age for groundwater reaching well CP-18A, as confirmed by the average apparent age of water determined from tracers.

Local-scale particle-tracking models were used to predict nitrate concentrations in the three monitor wells and three springs from 2002 to 2050 for three nitrogen management scenarios: (1) fixed input of nitrate at the 2001 level, (2) reduction of nitrate inputs of 4 percent per year (from the previous year) from 2002 to 2050, and (3) elimination of nitrate input after 2001. Simulated nitrate concentrations in well CP-21A peaked at 7.82 milligrams per liter in 2030, and concentrations in background well RF-41 peaked at 1.10 milligrams per liter in 2020. The simulated particle travel times were longer than indicated by age dating analysis for groundwater in well CP-18A; to account for the poor calibration fit at this well, nitrate concentrations were shifted 21 years. With the shift, simulated nitrate concentrations in groundwater at CP-18A peaked at 13.76 milligrams per liter in 2026. For groundwater in Baltzell Springs Group, Jackson Blue Spring, and Sandbag Spring, simulated nitrate concentrations peaked at 3.77 milligrams per liter in 2006, 3.51 milligrams per liter in 2011, and 0.81 milligram per liter in 2018, respectively, under the three management scenarios. In management scenario 3 (elimination of nitrate input after 2001), simulated nitrate concentrations in Baltzell Springs Group decreased to less than background concentrations (0.10 milligram per liter) by 2033,

and in Sandbag Spring concentrations decreased to less than background by 2041. Simulations using nitrate management scenarios 1 (fixed input of nitrate at 2001 levels) and 2 (reduction of 4.0 percent per year) indicate that nitrate concentrations in groundwater may remain above background concentrations through 2050 at all sites.

Introduction

Elevated nitrate concentrations in groundwater constitute an important ecological and human-health concern in the Dougherty Plain and Marianna Lowlands in the lower Apalachicola–Chattahoochee–Flint River Basin (ACFB) in southwestern Georgia, northwestern Florida, and southeastern Alabama (fig. 1). Groundwater provides the primary source of drinking water and irrigation supply in the area. Elevated nitrate concentrations in drinking water are a health concern because infants under 6 months of age who ingest water containing nitrate concentrations above the U.S. Environmental Protection Agency (USEPA) maximum contaminant level of 10 milligrams per liter (mg/L) as nitrogen can become seriously ill with blue baby syndrome (U.S. Environmental Protection Agency, 2012). In addition, groundwater supplies base flow to streams and, therefore, supports critical habitat for several endangered and threatened mussel species (Albertson and Torak, 2002).

Groundwater quality in the Dougherty Plain and Marianna Lowlands reflects the dominant land use—row-crop agriculture (cotton, corn, soybeans, peanuts)—as well as the vulnerability of the karst carbonate aquifer. Nitrate concentrations in groundwater samples collected by the U.S. Geological Survey (USGS) as part of the National Water-Quality Assessment (NAWQA) Program between 1994 and 2007 from the surficial aquifer system and Upper Floridan aquifer in the Dougherty Plain and Marianna Lowlands had high nitrate concentrations compared to other study areas within these two aquifers (Frick and others, 1998; Berndt and Crandall, 2009). The median nitrate concentrations in the Upper Floridan aquifer were about 2.5 mg/L for water from domestic wells in the lower ACFB compared to a median of less than 0.1 mg/L for domestic wells outside of the study area. Nitrate concentrations also were elevated in springs in the study area (Berndt and others, 2005). A trend analysis indicated a significant upward trend for nitrate in water from the Chipola River (Frick and others, 1996).

Concerns about water quality in domestic wells and springs in the lower ACFB led the Florida Department of Environmental Protection (FDEP) to fund a study in 2007 to examine water quality in groundwater and springs that provide base flow to the Chipola River. Additionally, the USGS NAWQA Program provided funds to collect data in other areas of the ACFB. The primary objective of this study was to predict trends in nitrate contamination in groundwater in the lower ACFB. Regional- and local-scale groundwater-flow models were developed, calibrated, and used with particle-tracking simulations of transport to meet this objective.

Groundwater-flow models and particle-tracking simulations can be used to determine the areas contributing recharge (ACR) and the travel times of water to selected receptor sites. Additionally, water particles can be used as proxies for conservative water-quality constituents, such as nitrate, in an oxidized flow environment. Particle tracking outlines the paths that water, and the dissolved nitrate moving with water particles, is most likely to take from locations where recharge occurs at the water table to discharge locations, yielding a travel time and a contributing area for each particle. Using particle travel times and an input function time series for a known water-quality constituent of interest, such as nitrate, future constituent concentrations can be estimated. The constituent is assumed to be transported conservatively by advection, moving with water molecules, and without adsorption, degradation, dispersion, or other processes that might reduce the constituent concentration.

Purpose and Scope

The purpose of this report is to (1) describe spring and monitor-well networks, sampling, data, and age-dating estimates, (2) describe and document groundwater-flow models, calibration, and particle-tracking simulations, and (3) simulate and predict nitrate concentrations (2002–50) in groundwater at three springs and three monitor wells within the ACFB area using the particle-tracking models and a nitrate input function. Simulations were based on three nitrogen management scenarios proposed by the USGS NAWQA Program.

Previous Studies

Many investigators have studied the geology, physiography, geohydrology, and groundwater resources of the study area. The most recent studies have concentrated on updating geohydrology and establishing groundwater-flow models. Torak and others (1993, 1996) and Torak and McDowell (1996) provided updates of the geohydrology in parts of the lower ACFB. Hayes and others (1983) evaluated stream-aquifer relations and water-resources potential and simulated the effects of groundwater withdrawals on streamflow and water levels in the Upper Floridan aquifer. Mosner (2002) described stream-aquifer relations and groundwater-level conditions in the lower ACFB during the drought of 1999 and 2000 and computed aquifer contributions to streamflows for specific reaches. Jones and Torak (2004) described the geohydrology of the area surrounding Lake Seminole in southeastern Alabama and southwestern Georgia and simulated the effects of impoundment on groundwater flow in the Upper Floridan aquifer. Torak and others (2006) cited physical and hydrochemical evidence of a hydraulic connection between surface water and groundwater beneath and around Lake Seminole and Jim Woodruff Lock and Dam (fig. 1),

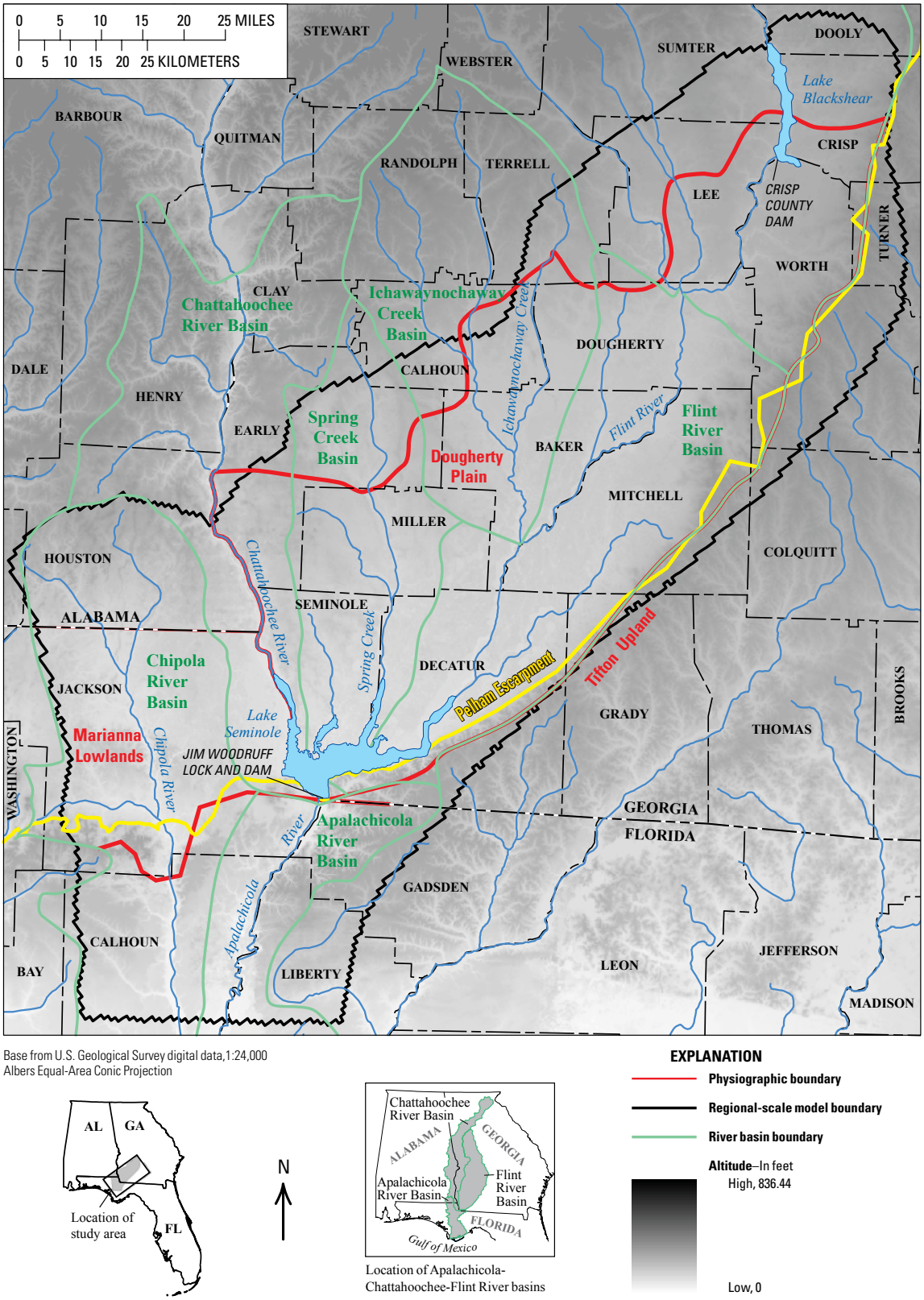

Figure 1. Location of the study area, major rivers and lakes, river basin divides, the Apalachicola–Chattahoochee–Flint River Basin, and major local physiographic provinces in southwestern Georgia, northwestern Florida, and southeastern Alabama.

and documented the complex exchange of surface water and groundwater between the lake, streams, and aquifer. Torak and Painter (2006) described the geologic and hydrologic framework of the lower ACFB and incorporated borehole and aquifer test data. Crandall (2007), Crandall and others (2009), and Katz and others (2007) demonstrated a methodology for using MODFLOW (Harbaugh and others, 2000) and MODPATH (Pollock, 1994) with age tracer and contaminant concentration data to estimate the area contributing recharge, groundwater travel times, and flow paths to discharge features (Eberts and others, 2005). Frick and others (1996) described nitrogen sources in the lower ACFB. Groundwater quality in the lower ACFB also was described in Frick and others (1998), Frick and Dalton (2007), and Dalton and Frick (2008).

Description of the Study Area

The study area is primarily in the Dougherty Plain and Marianna Lowlands physiographic regions within the lower ACFB in southeastern Alabama, northwestern Florida, and southwestern Georgia (fig. 1). The area is underlain by the surficial and Floridan aquifer systems. In the study area, the Upper Floridan aquifer is the predominant water-bearing unit of the Floridan aquifer system and has variable confinement, ranging from confined to unconfined (fig. 2). The Upper Floridan aquifer is a relatively closed hydrologic system containing unique geochemistry, recharge, and discharge zones. Groundwater discharges almost entirely within the lower ACFB, providing base flow to rivers, streams, and springs within the study area (figs. 1 and 2).

Physiography

The study area is in the coastal plain of the southeastern United States in southeastern Alabama, northwestern Florida, and southwestern Georgia (fig. 1). Most of the study area comprises three distinctive physiographic regions: two karst regions called the Dougherty Plain and the Marianna Lowlands, and a region of dissected remnant hills and sand-hill ridges on the southeastern and southern boundaries called the Tifton Upland (fig. 1). Springs are numerous along streams in the study area (figs. 2 and 3). Surface altitudes on the northern side of the Dougherty Plain and Marianna Lowlands range from about 300 feet (ft) in the northwest to about 500 ft in the northeast; altitudes on the southern side range from about 200 to 300 ft (fig. 1). All altitudes are referenced to the North American Vertical Datum of 1988 (NAVD 88) unless otherwise noted.

Sinkholes, which are closed-basin depressions, are prominent features of the Dougherty Plain and Marianna Lowlands. Sinkholes result when limestone dissolves, and the overburden collapses into a cavity. Most sinkholes are shallow, flat-bottomed, or rounded depressions (Fenneman, 1938) that can range in size from a few feet to several hundred feet. Sinkholes dot the landscape in the study area and provide evidence of active dissolution of the underlying limestone (Herrick and LeGrand, 1964; LeGrand and Stringfield, 1966; Longwell and others, 1969). Infiltrating water may enter the aquifer directly through sinkholes, facilitating the rapid transport of recharge water into the aquifer. Some sinkholes may become filled with silt and clay that plug the cavity, thereby preventing recharge, and creating sinkhole ponds (Sever, 1965a; fig. 3).

The southeastern part of the study area is bordered by the steeply sloped Pelham Escarpment along the Flint River Basin divide that continues in a southwesterly direction to form the eastern impoundment arm of Lake Seminole (fig. 1). This solution escarpment provides as much as 125 ft of local relief, and the ridge of the escarpment forms a topographic groundwater and surface-water divide between the Flint/Apalachicola River Basins and the Ochlockonee River Basin to the east (fig. 1) (Sever, 1965a; Torak and others, 1996). The base of the solution escarpment contains cavities, sinkholes, and springs in the study area (Hicks and others, 1987). The top of the escarpment is formed by the Hawthorn Group (fig. 4), which is known to be resistant to erosion (Torak and others, 2006).

Climate

The climate of the study area is humid subtropical with long, hot summers and mild winters (Sever, 1965a). Temperatures and precipitation are seasonally and areally variable due to the proximity to the Gulf of Mexico (Torak and Painter, 2006). The long-term mean annual air temperature is 66.4 degrees Fahrenheit (°F; 1957–2003) at Marianna, Fla, in the southern part of the study area and about 64 °F (1956–2003) at Plains, Ga., in the northern part of the study area (Torak and Painter, 2006). The long-term annual average precipitation ranges from 49.4 inches (in.) in Plains, Ga., to 54.69 in. in Jackson County, Fla, for the 30-year period 1961–90 (National Oceanic and Atmospheric Administration, 2003). Recharge to the aquifer occurs mainly during the winter, when cold fronts produce low-intensity precipitation of long duration. Aquifer recharge in the area can exceed 2 to 3 in. per precipitation event, because evapotranspiration occurs at a relatively low rate during the winter months. Rainfall is of a high intensity and short duration during the summer months and can result in low infiltration and high runoff (Torak and Painter, 2006).

Hydrogeology

Sand, clay, and limestone underlie the study area, and compose the surficial aquifer system and Upper Floridan aquifer. The sandy surficial aquifer system, found mainly in valleys, is discontinuous and is intersected by clayey deposits, hereafter called “residuum,” which are found mostly on ridges. The Upper Floridan aquifer is the major hydrogeologic unit in the study area and underlies the entire region.

The surficial aquifer system consists of a series of sandy marine and fluvial-terrace deposits (Moore, 1955; Reves,

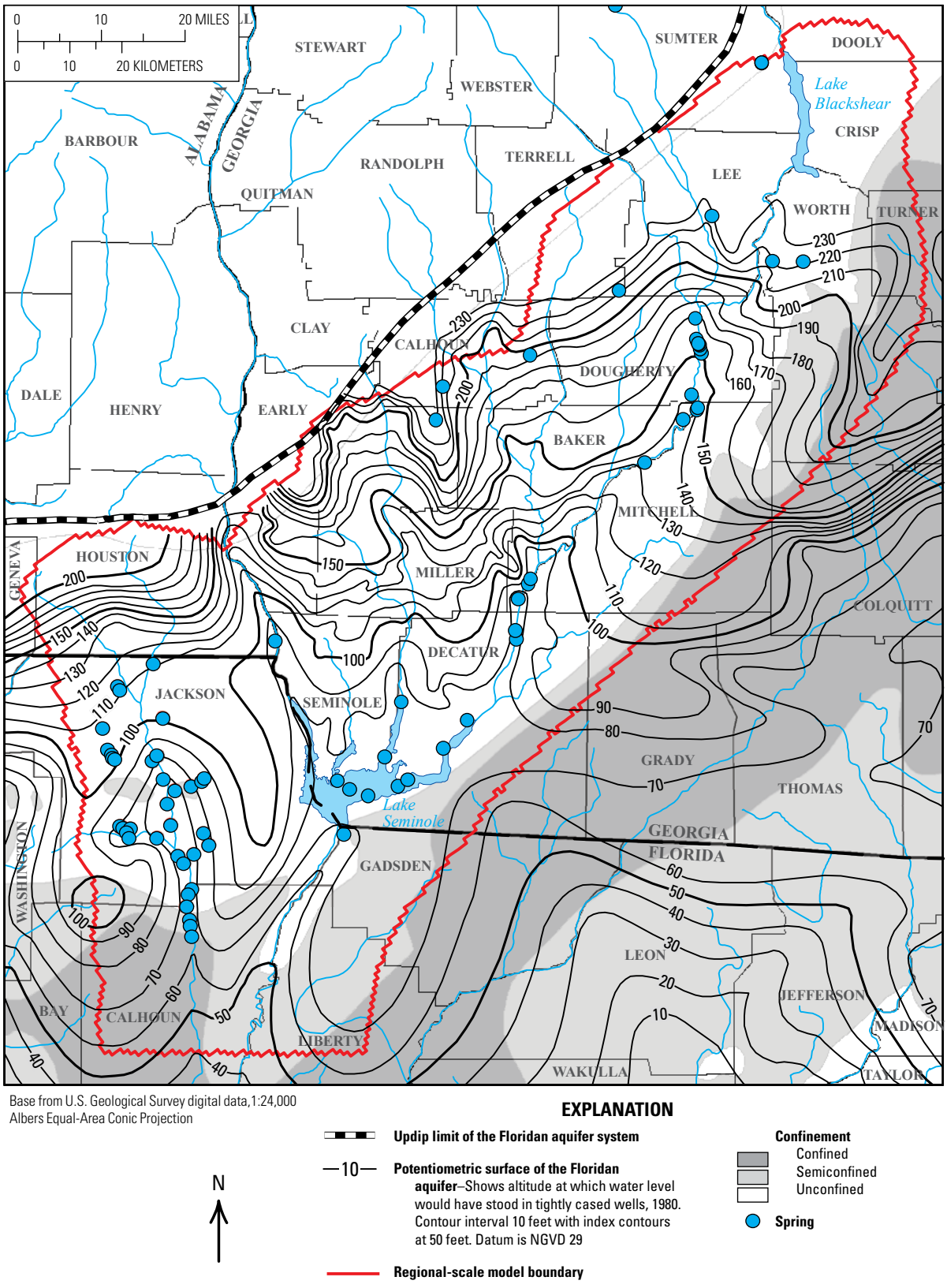

Figure 2. Location of springs in the study area; unconfined, semiconfined, and confined areas of the Upper Floridan aquifer; and 10-foot contour interval lines from the regional potentiometric surface, 1980.

Figure 3. Crack-In-The-Woods Spring along the Chipola River.

1961; Scott, 1992; Torak and others, 2006) and unconsolidated to poorly indurated clastic deposits (Florida Geological Survey, 1986). These deposits collectively represent the permeable hydrogeologic units contiguous with land surface that make up the aquifer. The thickness of surficial deposits in the study area ranges from less than 10 ft in the northwestern, upland-outcrop areas of the Upper Floridan aquifer and in stream valleys to greater than 600 ft in southern parts of the study area (fig. 5).

An intermediate confining unit overlies the Upper Floridan aquifer along the southern and southeastern boundaries of the study area, confining the aquifer in these areas. The unit consists of a dense clay lithology of the Hawthorn Group and in some places the Tampa Limestone, separating the surficial aquifer system from the Upper Floridan aquifer. The intermediate confining unit in southwestern Georgia averages about 90 ft thick on the southern and eastern parts of the study area (fig. 5; Camp, Dresser & McKee Inc., 2001); however, the confining unit is thin or absent in much of the Dougherty Plain and Marianna Lowlands (David W. Hicks, Joseph W. Jones Ecological Research Center, written commun., October 2005).

The Upper Floridan aquifer is the principal hydrogeologic unit in the study area and consists of the following sequence of geologic units, arranged from youngest to oldest: Tampa Limestone, Chattahoochee Formation, and St. Marks Formation; Suwannee Limestone; Marianna Limestone; and Ocala Limestone southeast of the solution escarpment; and Suwanee Limestone, Ocala Limestone, and Clinchfield Sand northwest of the solution escarpment (fig. 4). These geologic units are not all present throughout the study area. The aquifer consists mostly of the Ocala Limestone on the southern boundary. The varieties of units that make up the aquifer create heterogeneities in hydraulic properties within the lower ACFB.

Average thickness of the Upper Floridan aquifer in the study area is about 250 ft. Thickness values were determined by subtracting the altitude of the base of the Ocala Limestone or Clinchfield Sand obtained from Miller (1986) from the altitude of the top of the Upper Floridan aquifer obtained from Jones and Torak (2006); Torak and others (1996); and Kwader and Schmidt (1978). The thickness of the Upper Floridan aquifer in the Dougherty Plain and Marianna Lowlands ranges from a few feet along the northwestern study area boundary,

near the updip limit of the aquifer, to more than 1,000 ft along the southern boundary (fig. 6). Aquifer thickness ranges from about 100 to 300 ft along the midsection of the Dougherty Plain and Marianna Lowlands between the outcrop area and solution escarpment and Tifton Upland (figs. 1 and 6). The altitude of the base of the Upper Floridan aquifer dips steeply to the south and east and is deepest at the southern boundary of the study area (fig. 7), ranging from 250 to –1,160 ft (NAVD 88). The base plunges as the aquifer thickens, thus reflecting the marine depositional history of the limestone sediments that make up the aquifer.

Confinement of the Upper Floridan aquifer ranges from unconfined to confined, but the aquifer is classified as unconfined throughout a large part of the study area (Miller, 1986). The intermediate confining unit overlies the Upper Floridan aquifer in the southern and southeastern parts of the study area (fig. 2). This unit is particularly extensive beneath the Tifton Uplands and along the southern boundary of the study area. Additionally, where clay residuum overlies the Upper Floridan aquifer, the aquifer may be locally confined. Limestone dissolution in the Upper Floridan aquifer has created sinkholes and conduits and has caused extreme variability in aquifer hydraulic properties and has facilitated groundwater flow to wells through interconnected systems of conduits (solution openings or cavities), fractures, and joints. The distribution of conduits and sinkholes has created local patterns of high transmissivity and a potential for preferential groundwater flow paths in the Upper Floridan aquifer near springs in the study area (fig. 2) (Torak and others, 1993). Limestone dissolution has also increased hydraulic connection between the aquifer and surface-water bodies through springs (figs. 2 and 3).

Transmissivity estimates derived from aquifer tests demonstrate the heterogeneity of the Upper Floridan aquifer. Reported transmissivity estimates in the Albany, Ga., area range from about 700 to about 283,000 feet squared per day (ft^2/d). These estimates vary considerably even within short distances (Hicks and others, 1987). Aquifer tests in other areas yielded transmissivity estimates ranging from about 1,600 to about 1,300,000 ft^2/d (Sever, 1965a, b; Hayes and others, 1983; Wagner and Allen, 1984). The largest

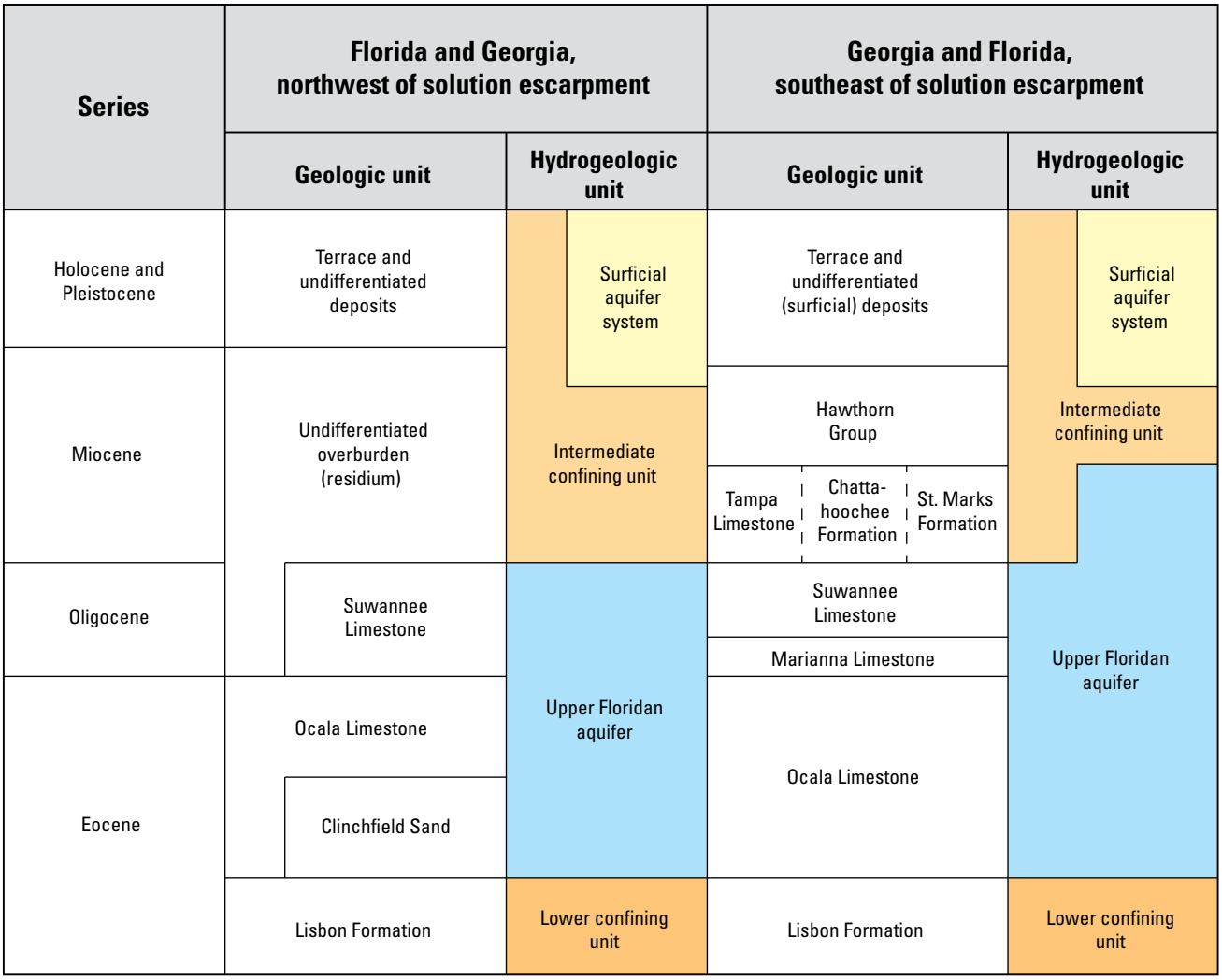

Figure 4. Geologic and hydrogeologic units in the study area.

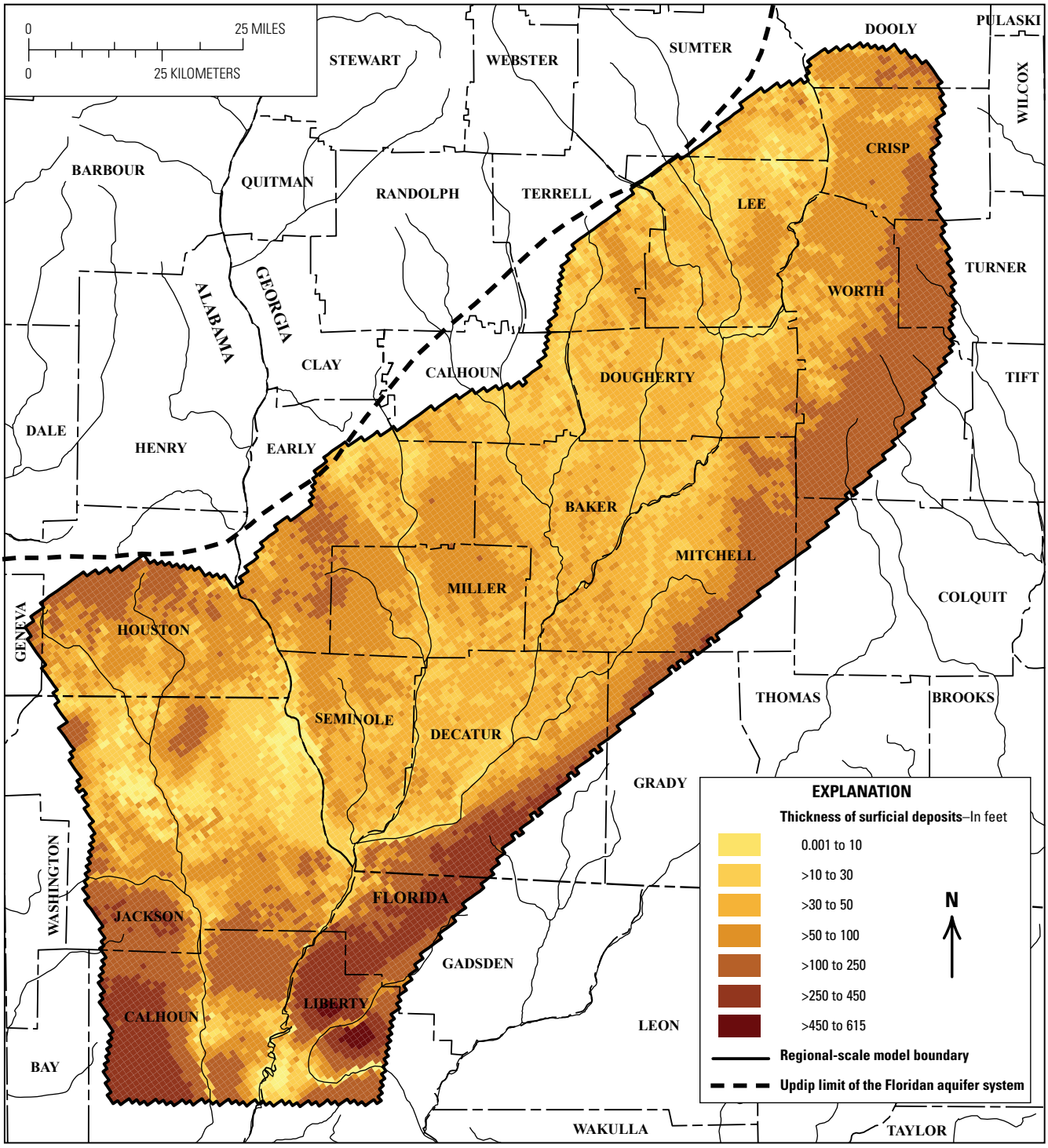

Base from U.S. Geological Survey digital data,1:24,000
Albers Equal-Area Conic Projection

Figure 5. Thickness of surficial deposits in the study area.

transmissivity (1,300,000 ft^2/d) was reported for an aquifer test from a well in Bainbridge, Ga. (Sever, 1965b; Katherine H. Zitsch, Project Manager, Camp, Dresser & McKee Inc., written commun., 2003). Reported hydraulic conductivities range from about 10 to about 600 feet per day (ft/d; Katherine H. Zitsch, Project Manager, Camp, Dresser & McKee Inc., written commun., 2003).

The presence of sand and clay surficial deposits and karst features control the rate of vertical leakage of groundwater into or out of the Upper Floridan aquifer. The vertical hydraulic conductivity of 16 relatively undisturbed core samples in the surficial sediments collected from wells in the Albany, Ga., area ranged from about 0.0004 ft/d for silty clay to about 23 ft/d for fine-to-medium sand (Charles A. Turner, Geologist,

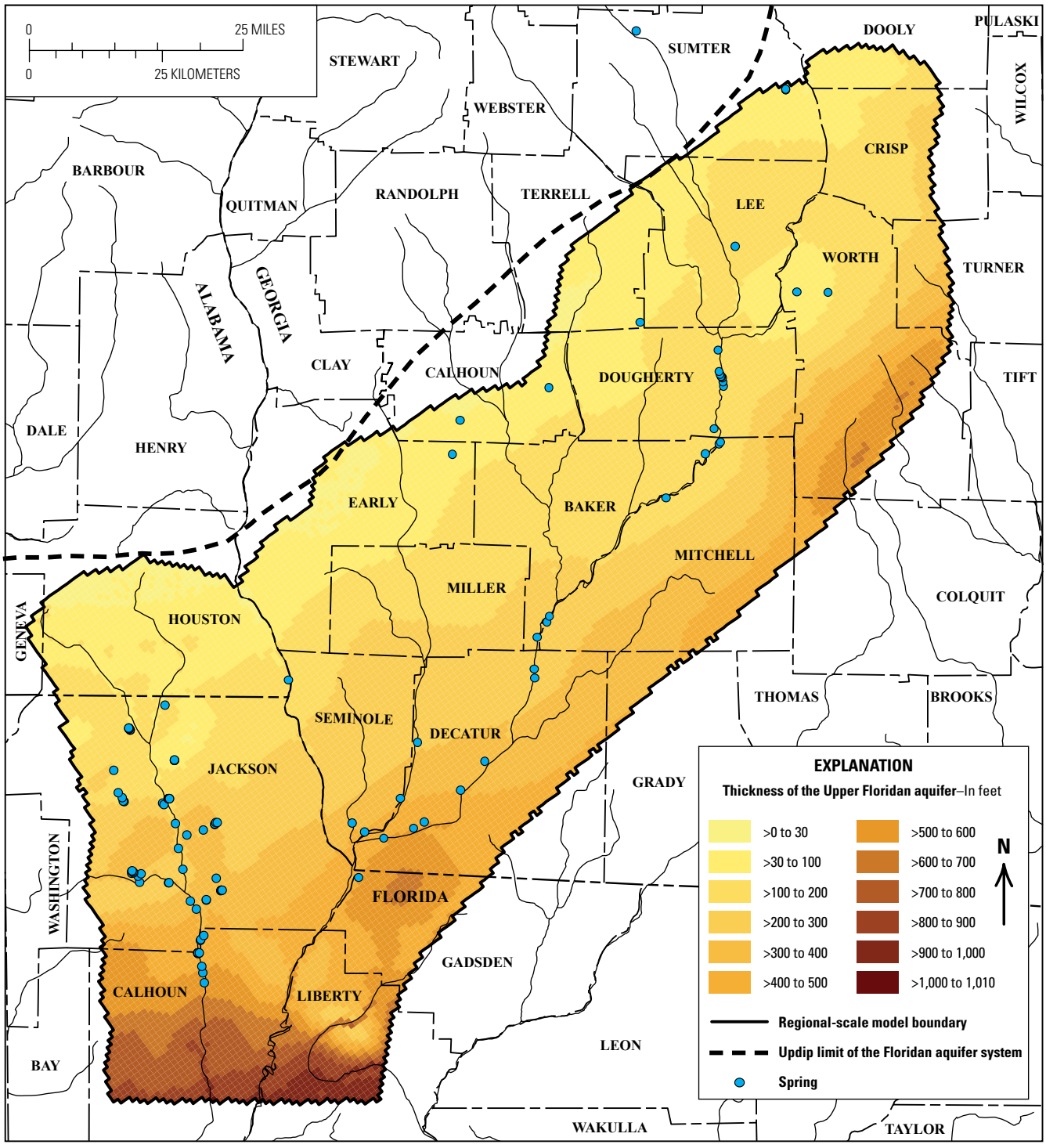

Base from U.S. Geological Survey digital data,1:24,000
Albers Equal-Area Conic Projection

Figure 6. Thickness of the Upper Floridan aquifer and locations of springs sampled in the study.

S&ME, Inc., written commun., 1988). Regional estimates of vertical hydraulic conductivity ranged from about 0.0001 to about 9 ft/d with a median value of about 0.003 ft/d (Hayes and others, 1983).

The confining unit underlying the Upper Floridan aquifer is the Lisbon Formation (fig. 4). This formation is made up of hard, sandy, clayey limestone with distinctly lower water-yielding characteristics than the units of the Upper Floridan aquifer (Watson, 1981). The Lisbon Formation acts as a nearly impermeable confining unit for the Upper Floridan aquifer (Hayes and others, 1983).

The surficial aquifer system, the Upper Floridan aquifer, and streams are hydraulically linked in the study area, especially where sandy or fluvial deposits rest directly on

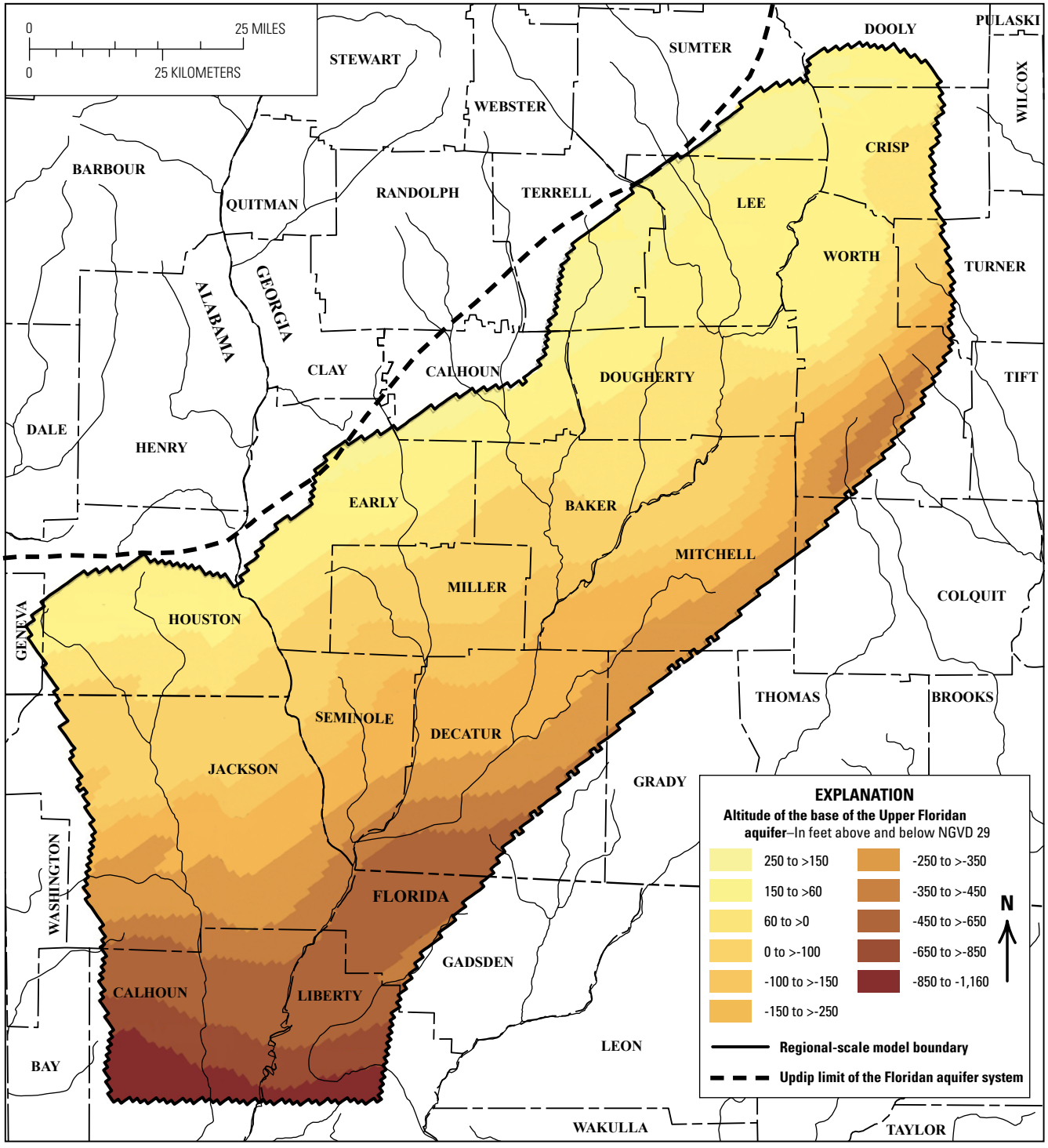

Base from U.S. Geological Survey digital data,1:24,000
Albers Equal-Area Conic Projection

Figure 7. Altitude of the base of the Upper Floridan aquifer in the study area.

the limestone units. The water table fluctuates with adjacent stream stage or with Upper Floridan aquifer water levels in places where the aquifers are hydraulically connected with the land surface. Residuum in other areas separates the surficial aquifer system from surface water and the Upper Floridan aquifer, forming perched water tables. Water levels in perched zones fluctuate independently of water levels in the Upper Floridan aquifer or adjacent streams.

Surface Water

Major surface-water features in the study area include the Chattahoochee, Flint, Apalachicola, and Chipola Rivers, Ichawaynochaway and Spring Creeks, Lake Blackshear, and Lake Seminole (fig. 1). Most river channels are incised into the units that form the top of the Upper Floridan aquifer, and limestone is exposed in many streambeds. Base flow is maintained during periods of little or no precipitation by aquifer discharge.

The Flint River flows through the northeastern part of the study area and is the main discharge feature for numerous springs and smaller tributaries in southwestern Georgia (figs. 1 and 8). Lake Blackshear is formed by the Crisp County Dam on the Flint River in the northern part of the study area (figs. 1 and 8). The Flint River also is one of the three main streams that are dammed to form Lake Seminole in the southern part of the study area on the shared border of Georgia, Florida, and Alabama (figs. 1 and 8).

Lake Seminole influences groundwater levels in the Upper Floridan aquifer near the lake and dam (fig. 2) because of its stable lake stage of about 77 ft. The creation of the impoundment in 1957 raised groundwater levels in the Upper Floridan aquifer by about 30 ft near the dam and caused smaller increases upstream from the dam (Torak and others, 2006). The impoundment creates backwater conditions that extend upstream nearly 50 miles (mi) along the Chattahoochee River and about 47 mi along the Flint River (fig. 2) (U.S. Army Corps of Engineers, 1948). Lake Blackshear, in the northern part of the study area, is maintained at an altitude near 237 ft above NAVD 88 by a flowthrough dam (fig. 2).

The Apalachicola River begins below Lake Seminole at the outflow from the Jim Woodruff Lock and Dam. The river flows about 107 mi southward and discharges into Apalachicola Bay and the Gulf of Mexico. The total drainage area of the Apalachicola River within the State of Florida is about 2,026 square miles (mi^2) and includes the Chipola River Basin (fig. 1) (U.S. Army Corp. of Engineers, 1973). The total drainage area of the Apalachicola River, including the Chattahoochee, Flint, and other rivers, is 19,256 mi^2. Flow in the Apalachicola River is important to the ecology and economy of the region, including the estuary. The mean annual flow of the Apalachicola River at Sumatra, Fla., (20.6 mi upstream from the mouth) is 26,500 cubic feet per second (ft^3/s) for water years (WY) 1978–95 (Franklin and Meadows, 1999). (Water year is the period from October 1 to September 30 and is defined by the year in which the period ends.)

The Chipola River, a major tributary to the Apalachicola River in Florida, is formed by the confluence of two creeks flowing out of Houston County, Alabama, into Jackson County, Florida (fig. 1). The Chipola River flows southward before joining the Apalachicola River. In the study area, the Chipola River is incised into the Upper Floridan aquifer, where limestone is exposed in the streambed. Base flow is maintained from groundwater discharge during periods of little or no precipitation. Along the upper and middle reaches, 68 named springs have been identified along the main stem of the river or its major tributaries (Barrios and Chellette, 2004; figs. 2 and 3). The average mean daily discharge of the Chipola River is 1,512 ft^3/s at the Altha gage in Florida (station number 02359000; 1913–98; fig. 8).

Land Use

Water quality concerns in the lower ACFB reflect dominant lands uses in the basin. Land use was compiled by category in subbasins of the lower ACFB for the period 1972–90 (Frick and others, 1996). Agriculture was the dominant land use (average 47.8 percent) in the Flint and Chattahoochee River Basins and Ichawaynochaway and Spring Creek Basins, closely followed by forest (average 43.4 percent; figs. 8 and 9). Forested land cover was dominant in the Apalachicola and Chipola River Basins, comprising nearly 60 and 50 percent of each basin, respectively. Agricultural land use is the second most common land use in the Chipola River Basin.

Fertilizer use in agricultural areas is probably the largest contributor (72 percent) to nitrogen loads in groundwater and surface water within the lower ACFB (Frick and others, 1996). Estimated annual nitrogen loads increased in the Flint, Chattahoochee, and Chipola River Basins during 1972–90 (Frick and others, 1996). Increased mean annual loads in the Chipola River Basin during 1972–90 were the largest in the Apalachicola Basin (Frick and others, 1996). Increases in nitrogen loads probably were related to increases in corn production, based on fertilizer sales data.

Methods for Predicting the Occurrence and Distribution of Nitrate in Groundwater

To address the need to predict the occurrence and distribution of nitrate in groundwater and to identify future trends in nitrate contamination in the lower ACFB, six sites with measureable nitrate concentrations were identified for water-quality sampling and particle-tracking flow simulations. A regional-scale groundwater-flow model was calibrated with data collected from September 19 to October 18, 1999, the same steady-state calibration period used by Jones and Torak (2006). The calibrated regional-scale model was used with long-term (through 2050) steady-state climate conditions and average groundwater withdrawals to provide flow boundaries for two local-scale groundwater-flow and particle-tracking models (fig. 10). Porosity values in the local-scale groundwater-flow and particle-tracking models were calibrated with geochemical age dating information collected in 2007. Porosity is a variable used in transport to estimate the pore velocity of particles of water and is not a variable in groundwater-flow simulations. Groundwater-flow models estimate Darcy velocity from hydraulic gradient and hydraulic conductivity information. Porosity is inversely correlated to the Darcy velocity.

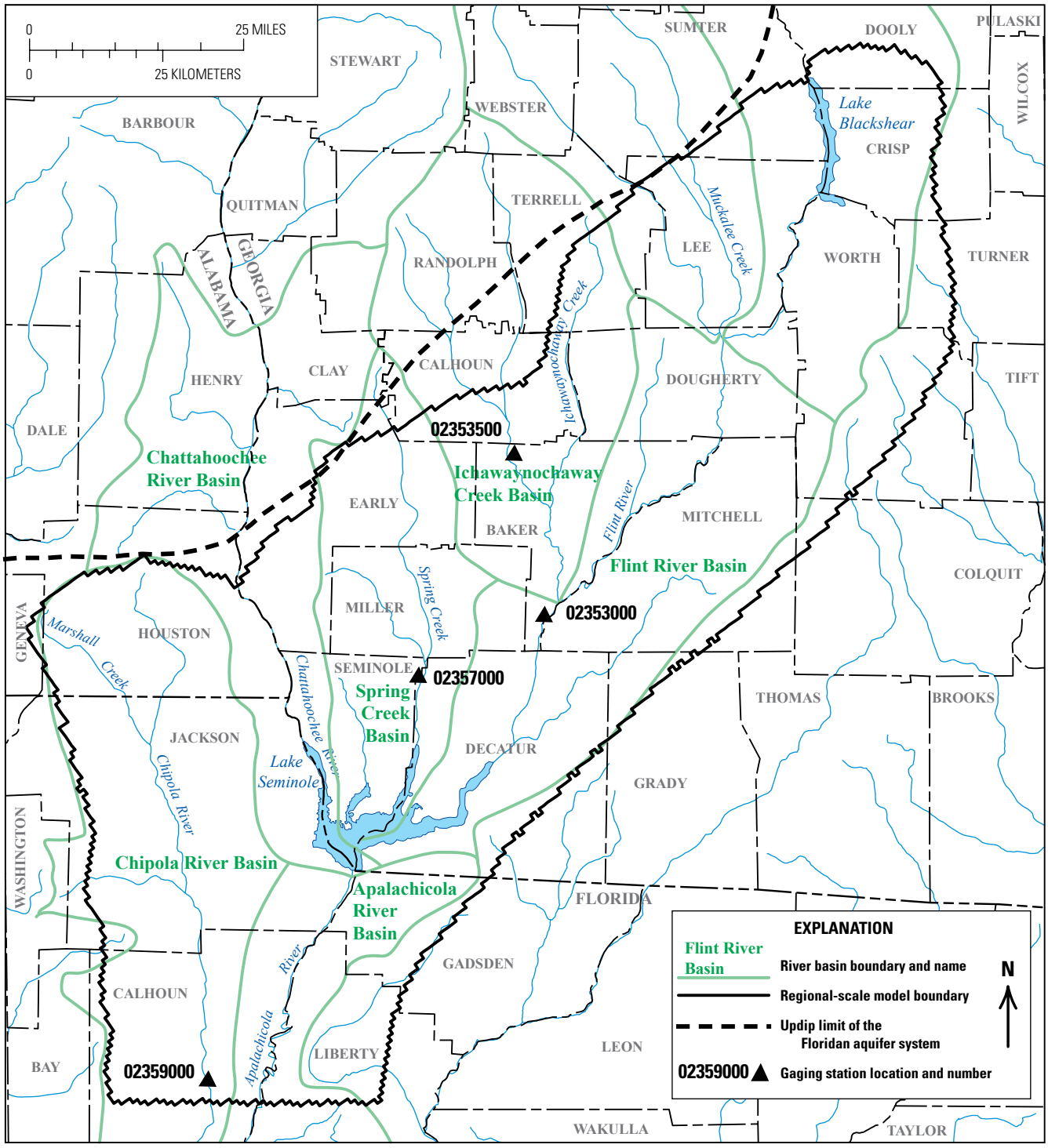

Base from U.S. Geological Survey digital data,1:24,000
Albers Equal-Area Conic Projection

Figure 8. Major rivers and lakes, river basin boundaries, and locations of gaging stations in the study area.

Porosity only affects time of travel of particles and it has no effect on groundwater recharge contributing areas. The local-scale and particle-tracking models were used to determine ACR and travel times (used in this report as surrogates for particle ages) of water. Finally, particle travel times were used to predict nitrate concentrations for three wells and three springs (fig. 10) during 2002–50 by using three nitrogen management scenarios. Nitrate concentrations were predicted through 2050 because predicted climate conditions were available for that time period.

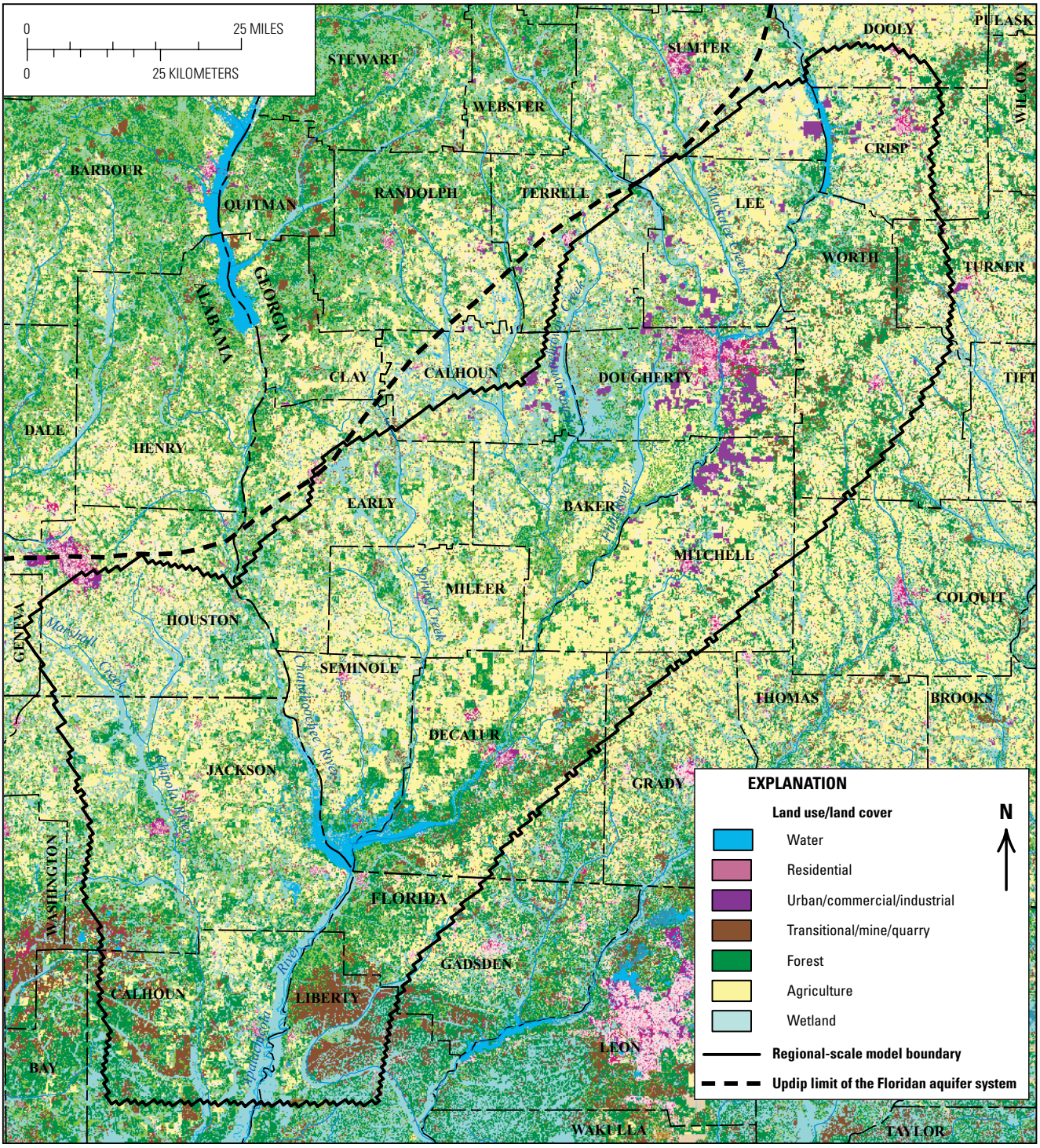

Base from U.S. Geological Survey digital data,1:24,000
Albers Equal-Area Conic Projection

Figure 9. Land use and land cover in the study area.

To estimate nitrate concentrations in selected wells and springs during 2002–50, a time series function of nitrate input to groundwater was developed from county level fertilizer sales and atmospheric deposition data (fig. 11) (Alexander and Smith, 1990; Battaglin and Goolsby, 1994; Frick and others, 1996; Ruddy and others, 2006). The input function was applied to determine the age of tracked particles to predict future nitrate concentrations at the six selected wells and springs. Although the input function changes over time, a steady-state flow field representing average flow conditions

during the period over which the transport occurred was used to create the steady-state flow field for particle tracking (Pollock, 1994; Eberts and others, 2005; Crandall, 2007; Katz and others, 2007; Crandall and others, 2009).

Water-Quality Sampling

Groundwater samples were collected from 11 long-term monitor wells as part of the NAWQA Program trends network. Data were collected approximately nine times from 1993 to 2007 to observe trends in groundwater quality in the lower ACFB. The samples were analyzed for major ions, nutrients, pesticides, volatile organic compounds, and field properties—temperature, pH, specific conductance, and dissolved oxygen. Additionally, during a synoptic sampling in the spring and early summer of 2007 in the upper Chipola River Basin, samples were collected from 33 springs and 17 surface-water sites (appendix). The sites were selected because they had been identified and sampled previously by the Northwest Florida Water Management District (NWFWMD). Water samples from the upper Chipola River Basin were analyzed for pH, dissolved oxygen, temperature, specific conductance, nitrate, total coliforms, and *Escherichia coli* (*E. coli*). Nitrate was measured using the field spectrophotometer method 10020 described by Hach Company (1992), and total coliforms and *E.coli* were measured using the IDEXX quick Colilert® method (IDEXX Corporation, 2006). All samples were collected using standard USGS water-quality sampling field procedures and protocols (Koterba and others, 1995), except where noted.

Synoptic water-quality data were used in conjunction with NAWQA, FDEP, and NWFWMD historical water-quality data to select three USGS long-term monitor wells and three springs in the Chipola River Basin for further study (fig. 10). Additionally, two upgradient monitor wells for each of the three springs were selected for further monitoring to help identify upgradient water quality and geochemical conditions along probable flow paths within each springshed (fig. 10). The three springs and their respective upgradient wells (and alternative names) are (1) Jackson Blue Spring and wells HWY 69 VISA (NWFWMD 80) and Baxter VISA (NWFWMD 85); (2) Baltzell Springs Group and wells JAPST001 (McArthur) and Malone No. 2; and (3) Sandbag Spring and wells Cottondale No. 3 and Hutton.

Three long-term monitor wells (CP-18A, CP-21A, and RF-41) were selected from the USGS NAWQA trends network for additional water-quality analyses (fig. 10). Analyses included major ions, nutrients, field properties, pesticides, isotopes of oxygen, hydrogen, and nitrate, and groundwater age tracers, including tritium (^{3}H), its radioactive decay product helium-3 (^{3}He), chlorofluorocarbons (CFC), and sulfur hexafluoride (SF_6). Quality-control samples accounted for 10 percent of the samples and included duplicates, replicates, spikes, and blanks.

Age Dating of Groundwater and Spring Samples

The average age or residence time of groundwater at selected wells or springs was determined using transient tracer techniques to differentiate between the relative proportions of young water from shallow parts of the aquifer and older water from deeper parts of the aquifer. Water samples were collected from selected wells and springs and analyzed for the transient environmental tracers ^{3}H, its radioactive decay product ^{3}He, CFC, and SF_6. Anthropogenic activities, such as industrial processes and atmospheric testing of thermonuclear devices, have caused SF_6, CFC, and ^{3}H to be released into the atmosphere in low, but measurable, concentrations (fig. 12). Precipitation that contains SF_6, CFC, and ^{3}H from the atmosphere infiltrates into the ground and carries a particular chemical or isotopic signature related to atmospheric conditions at the time of recharge to groundwater. The tritium/tritiogenic helium-3 ratio ($^3H/^3He_{trit}$), CFC, and SF_6 dating methods assume that gas exchange between the unsaturated zone and the atmosphere occurs quickly and that shallow groundwater remains closed to gas exchange after recharge (Schlosser and others, 1989; Plummer and Busenberg, 1999; Busenberg and Plummer, 2000).

Established protocols were used to collect and analyze samples for SF_6, $^3H/^3He$ (Ludin and others, 1998), and CFC (Busenberg and others, 1993). Dissolved gases (nitrogen gas, argon, carbon dioxide, and methane) were analyzed in groundwater samples at the USGS Chlorofluorocarbon Laboratory in Reston, Virginia. Dissolved gases were measured by gas chromatography after extraction in headspaces of glass samplers (Busenberg and others, 1998). Water samples from the selected wells and springs were analyzed for groundwater age-dating tracers—tritium, tritiogenic helium-3, CFC-11, CFC-12, and CFC-113, and SF_6. Results for these analyses produced an average apparent age of groundwater for each selected site.

Tritium and Tritiogenic Helium-3

The continued decrease in occurrence and the low concentrations of ^{3}H in rainfall in the southeastern United States have resulted in limited use of the ^{3}H method for age dating of groundwater recharged during the past 20–30 years. However, by measuring the tritiogenic helium-3 ($^3He_{trit}$), the stable daughter product of ^{3}H decay that has accumulated in groundwater systems, the dating range and precision can be enhanced (Plummer and others, 1998; Cook and Böhlke, 1999). Combined measurements of ^{3}H and its daughter product of radioactive decay, $^3He_{trit}$, define a relatively stable tracer of the initial ^{3}H input to groundwater, which can be used to calculate the $^3H/^3He_{trit}$ apparent age from a single water sample (Schlosser and others, 1988, 1989; Solomon and Sudicky, 1991). The $^3H/^3He_{trit}$ ratio is used in the following equation for

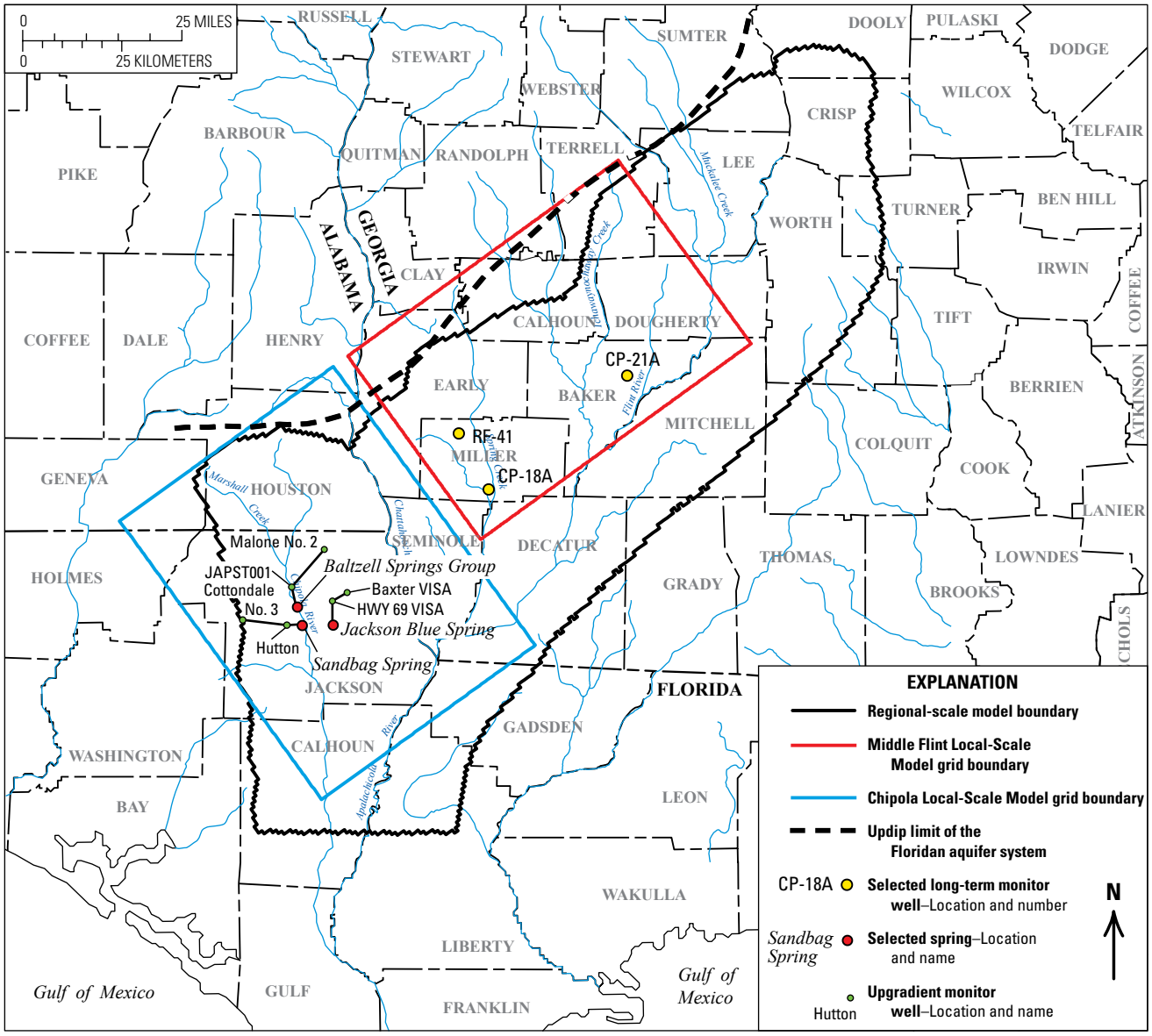

Base from U.S. Geological Survey digital data,1:24,000
Albers Equal-Area Conic Projection

Figure 10. Regional and local-scale model areas and locations of springs and wells selected for detailed study.

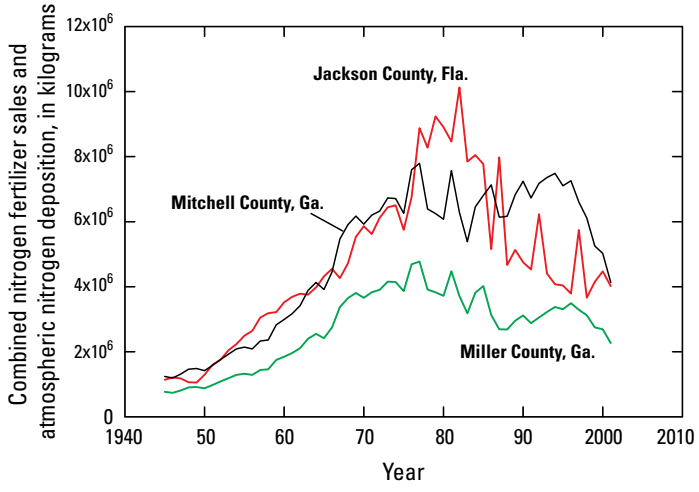

Figure 11. Nitrogen fertilizer sales and atmospheric nitrogen deposition by county.

the piston-flow assumption where the average apparent age (T, years) can be expressed as (Torgersen and others, 1979):

$$T = 1/\lambda_T[\ln (1 + {}^3He_{trit}/{}^3H)]$$

where

λ_T is the radioactive decay constant for the ^3H concentration in tritium units, and

$^3He_{trit}$ is the tritiogenic helium-3 content in tritium units.

A tritium unit is equal to 1 ^3H atom in 10^{18} hydrogen atoms and is equivalent to 3.2 picocuries per liter of water. A helium (He) isotope mass balance is used to calculate the amount of tritiogenic and non-tritiogenic ^3He in the sample. Non-tritiogenic ^3He (generally negligible in a shallow aquifer with local recharge) is corrected by using measured concentrations of helium-4 (^4He) and neon (Ne) in the water sample and assuming solubility equilibrium with air at the water temperature measured during sampling (Schlosser and others, 1988, 1989). In order to use ^3H and $^3He_{trit}$ concentrations to estimate the average apparent age of groundwater, it is assumed that ^3H and $^3He_{trit}$ concentrations in groundwater are not affected by contamination, sorption, and microbial degradation processes that can alter the concentrations of other transient tracers, such as CFC (Plummer and others, 1998). The distribution of ^3H and $^3He_{trit}$ can be affected by hydrodynamic dispersion and the mixing of different age waters (Solomon and Sudicky, 1991; Reilly and others, 1994).

Information about groundwater travel times can be obtained by comparing measured ^3H concentrations in groundwater with the long-term ^3H input function of rainfall measured at the International Atomic Energy Agency precipitation monitoring station in Ocala, Fla., which is about 190 mi southeast of the study area. Atmospheric weapons testing beginning in the early 1950s increased ^3H concentrations in rainfall in this area to a maximum of several hundred tritium units during the mid-1960s, followed by a nearly logarithmic decrease in concentrations to the present (fig. 12). Analytical uncertainty (one sigma) for ^3H using the low-level counting procedure is about plus or minus (±) 0.15 to 0.30 tritium units (Ludin and others, 1998).

Water samples for the determination of $^3H/^3He^{trit}$, ^4He, and Ne were collected in pinched-off copper tubes (10-millimeter (mm) diameter, 80-centimeter (cm) length, about 40-milliliter (mL) volume) while applying back pressure to prevent gas bubbles from forming. These samples were analyzed at the Noble Gas Laboratory of Lamont-Doherty Earth Observatory in Palisades, New York, by using quantitative gas extraction followed by mass spectrometric techniques (Schlosser and others, 1989; Ludin and others, 1998).

Chlorofluorocarbons and Sulfur Hexafluoride

The CFC and SF_6 age-dating techniques rely on the stability of these halogenated hydrocarbon and sulfur compounds in the hydrosphere, which has led to their effective use as tracers to date groundwater recharged during the past 50 years (Plummer and Busenberg, 1999; Busenberg and Plummer, 2000). The techniques presume that CFC and SF_6 concentrations in the aquifer have not been altered by biological, geochemical, or hydrologic processes.

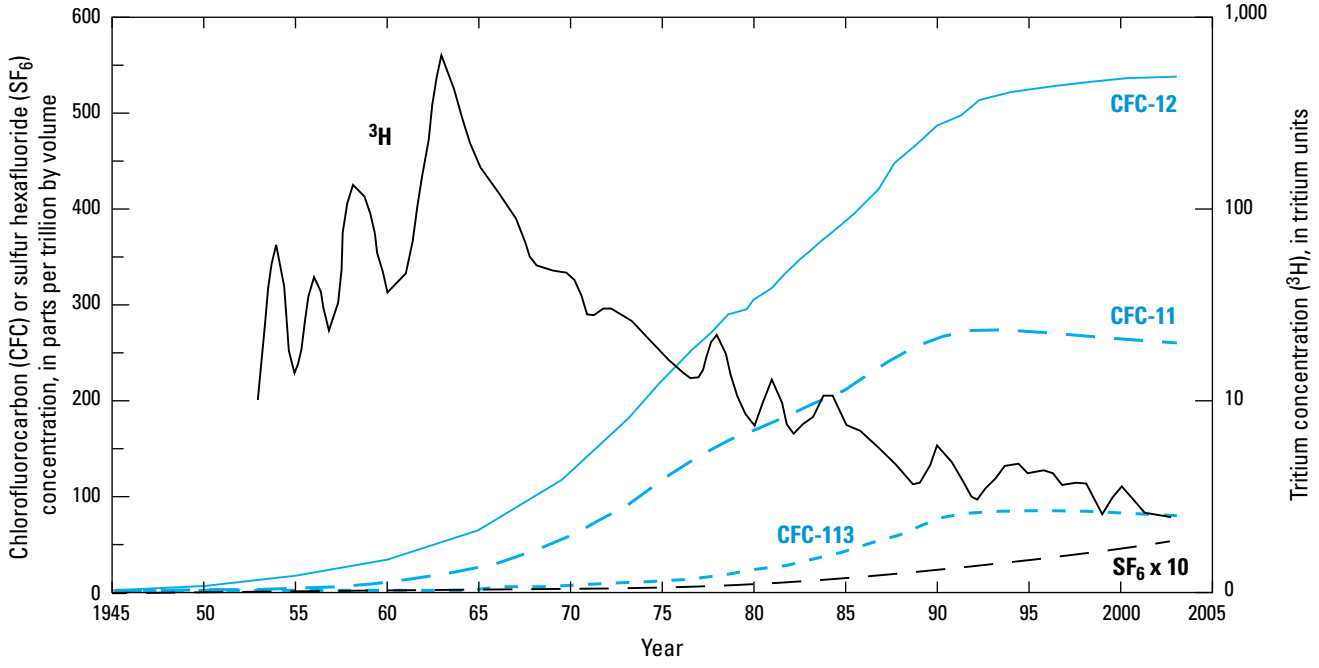

Figure 12. Concentrations of chlorofluorocarbon, sulfur hexafluoride, and tritium in the atmosphere from International Atomic Energy Agency precipitation monitoring station in Ocala, Florida, 1945–2005.

Apparent ages for CFC and SF_6 are estimated on the basis of equilibrium partitioning between recharging groundwater and the partial pressures of trichlorofluoromethane (CCl_3F, CFC-11), dichlorodifluoromethane (CCl_2F_2, CFC-12), trichlorotrifluoroethane ($C_2Cl_3F_3$, CFC-113), and SF_6 in the troposphere or soil atmosphere (fig. 12). Concentrations of CFC and SF_6 in groundwater are functions of the atmospheric partial pressures and the temperature at the base of the unsaturated zone during recharge. The recharge temperature and the quantity of dissolved excess air (Heaton and Vogel, 1981) are determined from gas-chromatography analyses of nitrogen (N_2) and argon (Ar) in the headspace of water samples collected in the field (Busenberg and others, 1993). An average apparent age of the sampled water is determined from a comparison of the partial pressure of each CFC compound and SF_6 in the sample, calculated from their measured concentrations using solubility data for each compound, with the record of atmospheric partial pressures over North America at different times (fig. 12). Input functions for CFC and SF_6 were obtained from their atmospheric input curves, assuming a ratio of summer-to-winter infiltration coefficient of 1.0. Concentrations of the three CFC compounds and SF_6 ideally provide four independent ages that can be used to cross check the sampling and analytical methods. Additional age information can be obtained from ratios of atmospheric CFC compounds (for example, CFC-113/CFC-12 and CFC-113/CFC-11) that have varied over time (Plummer and Busenberg, 1999). Discrepancies between ages obtained from CFC ratios and individual compounds provide important information about water mixtures. Analytical procedures for CFC and SF_6 sampling are described by Busenberg and others (1993) and Busenberg and Plummer (2000).

Groundwater-Flow Model Development and Simulations

Groundwater-flow models were developed at both regional and local scales. A regional-scale, steady-state, three-dimensional, finite-difference, groundwater-flow model was calibrated against data for September 19–October 18, 1999. Long-term (1975–2005) average steady-state recharge and withdrawal conditions were applied to the regional model for particle-tracking analysis. Two local-scale models that obtained parameters and boundary flows from the regional-scale steady-state simulation with long-term average conditions (1975–2005) were used for particle-tracking analysis and simulation of future nitrate concentrations.

The local-scale model areas contain the ACR for selected wells and springs as determined from regional particle tracking. The local-scale models, however, use refined discretization of the regional-scale model grid (more cells and layers) in order to have more mathematically accurate particle tracking for the simulation of nitrate transport (Pollack, 1994).

Regional-Scale Model

A regional-scale, steady-state, three-dimensional, finite-difference, groundwater-flow model was developed using information and data from two existing two-dimensional USGS MODFE finite-element groundwater-flow models (Cooley, 1992; Torak, 1993; Torak and others, 1996; Jones and Torak, 2006; fig. 13). Data from the MODFE models were extracted and used to provide base line and starting hydraulic parameters and boundary conditions for the three-dimensional models developed for this study using MODFLOW 2000 (Harbaugh and others, 2000). Both simulations for the regional-scale model are steady-state; however, one was used for calibration purposes (September 19–October 18, 1999; stress conditions) because the greatest number of head and flow observations was available during that period. The second regional-scale simulation used average recharge and withdrawal conditions for 1975–2005, the period during which most of the nitrate transport most likely occurred.

The regional-scale, steady-state, MODFLOW model was calibrated against data collected or estimated from September 19 to October 18, 1999 (Jones and Torak model, 2006). Boundary conditions from the Jones and Torak (2006) model were augmented with estimated or measured precipitation and withdrawal data for the additional area, because the MODFLOW model extends into the upper Chipola River Basin beyond the area of the 2006 model. The calibration was achieved using 328 groundwater level measurements and 68 streamflow measurements. For the purpose of this study, however, another steady-state simulation using long-term (1975–2005) average recharge and withdrawal conditions was needed for calibration of the two local-scale models to provide steady-state flow boundaries for the particle-tracking simulations.

Particle-tracking simulations require a fully three-dimensional groundwater simulation code in order to reproduce any variability in particle-age distributions. Additionally, it is assumed that the transport of nitrate occurs over a long period of time, such that the transient seasonal nature of both rainfall and groundwater withdrawals can be averaged and still produce reasonable estimates of contributing areas and travel times to the selected springs and wells. The period 1975–2005 was selected for the long-term average because this 30-year period would include wet, dry, and average conditions and it roughly corresponds to the period of time for which nutrient sources were estimated (Frick and others, 1996). A steady-state flow field can be used for the simulation of transport with particle tracking (Pollock, 1994). In this oxygenated flow system, nitrate entering the aquifer tends to be conserved and transported with the water molecules; thus, advective transport with particle tracking using a long-term average steady-state flow field is a reasonable approach (Eberts and others, 2005; Crandall and others, 2009).

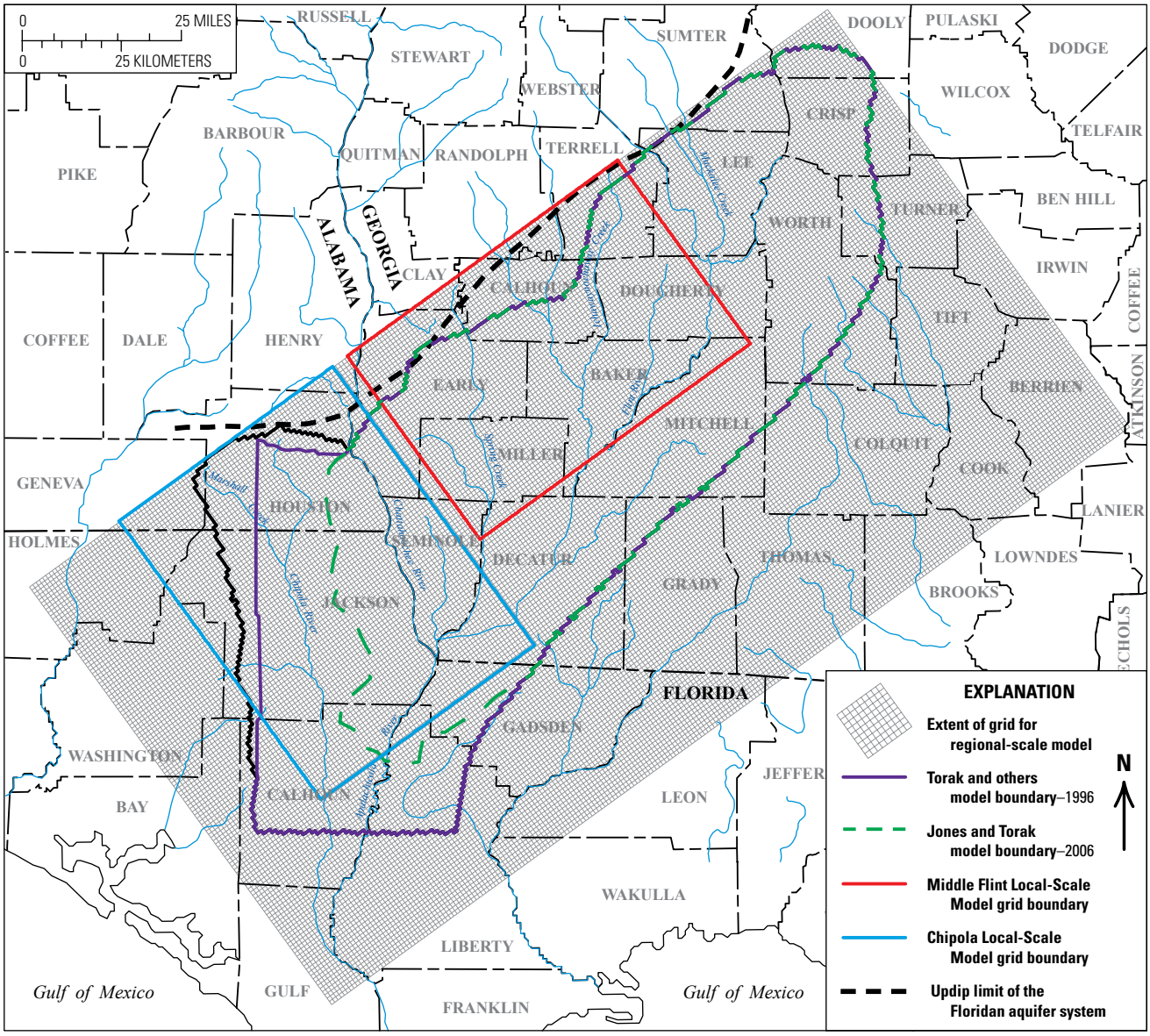

Base from U.S. Geological Survey digital data,1:24,000
Albers Equal-Area Conic Projection

Figure 13. Previous and current groundwater-flow model boundaries in the study area.

Model Geometry and Discretization

The regional-scale groundwater-flow model active area includes about 7,949 mi^2 of the Dougherty Plain and Marianna Lowlands (fig. 1), and the rectangular model grid consists of 4 layers, 130 columns, and 248 rows with a cell size of 3,281 ft on each side (fig. 13). Cell-size dimensions were selected on the basis of the average and minimum element side-length from the previous MODFE model. The regional-scale groundwater-flow model grid was rotated 306 degrees to align the grid approximately along dominant fracture feature traces identified through photolineaments (Vernon, 1951; Williams, 1985; Culbreath, 1988; Hazlett, 1989; U.S. Army Corps of Engineers, 2004).

The top of layer 1 represents land-surface altitude from the USGS National Elevation Dataset (NED) (Gesch, 2007; Gesch and others, 2009). The thickness of surficial deposits was obtained by subtracting the estimated altitude of the top of the Upper Floridan aquifer in Jones and Torak (2006) from the NED land-surface altitude. The resulting thickness of layer 1 was adjusted in stream channels and valleys where surficial sediments were absent or thin. Thickness of layer 1 ranges from a minimum of 10 to a maximum of 615 ft, and the median thickness is about 50 ft.

The top layer of the regional-scale model represents three distinctive hydrogeologic units—sandy sediments that form the surficial aquifer system, a clayey residuum, and the Upper

Floridan aquifer in the river channels. Zones that represent the geologic materials present were assigned to layer 1 of the model (fig. 14). The surficial aquifer system is present in layer 1 where the overlying sediments mostly consist of sand or clayey sand. Where the sediments mainly consist of sandy silt or sandy clay (primarily on small ridges that pinch out near streams), layer 1 represents residuum, and vertical leakage is appropriately smaller than where the sediments contain more sand (Jones and Torak, 2006; Torak and Painter, 2006). Layer 1 represents the Upper Floridan aquifer in river beds and areas where the Ocala Limestone crops out or is close to the land surface (fig. 14).

Model layers 2 through 4 represent the Upper Floridan aquifer. The hydraulic and thickness properties of the layers

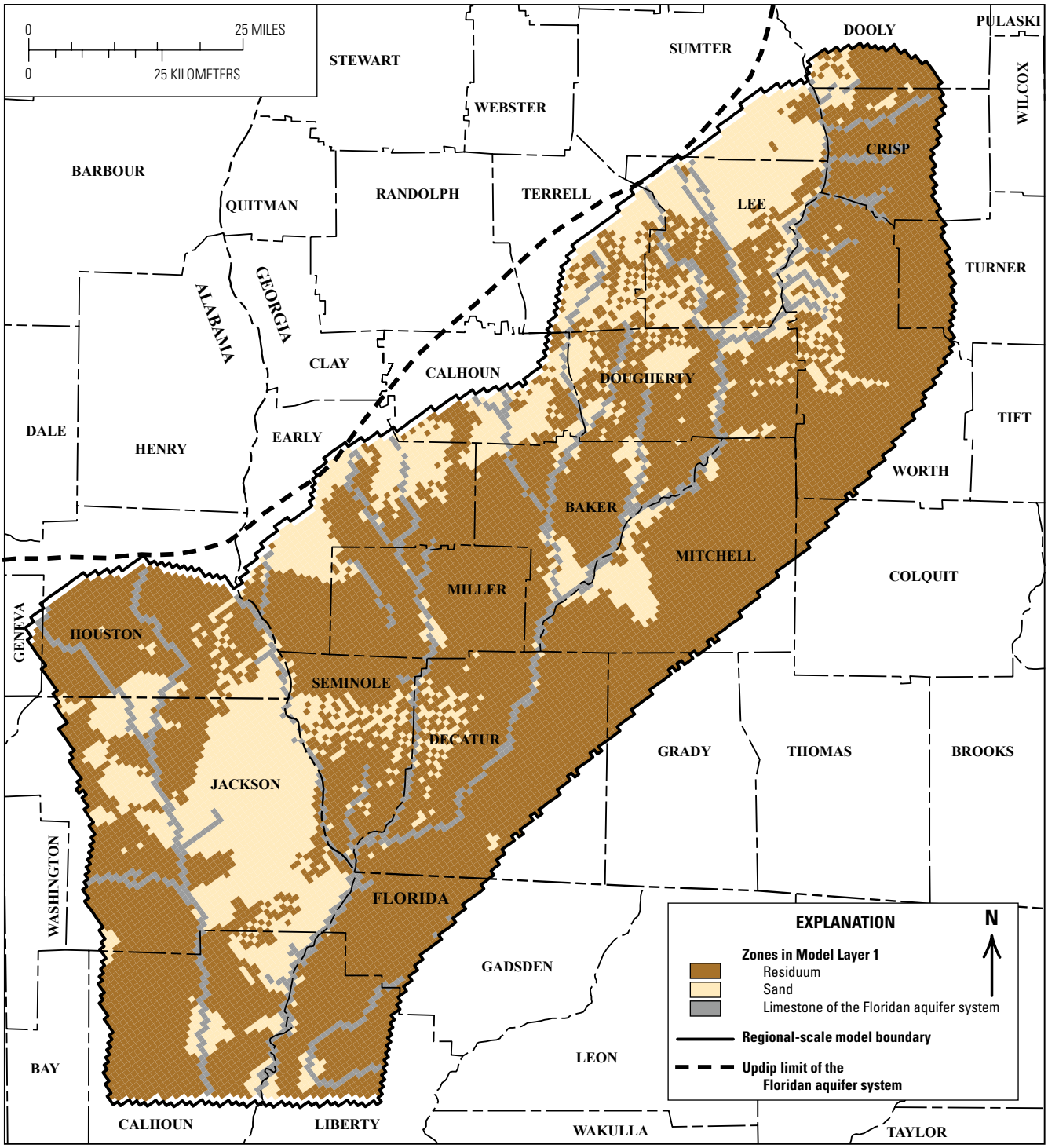

Base from U.S. Geological Survey digital data,1:24,000
Albers Equal-Area Conic Projection

Figure 14. Zones representing residuum, sand, or limestone of the Floridan aquifer in model layer 1 of the regional-scale model.

are identical. The total thickness of model layers 2 through 4, representing the entire aquifer, ranges from 29.5 ft (a minimum of nearly 10 ft per layer) on the northern boundary of the modeled area to approximately 1,009 ft near the southern boundary. The thicknesses of layers 2 through 4 are divided evenly so that they make up one-third of the total aquifer thickness in most places except where rivers are designated. The Floridan aquifer system may have additional thickness in layer 1 in river channels. The median thickness of the sum of layers 2 through 4 is approximately 200 ft.

Boundary Conditions and Model Stresses

Lateral boundary conditions for the regional-scale models include a constant (specified) head on the northwestern and southern boundaries (fig. 15), head-dependent flux using the MODFLOW general-head package on the northeastern, eastern, and southeastern boundaries of the model—essentially the same boundary conditions applied by Jones and Torak (2006)—and a no-flow boundary on the northern and the western boundaries (fig. 15) that approximately follows the Upper Floridan aquifer divide based on historical published potentiometric surfaces. A constant-head boundary was applied to the top active grid layer using the MODFLOW recharge package for the calibration and long-term average stress periods. Minimal flow between the aquifer and the confining unit was assumed to occur along the bottom layer of the model; therefore, a no-flow boundary condition was used beneath model layer 4.

Net recharge (precipitation minus evapotranspiration and surface runoff) was simulated in the regional-scale calibration model by applying 23 percent of the total precipitation from September 19–October 18, 1999, to the top face of the highest active grid cell (layer 1) in areas where the top layer is zoned as limestone (the Upper Floridan aquifer) or sandy sediments—identical to the procedure used by Jones and Torak (2006). In areas where the overburden is categorized as residuum, scaled precipitation totals were reduced another 30 percent to simulate the effects of additional evapotranspiration in the residuum, which further reduces groundwater recharge. Theissen polygons of precipitation combined with percentage reductions for the different zones of layer 1 (residuum, sand, or limestone shown in figure 14) result in the distribution of net recharge shown in figure 16. The areal average net recharge was 7.44 inches per year (in/yr). The maximum and minimum amounts of net recharge were 37.47 in/yr and 2.32 in/yr, respectively.

Net recharge for the steady-state, long-term, regional-scale and local-scale models was developed by scaling the long-term (1975–2005) average precipitation from 20 climate stations within and outside of the active modeled area and distributing recharge using Theissen polygons (fig. 17). A total of about 5 percent of the long-term average precipitation was applied where layer 1 represents residuum and 23 percent of the total long-term average precipitation was applied in other areas. The long-term areal average recharge for the steady-state regional-scale model is 6.63 in/yr. The maximum and minimum amounts of simulated recharge were 18.21 and 3.03 in/yr, respectively. The patterns of simulated recharge reflect both the location of weather stations and the different zones in layer 1 (residuum, sand, or limestone shown in figure 14).

Rivers were simulated in the local- and regional-scale models (fig. 15) using the MODFLOW river package. A total of 826 rivers cells, which are set in layer 1, were used in the regional-scale model. Original river stage and riverbed conductance values were obtained from Jones and Torak (2006). Values were modified slightly in the calibration. A detailed discussion describing the development of withdrawal and river stage data for the Dougherty Plain portion of the calibration model can be found in Jones and Torak (2006). Stage between gages in the Chipola River Basin was estimated using the NED and adjusted regressions. Stage and river bottom altitudes for tributaries with no gaging stations were estimated using the Digital Elevation Model (DEM) for land surface and constants based on available measured stages and river bottom altitudes at gaging stations (fig. 8). River bottom altitudes were set at a constant 10.0 ft below stage values if this would allow river bottom altitudes to remain above the bottom of layer 1. Where the bottom of layer 1 is less than 10 ft below the stage in model grid cells, river bottom altitudes were set above the bottom of the layer 1, but below the stage (generally 1 ft above the bottom of layer 1).

The MODFLOW drain package was used to simulate discharge from the Upper Floridan aquifer from springs and non-perennial streams in the regional-scale model (fig. 15). Drain cells were specified in 579 cells in layer 1 of the regional models or at the bottom of the surficial aquifer system (top of the Upper Floridan aquifer). The altitude of drains was based approximately on land-surface altitude or stream stage, if available, or otherwise estimated from land-surface altitude.

The regional-scale model includes 2,938 public-supply, domestic, industrial, and irrigation wells (fig. 15). Estimated withdrawals were averaged for the calibration period (September 19–October 18, 1999; Jones and Torak, 2006). Withdrawals estimated from the Jones and Torak (2006) report totaled 133 million gallons per day (Mgal/d). Withdrawals in the upper Chipola River Basin in Florida and Alabama totaled an additional 14.5 Mgal/d. Withdrawals for 53 irrigation wells in the Alabama portion of the upper Chipola River Basin (totaling 2 Mgal/d) were estimated based on the latitude and longitude of each irrigation pivot using Google Earth™ and on probable crop type. For example, water use for corn was estimated at 9 in/yr of irrigation water per crop (R.L. Marella, U.S. Geological Survey, oral commun., 2008). Withdrawals in the Chipola River Basin in Florida were estimated using permitted average values obtained from the Northwest Florida Water Management District (1999–2007) and totaled 12.5 Mgal/d. Withdrawals in the regional-scale calibration model totaled 147.5 Mgal/d for the calibration period. Overall, withdrawal rates per grid cell (withdrawals may consist of one or more wells per grid cell) ranged from a

minimum of 11 gallons per day to a maximum of 8.0 Mgal/d; the average withdrawal rate was 0.051 Mgal/d for the period September 19–October 28, 1999.

Withdrawals for the steady-state, long-term, regional-scale model were based on estimated withdrawals for average climate conditions from Hook and others (2010), the percentage acreage in agricultural production of the modeled area in each county, and other long-term average withdrawal data for Georgia. Withdrawal locations were taken from the calibration model, but scaled to estimate and distribute long-term withdrawals under average climate conditions. Estimated total steady-state withdrawals under average climate conditions are 285.5 Mgal/d for Georgia. Estimated withdrawals in the Chipola River Basin (obtained from the calibration model)

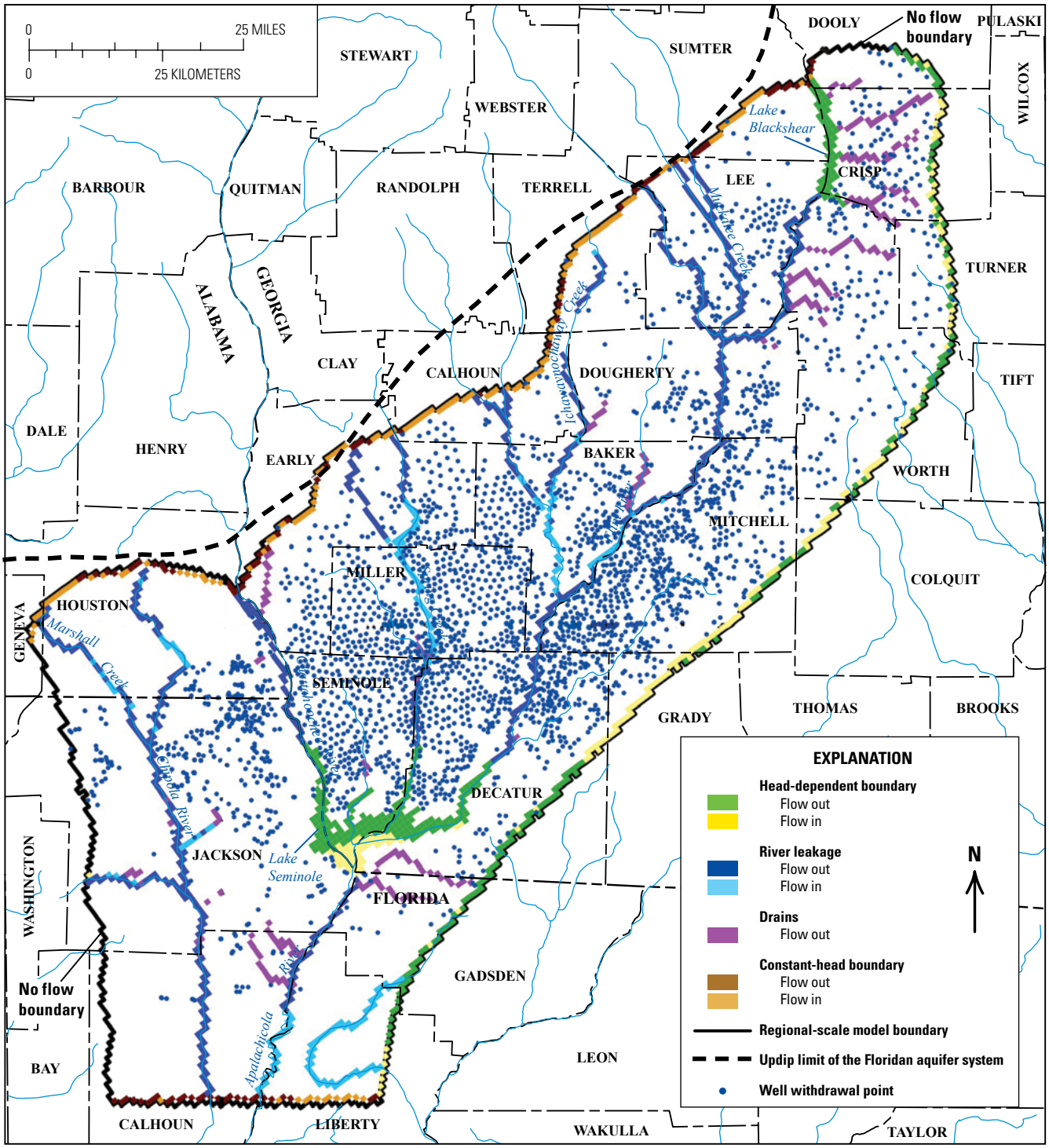

Base from U.S. Geological Survey digital data,1:24,000
Albers Equal-Area Conic Projection

Figure 15. Regional-scale model boundary conditions and locations of rivers, drains, and wells.

remained unchanged in the steady-state model. Total withdrawals in the steady-state, long-term, regional-scale model totaled approximately 300 Mgal/d for Georgia, Alabama, and Florida. The long-term average withdrawal is greater than that of the calibration period because the calibration period was at the end of the growing season and irrigation withdrawals were less than average.

Head-dependent flux boundaries and the general head boundary package of MODFLOW-2000 (Harbaugh and others, 2000) were used to simulate stage and flows in and out of Lake Seminole and Lake Blackshear in the regional-scale model. The use of the head-dependent boundary requires a stage and lakebed conductance term. Lakebed conductance is defined as the product of the vertical hydraulic conductivity of

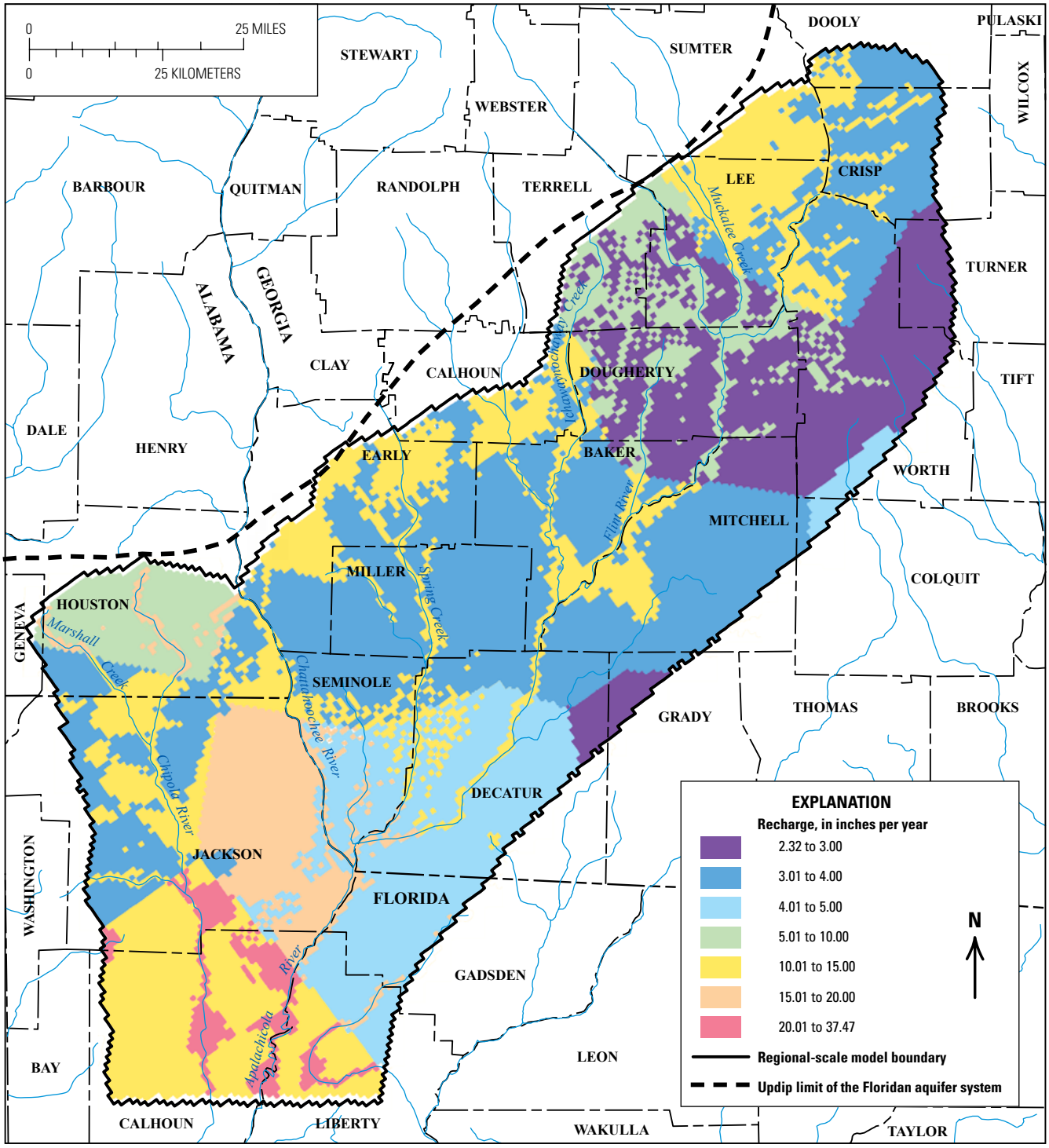

Base from U.S. Geological Survey digital data,1:24,000
Albers Equal-Area Conic Projection

Figure 16. Distribution of net recharge in the regional-scale calibration model.

lake sediments and the area of the lake within the model-grid cell divided by the thickness of the lake sediments. Stage was set at 237.00 ft and 75.9 ft for Lakes Blackshear and Seminole, respectively. The vertical hydraulic conductivity for lakebed sediments in these two lakes are within the range of observed values reported in selected literature (10^{-3} to 10^{-6} ft/d; Taylor and Cherkauer, 1984; Cherkauer, and others, 1987). Lakebed hydraulic conductivities for Lake Blackshear ranged from 9.3×10^{-5} to 6.6×10^{-4} ft/d (average of 2.8×10^{-4} ft/d) and for Lake Seminole they ranged from 1.4×10^{-4} to 7.9×10^{-3} ft/d (average of 3.0×10^{-3} ft/d).

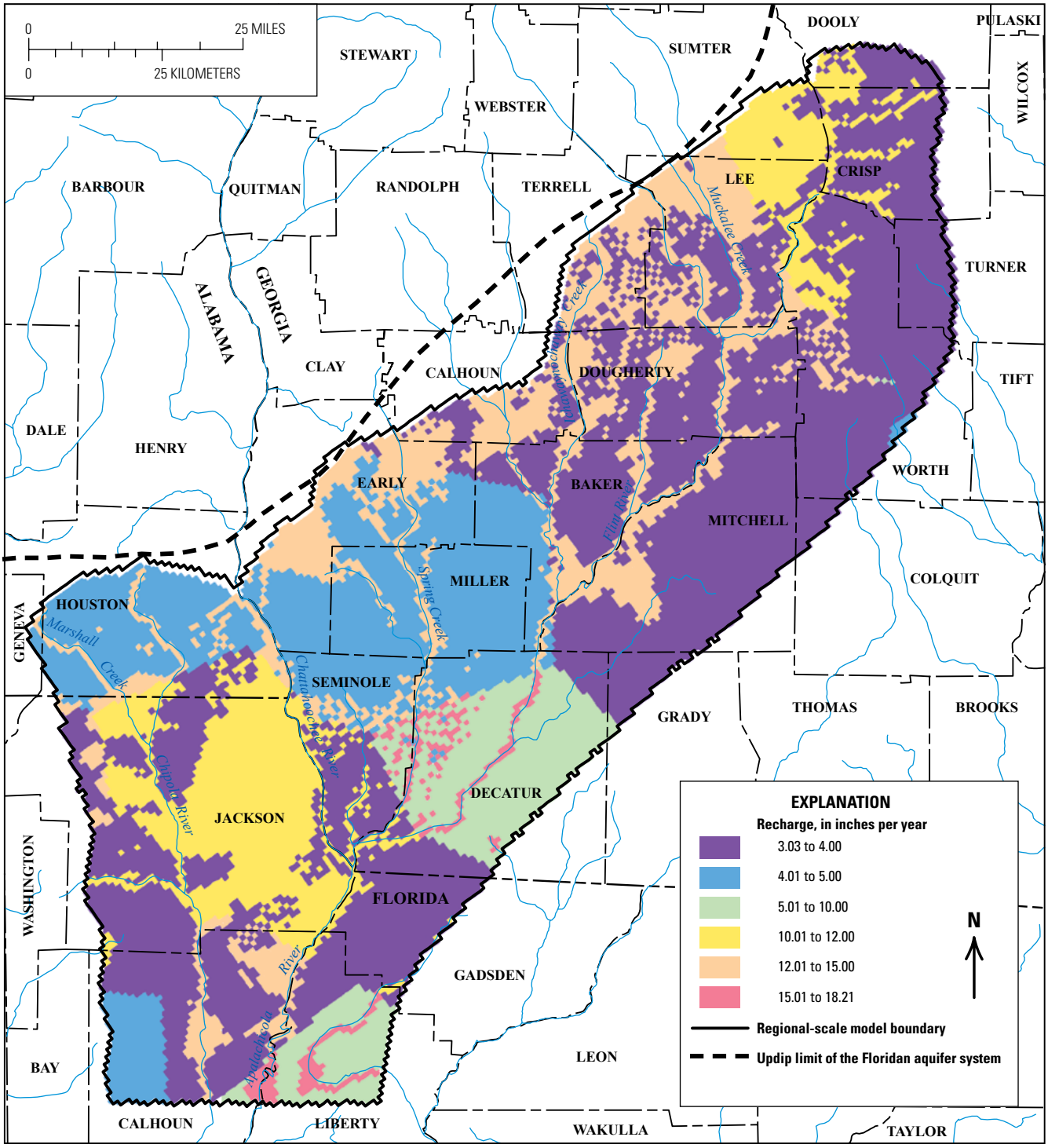

Base from U.S. Geological Survey digital data,1:24,000
Albers Equal-Area Conic Projection

Figure 17. Distribution of net recharge in the regional-scale long-term model.

Calibration Criteria and Strategy

Calibration of the regional-scale model was achieved using parameter estimation in MODFLOW-2000 (Harbaugh and others, 2000). Parameter estimation in MODFLOW-2000 uses regression to minimize the weighted sum of squared errors on the basis of observed data compared to simulated head and flow data. The program iterates between model runs, calculating the total weighted sum of squared errors, updating the parameter values, and finally running the model again. The program continues until the convergence criteria are met and values of the parameters are optimized (Hill and Tiedeman, 2007). Additionally, the use of parameter estimation means that hydraulic properties and (or) stresses can be grouped together into parameters that are estimated by the regression by defining zones and (or) multiplier arrays.

The regional-scale model was based on two previously completed one-layer models of the Floridan aquifer system that were calibrated with a trial and error approach. Water levels in wells and flow observation locations are shown in figure 18. Thus, the calibration criteria were similar to past models and were based on the average accuracy of the observed data. Most of the water levels are accurate to ±5 ft. Accuracy of streamflow gains and losses for the river reaches or for spring discharge is difficult to determine because streamgaging accuracy typically is defined as a percentage, and the subtraction of two flow measurements may magnify the error in an individual measurement. Additionally, simulated small flows could be widely inaccurate, but would not be a substantial quantity of the simulated water budget. Thus, no absolute number criterion or range in flow was established, as in Jones and Torak (2006). Weighting of the residuals for flows was based on an assumption that the observed flows are accurate within 30 percent.

Flow observations used for the calibration model included 53 river reaches, springs, and non-perennial streamflows (fig. 18). Flows were measured along reaches in the Flint River and other smaller tributary streams in the lower ACFB. In the Chipola River, no flows for the specified time period were available for Jackson Blue Spring, Baltzell Springs Group, Sandbag Spring, Cowarts Creek, and Marshall Creek, so an average flow and stage were used for reference. Four additional gaging stations along reaches were added from the Chipola River Basin to calibrate the regional-scale model in that basin. Groundwater levels (treated as local aquifer head observations in the model calibration procedure) from 328 wells open to the Upper Floridan aquifer in the Dougherty Plain and Marianna Lowlands also were used to calibrate the model (fig. 18). The range in the observed water levels is 232 ft. The water-level residual calibration criteria ideally is achieved when the average residual is close to 0.0 ft (less than 1 ft), the weighted sum of squared errors of the residual is less than 10 ft (about twice the accuracy), and the weighted sum of square errors of the residual divided by the range is less than 0.1.

When flow and water-level observations are used in parameter estimation, weighting is required in order to have similar ranges in values and dimensionless units in the least-squares minimization objective function (Hill and Tiedeman, 2007). Often the inverse of the variance of the observations is used because this results in dimensionless units and incorporates some statistics related to observation error or accuracy. Sometimes weights can be used to emphasize or de-emphasize observations. Observations that are more accurate, for example water levels from wells that are surveyed with spirit leveling, could have been given a relatively greater weight than those that are not surveyed with spirit levels; however, a weighting factor of 1.00 ft^{-2} was used for all water-level measurements (water-level observations calibrated in the model).

Weighting of flow observations is more complex because the range in flow is quite large and the accuracy is based on a percentage of the observed flow. The inverse of flow observation squared multiplied by a factor of 0.1 was used to weight all flow observations. This computation results in weights decreasing as observed flow increases and may result in weighted residuals having similar magnitudes. This method represents a coefficient of variation approach and is appropriate for accuracies based on percentage error. The multiplication factor of 0.1 results in a coefficient of variation of 0.31 (to match the assumption that the observed gains or losses are accurate within 30 percent).

Strategy for Calculating Hydraulic Properties and Other Estimated Parameters

The current modeling effort is designed to investigate the transport of nutrients in the aquifer, whereas previously published models were developed to investigate groundwater/surface-water interactions for the study area. The major change in this model compared to models by Torak and other (1996) and Jones and Torak (2006) is the incorporation of karst features to simulate advective transport with particle tracking. A fully three-dimensional model was needed for the simulation. Lindsey and others (2010) determined that carbonate aquifers with high sinkhole density (greater than 25 sinkholes per square kilometer) generally had higher concentrations of nitrate in groundwater than areas with low sinkhole density (less than 1 sinkhole per square kilometer). To incorporate karst features, vertical and horizontal hydraulic conductivities for the Upper Floridan aquifer were multiplied by an array that increases with the presence and density of sinkholes. Sinkhole area and density per grid cell were determined using data from the NED. For much of the study area, digital versions of the original 1:24,000-scale topographic maps were the best available sources of information. The resolution of the NED in the study area is 5 meters. Geographic information system (GIS) tools were used with the NED to identify areas where topographic data form closed contours or closed-basin depressions likely to be sinkholes. These depressions or sinkholes commonly occur in

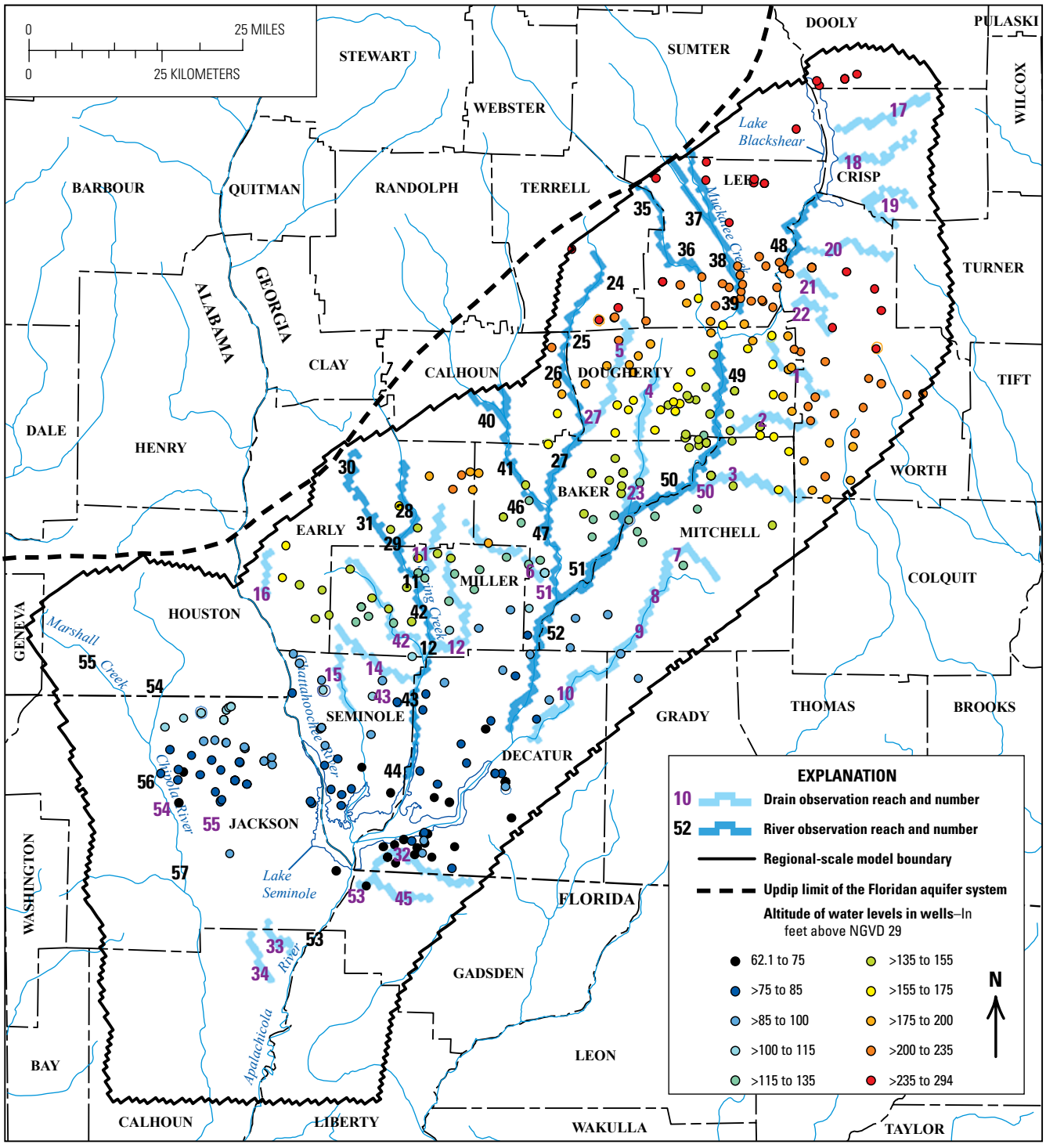

Base from U.S. Geological Survey digital data,1:24,000
Albers Equal-Area Conic Projection

Figure 18. Measured water levels in wells, September 1999 through October 2000, and locations of river and drain observation reaches and reach numbers.

karst terrain where internal drainage is the primary mechanism of recharge to aquifers.

A sinkhole multiplier array was created to incorporate karst features into the groundwater-flow model. The array initially was created by scaling the product of the number of closed-basin depressions multiplied by the total contributing area of all closed-basin depressions per grid cell. The total drainage area of closed-basin depressions was limited to less than or equal to the total area of a model-grid cell. The resultant multiplier array was biased in both the number and locations of closed-basin depressions. The initial sinkhole multiplier array showed a strong bias along the boundaries of each

1:24,000-scale topographic map and among different maps (created by different cartographers and at different times). An edge effect was created where the contour lines spanning more than one topographic map do not match up exactly; the differences caused the sinkhole identification routines to overestimate the number of closed-basin depressions along map edges (U.S. Geological Survey, 2009). The edge effect among adjacent maps created substantial differences in the multipliers along the boundaries of adjacent maps, thereby negatively affecting model calibration. Also, the closed-basin depressions in relatively flat areas were underestimated. Different methods of developing the 1:24,000-scale topographic maps emerged as technology improved. As a result, inconsistent values were produced for mapped adjacent areas (noticeably greater or smaller sinkhole density than adjacent maps).

To compensate for the problems, individual map areas were normalized to correct the multiplier array. Separate additional multipliers were developed for individual topographic map extents using a trial-and-error approach until the array was relatively similar and random throughout the study area (fig. 19). The scaled sinkhole multiplier array then was used to increase hydraulic conductivities in layers representing the Upper Floridan aquifer. Final values of the sinkhole multiplier array range from 1.0 (the minimum—where there are no sinkholes or the overburden is greater than or equal to 100 ft) to 19.9.

Local-Scale Models

Two local-scale groundwater-flow models were nested within the boundaries of the regional-scale model (fig. 13) and used to predict nitrate concentration over time in selected wells and springs under three different nitrogen management scenarios. Model geometry, discretization, boundary conditions, stresses, and parameters were taken from the regional-scale simulation of long-term average (1995–2005) steady-state conditions. The local-scale models included the areas contributing recharge to the selected wells and springs and are a refinement of the regional-scale model grid. Spatial refinement is necessary to improve estimates of travel time from the recharge area to selected springs or wells with particle tracking (Pollock, 1994).

The Chipola Local-Scale Model (CLSM) active model area covers 1,653 mi^2 in the upper Chipola River Basin in the unconfined and semiconfined areas of the Upper Floridan aquifer (fig. 10), and includes the area contributing recharge to the three selected springs—Jackson Blue Spring, Baltzell Springs Group, and Sandbag Spring (fig. 10). The CLSM model grid has 11 layers, 198 rows, and 255 columns. The Middle Flint Local-Scale Model (MFLSM) active model area covers 1,383 mi^2 in the central-northern Flint River Basin in the study area (fig. 13), and includes the area contributing recharge for the NAWQA long-term monitor wells (CP-18A, RF-41, and CP-21A) selected for detailed study (fig. 10). The MFLSM model grid has 11 layers, 252 rows, and 171 columns.

Local-Scale Model Geometry and Discretization

Local-scale model grids were created by dividing the regional-scale model-grid cells in layers 1–3 by 3 in vertical and horizontal (XYZ) directions. Layer 4 of the regional-scale model was divided by 2 in the vertical direction and by 3 in each of the x and y directions. The resultant local-scale model grids have 11 layers; layers 1–3 correspond to layer 1 of the regional-scale model, and layers 4–11 correspond to layers 2–4 of the regional-scale model. Regional-scale model layers 2 and 3 form local-scale model layers 4–9. Regional-scale model layer 4, divided into two layers in the vertical, forms local-scale model layers 10 and 11.

Boundary Conditions and Model Stresses

Both local-scale models use constant-head boundary conditions on the northwestern boundaries and specified flux on all other boundaries with the exception of the western boundary of the CLSM, which is a no-flow boundary. Specified flows were obtained from the steady-state long-term (1995–2005) average regional-scale simulation and distributed on the corresponding eastern, western, and southern boundaries. Specified flows represent average steady-state flow that passes through a regional-scale model-grid cell coincidentally located along the boundary of a local-scale model-grid cell. Flow boundaries were obtained for each grid cell of the shared local-regional-scale grid-cell boundary. The flow represents the water that passes in or out of the cell on the outer vertical boundary face. Total flows from the regional-scale shared cell face are divided by a factor of 9 for each local-scale grid cell except in regional-scale model layer 4 (local-scale model layers 10 and 11). In layer 4, flows are divided by 6 because there are only two layers in the vertical direction. Flows were distributed evenly within each shared local-regional-scale grid cell.

Porosity, the only new parameter in the local-scale models, is needed for particle tracking. The groundwater-flow model calculates the Darcy flux and Darcy velocity. To calculate the pore velocity, the Darcy velocity is divided by the porosity in the particle-tracking program (Pollock, 1994). The pore velocity is used to calculate the time for water particles to travel through the aquifer from the water table below an area contributing recharge to the final discharge or observation point (a spring or well). Effective porosity values are based on published values for the Upper Floridan aquifer, sand, and clays (Knochenmus and Robinson, 1996; Langevin, 1998); however, effective porosity values were distributed using the sinkhole multiplier array for layers representing the Upper Floridan aquifer. The effective porosity was set at 0.01 (faster velocities in karst areas) in grid cells that had a relatively high sinkhole multiplier (greater than 18); grid cells that had lower values for the sinkhole multiplier array (less than or equal to 18) had porosities that were set at 0.15—a common value for porous block limestones (Langevin, 1998). Porosities for layer 1 were distributed using zones of residuum and sand overburden from Torak and others (1996) and Jones and Torak (2006).

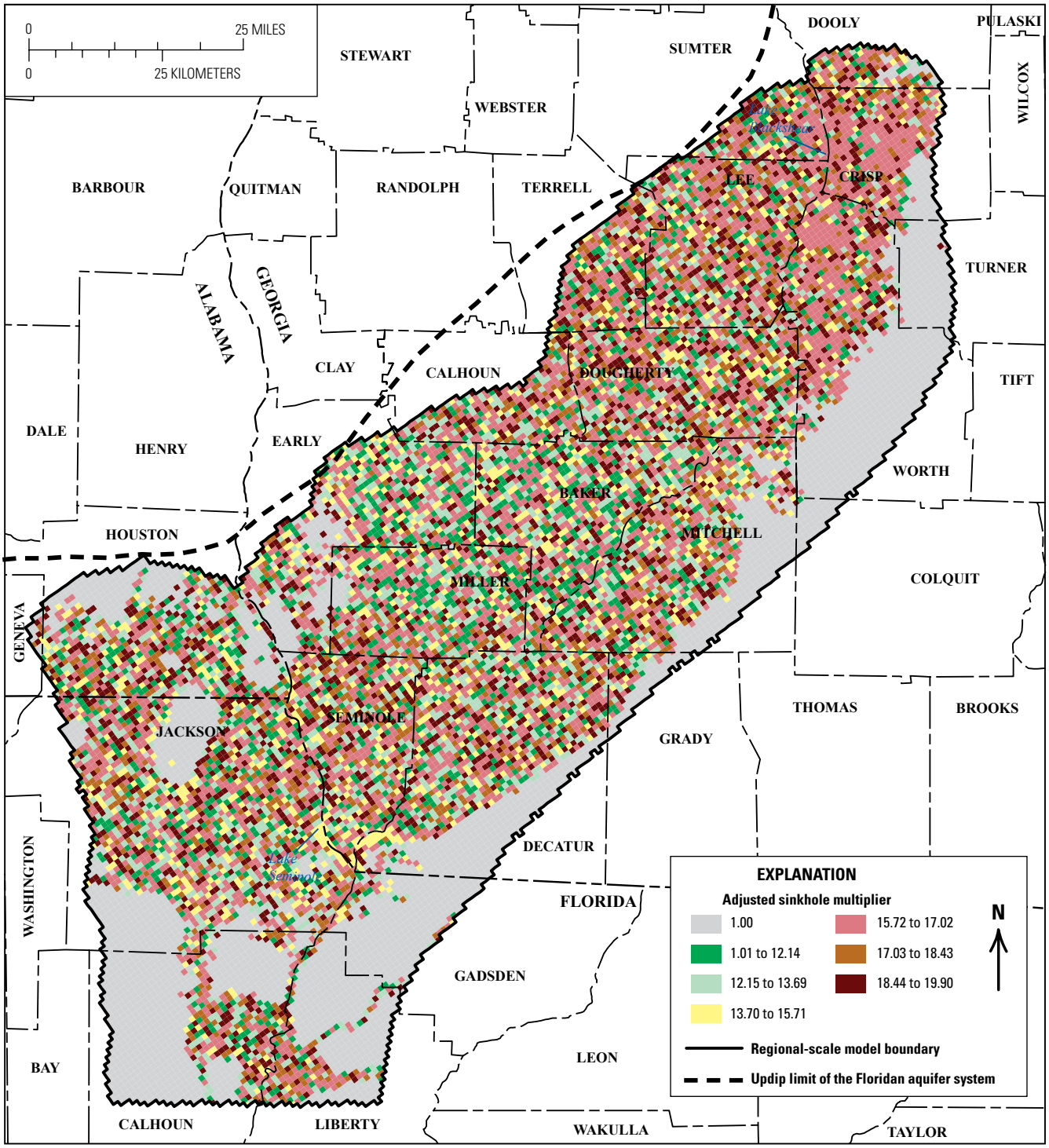

Base from U.S. Geological Survey digital data,1:24,000
Albers Equal-Area Conic Projection

Figure 19. Spatial distribution of adjusted sinkhole multipliers.

Porosities in grid cells identified as residuum in layer 1 were set at 0.30 (a typical porosity for clay); porosities at grid cells identified as sand were set at 0.10 (a typical porosity for sand). Average particle travel times (used in this report as surrogates for age) were compared to the measured apparent average age derived from multiple age tracers (CFC, SF_6, and $^3H/^3He_{trit}$) to validate porosity values.

Simulation of Particle Tracking

Particle tracking was used to identify flow paths, ACR, advective travel times, and zones of contribution for the selected receptor wells and springs, and to estimate temporal nitrate concentrations in the selected wells under three management scenarios. The management scenarios were:

(1) nitrate input to groundwater remained constant at 2001 levels from 2002 to 2050, (2) nitrate input to groundwater decreased at a rate of 4 percent per year from 2002 to 2050, and (3) nitrate input to groundwater ceased altogether after 2001.

The ACR was defined as the areal expression at land surface that contributes recharge water to a specific receptor (a well or spring) that intersects the water table, assuming that water particles travel mostly vertically downward through the unsaturated zone from land surface to the water table (Focazio and others, 2002). The travel times simulated by this method represent the range and distribution in travel times for particles reaching a receptor or discharge point. A conservative water-quality constituent, such as nitrate in an oxygenated environment, can travel coincidently with water particles. Particle tracking does not consider the effects of dispersion, diffusion, adsorption, retardation, degradation, or other processes that can affect concentrations of water-quality constituents. The simulated distribution of travel times at a well or spring is computed by tracing water particles either backward from the monitor well or spring to an area contributing recharge or forward from the area contributing recharge to a selected receptor well or spring (Pollock, 1994).

A backward particle-tracking simulation was performed for each well and spring; simulations were used to track particles from selected wells or springs toward the corresponding area contributing recharge to calculate the average age of water for each selected well or spring. Forward particle-tracking—simulations that track particles from the water table to the receptor—was performed to identify potential additional ACRs to each spring. For the backward simulations, 999 particles were evenly distributed over each cell face in the layers containing the open interval of the well or spring. For the forward simulations, one particle was placed on the top face over the entire active local-scale grid. Particles moving to the three selected receptor springs were tracked and analyzed. A total of 1,015 particles were used to track particle travel times (as a surrogate for age) at Sandbag Spring. Approximately 2,133 and 16,845 particles were used for particle tracking from Baltzell Springs Group and Jackson Blue Spring, respectively.

Distribution of Nitrate in Groundwater and Estimated Nitrate Concentration at Selected Wells and Springs

Nitrate concentrations were measured in water samples from wells and springs in the study area. Three springs and six flow-path wells in the Chipola River Basin, and three long-term monitor wells in the Flint River Basin were sampled to identify water-quality and geochemical conditions and determine the age of water. A regional-scale groundwater-flow model was developed and calibrated against measured groundwater levels and flows. Two local-scale groundwater-flow models were developed and used to generate particle-tracking models that delineate areas contributing recharge and particle travel times for selected wells and springs. Additionally, future nitrate concentrations were predicted with model simulations under three different nitrate management scenarios.

Occurrence and Distribution of Nitrate from Water-Quality Sampling

Nitrate concentrations in water samples collected during 1993-2007 from the selected wells and springs in the study area were elevated above background concentrations (less than 0.10 mg/L). Nitrate concentrations were measured in groundwater samples from each of three selected long-term monitor wells from 1993 to 2007 (fig. 10; tables 1 and 2). Among the three wells, measured nitrate concentrations were highest in well CP-18A and ranged from 4.70 to 12.73 mg/L. Nitrate concentrations in well CP-21A ranged from 3.40 to 6.10 mg/L, and nitrate concentrations in well RF-41, a background well, ranged from 0.86 to 1.04 mg/L (table 1).

Nitrate concentrations were analyzed in water samples from three selected springs—Jackson Blue Spring, Baltzell Springs Group, and Sandbag Spring—between 2001 and 2007 (table 2). Samples also were collected from two adjacent wells along approximate flow paths to each of these springs (table 2; fig. 20). Nitrate concentrations were highest in the Baltzell Springs Group and its two adjacent flow-path wells; the average concentration was 3.74 mg/L in the spring and about 6.4 mg/L in both wells). Jackson Blue Spring had the second highest nitrate concentration (3.24 mg/L in the spring, and 3.27 and 3.81 mg/L in the two upgradient flow-path wells). Sandbag Spring had the lowest nitrate concentrations (0.49 mg/L in the spring, and 0.37 and 0.99 mg/L in flow-path wells).

Measured Age-Tracer Concentrations and Age of Recharge Water

Measured age-tracer concentrations ($^3H/^3He$, CFC, and SF_6) were used to assess the age of recharge water and particle travel times in the aquifer. Lumped parameter models were used in this study to evaluate mixing of different age waters and to estimate the mean transit time of groundwater. These multiple models treat the aquifer system as a homogeneous compartment in which tracer input concentrations are converted to tracer output concentrations according to the system response function used and how the flow system is described (Zuber, 1986; Maloszewski and Zuber, 1996; Ozyurt and Bayari, 2003). The lumped parameter models assume a steady-state flow system and assume that the selected tracers behave like a water molecule. This assumption typically is valid for ^3H, which is part of the water molecule, but the gas tracers (CFC and SF_6) can show substantial variation due to sorption and other biogeochemical processes (Cook and others, 1995; Plummer and Busenberg, 1999). The lumped parameter

Table 1. Measured dissolved oxygen, dissolved organic carbon, iron, and nitrate in groundwater samples from selected wells, 1993–2007 and calculated nitrate concentrations during measured year.

[mg/L, milligrams per liter; *, sum of flow-weighted concentrations in particles for year; <, less than; --, not measured; E, estimated]

Sample date	Dissolved oxygen, in mg/L	Dissolved organic carbon, in mg/L	Iron, in mg/L	Nitrate as nitrogen, in mg/L	Simulated year	Simulated* nitrate concentration, in mg/L
Well CP-18A; Station ID 310552084435601; Well depth 68.8 feet						
8/25/1993	6.8	0.1	<0.1	4.70	1993	7.84
4/5/1994	7.6	0.2	<0.1	5.20	1994	8.02
9/15/1999	7.32	--	--	6.98	1999	9.99
4/11/2002	7.1	E0.3	0.09	7.97	2002	10.55
10/26/2004	7.1	--	<0.1	11.10	2004	11.64
1/26/2005	7.88	--	<0.1	10.05		
4/19/2005	7.55	--	0.059	11.45	2005	11.06
7/21/2005	6.6	--	0.1	11.67		
8/15/2007	7.42	--	<6.0	12.73	2007	12.73
Well CP-21A; Station ID 312119084215601; Well depth 48.8 feet						
8/31/1993	6.6	0.3	<0.1	6.00	1993	3.71
4/4/1994	5.5	0.2	0.1	3.40	1994	3.82
6/26/2001	6.4	--	--	4.12	2001	4.83
4/8/2002	5.7	0.2	<0.1	4.37	2002	4.90
12/21/2004	7.2	--	<0.1	4.97	2004	4.95
1/26/2005	6.54	--	<0.1	4.69		
4/19/2005	6.6	--	<0.1	5.88	2005	5.14
7/21/2005	6.09	--	<0.1	6.10		
8/16/2007	5.35	--	<6.0	4.78	2007	5.63
Well RF-41; Station ID 311327084484101; Well depth 69 feet						
8/26/1993	5.4	--	<0.1	0.86	1993	0.54
4/5/1994	6.5	0.1	<0.1	1.00	1994	0.56
9/14/1999	4.8	--	--	1.02	1999	0.74
10/31/2000	5.1	--	--	1.01	2000	0.73
3/21/2002	4.6	E0.2	<0.1	0.98	2002	0.73
1/25/2005	5.01	--	<0.1	1.00		
4/18/2005	5.03	--	0.1	1.04	2005	0.88
7/28/2005	4.37	--	0.1	1.03		
8/15/2007	4.48	--	<6.0	1.04	2007	0.95

models are consistent with different configurations of groundwater flow from a recharge area in the aquifer to a discharge location (well or spring) in the aquifer. The lumped parameter models assume recharge occurs across the unconfined Upper Floridan aquifer in the study area.

Several lumped parameter models are appropriate for estimating the age of recharge water and travel times for the groundwater-flow system in the study area. These lumped parameter models include a piston-flow model, exponential mixing model, exponential piston-flow model, and binary mixing model . The lumped parameter models account for groundwater flow from a recharge area to a point of discharge (well or spring) and are represented mathematically as exit age (transit time) distribution functions (Maloszewski and Zuber, 1996). Model-simulated tracer concentrations at a well or spring are calculated from the tracer input history in the recharge area (fig. 12), the exit age distribution function, and the decay function that applies for tritium.

Table 2. Well depth and measured concentrations of dissolved oxygen, organic carbon, dissolved iron, nitrate, delta $^{15}N/^{14}N$, and calculated nitrate concentrations in three springs and upgradient wells, 2007.

[mg/L, milligrams per liter; *, sum of flow-weighted concentrations in particles for the year; <, less than]

	Station name (alternative name)	Well depth, in feet	Dissolved oxygen, in mg/L	Dissolved organic carbon, in mg/L	Dissolved iron, in mg/L	Nitrate as nitrogen, in mg/L	Delta $^{15}N/^{14}N$, in per mil	Simulated year	*Simulated nitrate, in mg/L
Baltzell Springs Group and flow-path wells									
305725085094102	Malone No. 2	115	6.6	<0.3	<6	6.43	3.46		
305219085144901	JAPST001 (McArthur)	37	8.5	0.6	<6	6.39	3.85		
304948085140501	Baltzell Springs Group		9.5	<0.2	<6	3.74	3.13	2007	3.75
Sandbag Spring and flow-path wells									
304746085223201	Cottondale No. 3	128	3	0.6	30	0.99	7.36		
304707085153301	Hutton	70	8	0.4	<6	0.37	7.62		
304718085132000	Sandbag Spring		5.4	<0.3	<6	0.49	7.01	2007	0.48
Jackson Blue Spring and flow-path wells									
305137085060301	HWY 69 VISA (NWFWMD 80)	65	8.5	<0.4	<6	3.81	2		
305025085082101	Baxter VISA (NWFWMD 85)	85	7	<0.3	<6	3.27	2.23		
02358795	Jackson Blue Spring		10	<0.3	<6	3.24	2.31	2007	3.41

The piston-flow model assumes that after a tracer is isolated from the atmosphere (at the time of groundwater recharge), it becomes incorporated in a parcel of water that moves from the recharge area with the mean velocity of groundwater. The mean groundwater velocity is represented with the steady-state groundwater velocity from the local models. All flow lines to the sampled well or spring are assumed to have similar velocities and hydrodynamic dispersion, and molecular diffusion of the tracer is assumed to be negligible.

The exponential mixing model represents an unconfined aquifer system where there is vertical stratification of groundwater age, which increases logarithmically from zero at the water table (assuming short travel times through the unsaturated zone) to ages that approach infinity at great depths in the aquifer. Mixing occurs in the well bore during pumping or in conduits feeding the spring. Spring flow is composed of recharge waters with a large range in ages; however, the contributions to spring discharge decrease exponentially from the most recent recharge (young water) to that which has occurred in the distant past (older water). Groundwater moves slowly through small openings in the carbonate matrix, fractures or fissures, and much more rapidly through large conduits or caverns.

The exponential piston-flow model represents an aquifer system that contains two components of flow in series, a component of exponential flow followed by a segment of piston flow. The exponential piston-flow model is also applicable for piston-flow transport through the unsaturated zone followed by exponential mixing in springs or wells in the aquifer. The exponential piston-flow model has an additional parameter—the ratio of the exponential flow to piston flow. Exponential piston-flow model ratios greater than 1 produce

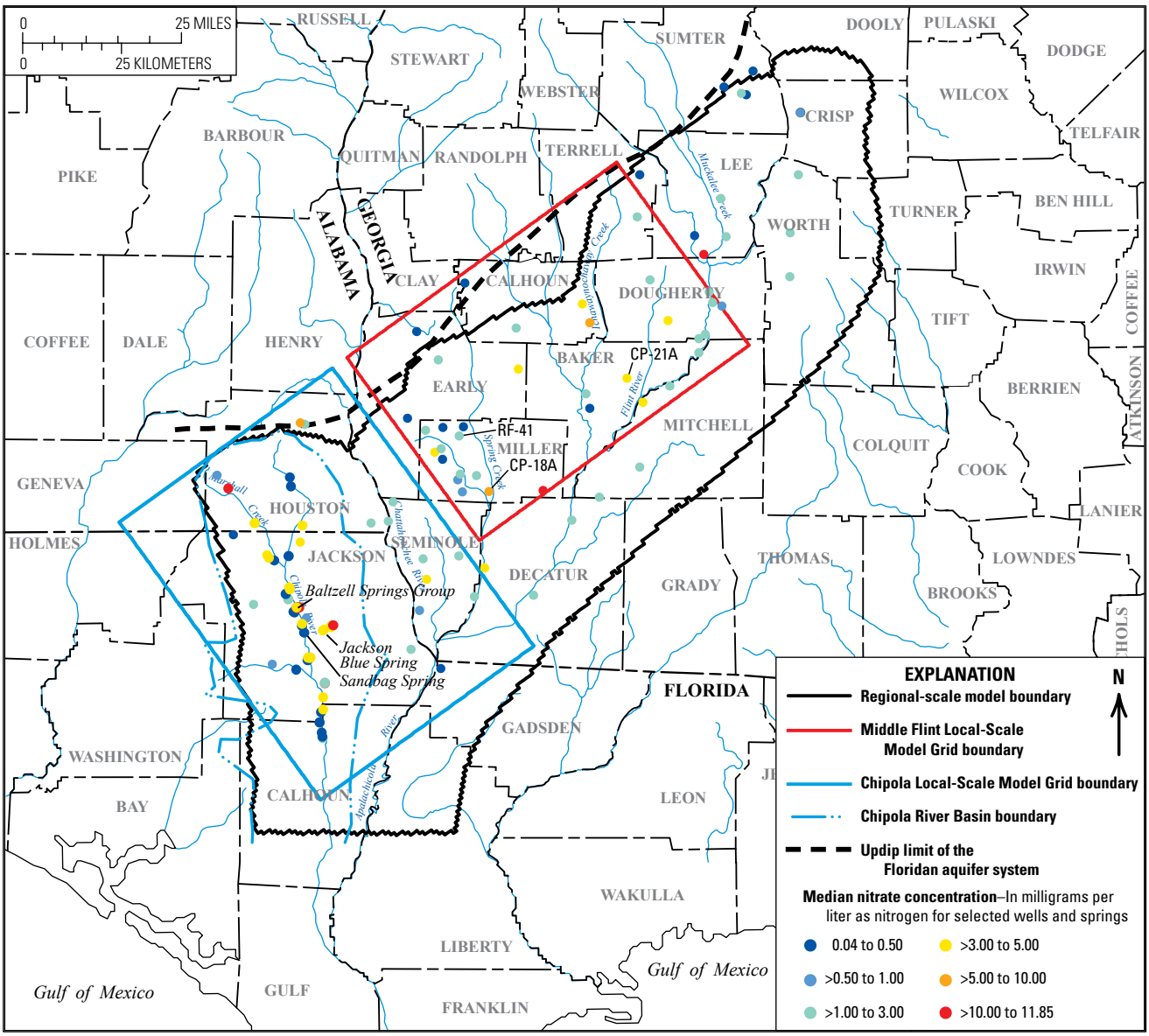

Base from U.S. Geological Survey digital data,1:24,000
Albers Equal-Area Conic Projection

Figure 20. Median nitrate concentrations in springs and streams in the study area.

more piston-flow model behavior, whereas ratios less than 0.1 produce more exponential mixing model behavior. The exponential piston-flow model ratio used in this study was 0.5.

The binary mixing model is used to evaluate mixing scenarios involving groundwater with two age components: (1) relatively young water (recharged within the past 5–10 years) from the shallow (or a highly transmissive) part of the flow system, and (2) older aquifer matrix water (decades or older) presumably from the deeper parts of the aquifer (Katz and others, 2001). Both end members of a binary mixture can be of any age, but the calculation is greatly simplified if it is assumed that one end-member water is "young" (recharged after 1995 when CFC concentrations in the atmosphere have been relatively constant) and the other end-member water is "old" (recharged before 1940 with undetectable CFC or SF_6 concentrations). The output from the binary mixing model for the tracers used in this study produced a straight line that originates from the output concentration of the old end-member water and ends at the concentration of the young end-member water.

The total mean age of a water sample is defined as the mean age or travel time in the saturated zone plus the travel time through the unsaturated zone. Travel time of recharge water through the unsaturated zone to the Upper Floridan aquifer is assumed to be less than 1 year, so the total mean age is approximately equal to the mean age of the saturated zone travel times. The total mean age for the binary mixing model is obtained by the following expression:

$$\text{Total mean age} = f_{young} * \text{age}_{\text{young water}} + (1 - f_{young}) * \text{age}_{\text{old water}} + UZ$$

where

f_{young} is the fraction of young water in the mixture, and UZ denotes the travel time through the unsaturated zone.

Measured tracer concentrations are plotted relative to each other and the output curves for the different models. Groundwater ages estimated using multiple tracers are more effective in reducing the uncertainty that arises from the use of a single tracer. Lack of agreement between the apparent ages of groundwater based on individual tracers can occur if complex mixtures of groundwater are contributed from different parts of the Upper Floridan aquifer where contamination is unlikely from non-atmospheric sources of CFC or SF_6. The CFC and SF_6 data were used to estimate groundwater age in this study where contamination from non-atmospheric sources was considered unlikely in an attempt to assess and quantify various groundwater mixing scenarios from the evaluation of multiple tracer data. Non-atmospheric sources for CFC include improper disposal of refrigerants, and for SF_6 include the intentional introduction into the aquifer as a tracer of groundwater flow and (or) natural sources in the subsurface. A comparison of the apparent ages of groundwater based on SF_6 and CFC concentrations in all samples (fig. 21) indicates that the CFC apparent ages are slightly older than the SF_6 apparent ages.

The SF_6 concentration was plotted relative to CFC-12, CFC-113, and tritium (figs. 22–24) and compared to output curves for the lumped parameter models (Böhlke, 2006) that represent the groundwater-flow scenarios previously described. The four water samples with useable CFC-12 and SF_6 concentrations (Malone No. 2, Hwy 69 VISA, Baxter VISA, and JAPST001) plot near the output curves for all four models (fig. 22). For the SF_6 versus CFC-113 plot, four water samples (Jackson Blue Spring, Hwy 69 VISA, Malone No. 2, and Baxter VISA) cluster along the exponential mixing model output curve, but three other samples (Cottondale No. 3, JAPST001, and Sandbag Spring) plot closer to the piston-flow model output curve (fig. 23). Most tracer concentrations from groundwater and springs cluster along curves that represent exponential mixtures of waters for the tritium versus SF_6 plot (fig. 24). However, generally older apparent CFC-12 ages than apparent CFC-113 ages could account for the clustering of points near the piston-flow model and exponential piston-flow model curves for the same four sites (Malone No. 2, Baxter VISA, Hwy 69 VISA, and JAPST001).

The piston-flow model yields an estimate of mixed-age waters. The average apparent age derived from the piston-flow model varies depending on the amount of water in the mixture from end-member components. Tracer concentrations (CFC-11, CFC-12, CFC-113, and SF_6) in water samples did not yield concordant ages based on atmospheric equilibration data (table 3). The average apparent ages based on CFC concentrations were older than those based on SF_6 concentrations (table 3) with the exception of samples from Cottondale No. 3, Sandbag Spring, and JAPST001 (table 3). Older CFC-11 apparent ages (compared to CFC-12 or CFC-113 apparent ages) are attributed to microbial degradation in the aquifer system under reducing conditions (Plummer and Busenberg, 1999). Several sites (Jackson Blue Spring, Hutton, Sandbag Spring, Cottondale No. 3, Baltzell Springs Group, and Malone No. 2) have at least one CFC compound with a concentration higher than what is possible for equilibrium with modern air. These concentrations were not reported in table 3 and samples are considered to be contaminated. Local non-atmospheric sources of CFC (likely the causes of the CFC contamination) could result from improper disposal of refrigerants on the land surface, particularly near sinkholes.

The average date of likely recharge based on the piston-flow model analysis ranged from mid-1970s to early 1990s for selected wells and springs (table 3). The average apparent age of recharge water reaching wells RF-41, CP-18A, and CP-21A was 32, 23, and 29 years, respectively, indicating that recharge of the aquifer near these wells occurred in the mid-1970s to the mid-1980s (table 3). The average apparent age using SF_6 ranged from about 13 years at Malone No. 2 to about 30 years at Cottondale No. 3 (table 3). The average apparent age (16–21 years) for water sampled in 2007 at Jackson Blue Spring was consistent with the apparent age reported in a previous study (9–13 years; Katz, 2004).

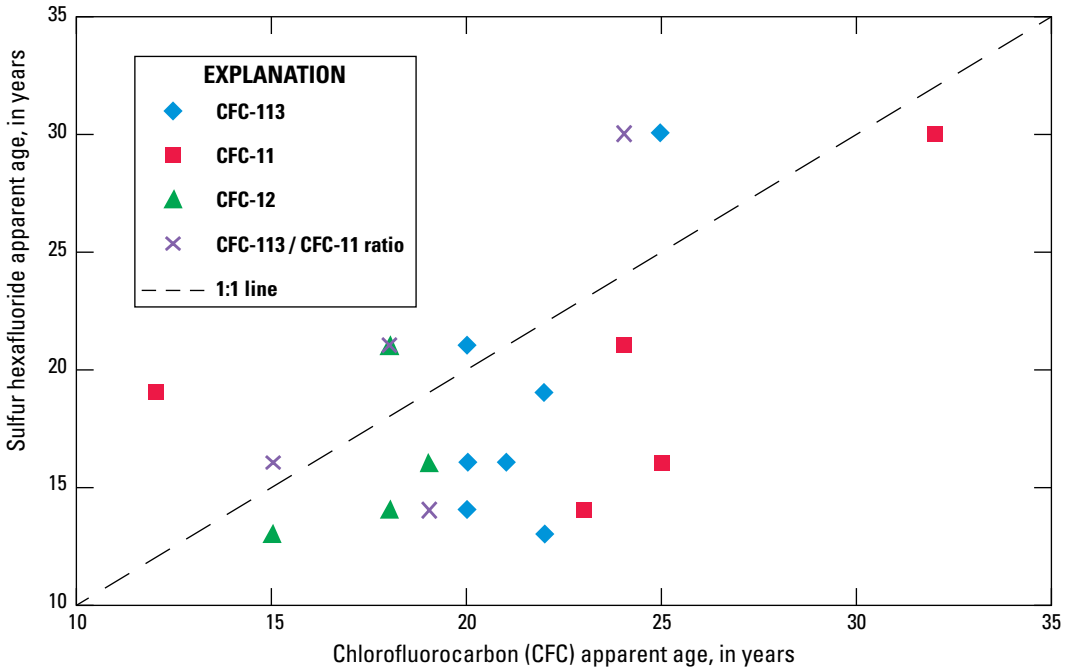

Figure 21. Comparison of apparent ages of groundwater based on measured concentrations of chlorofluorocarbons and sulfur hexafluoride in all samples.

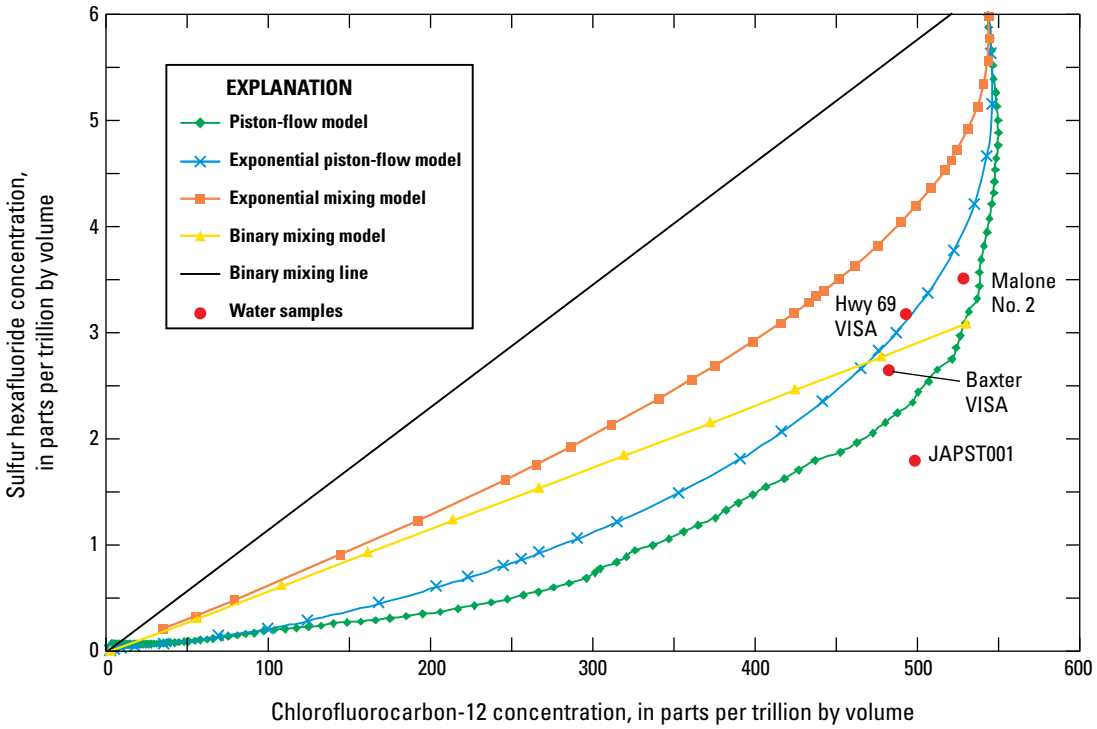

Figure 22. Measured concentrations of sulfur hexafluoride and chlorofluorocarbon-12 in groundwater from wells, and lumped-parameter modeled curves for groundwater-age distributions in the study area.

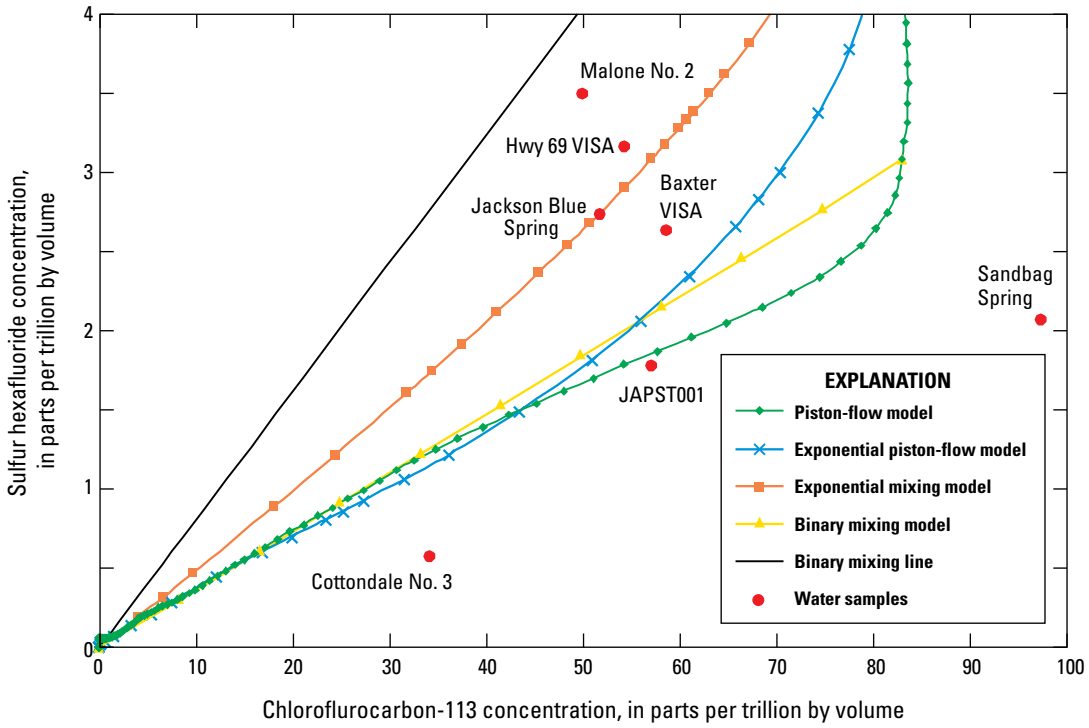

Figure 23. Measured concentrations of sulfur hexafluoride and chlorofluorocarbon-113 in groundwater from wells, and lumped-parameter modeled curves for groundwater-age distributions in the study area.

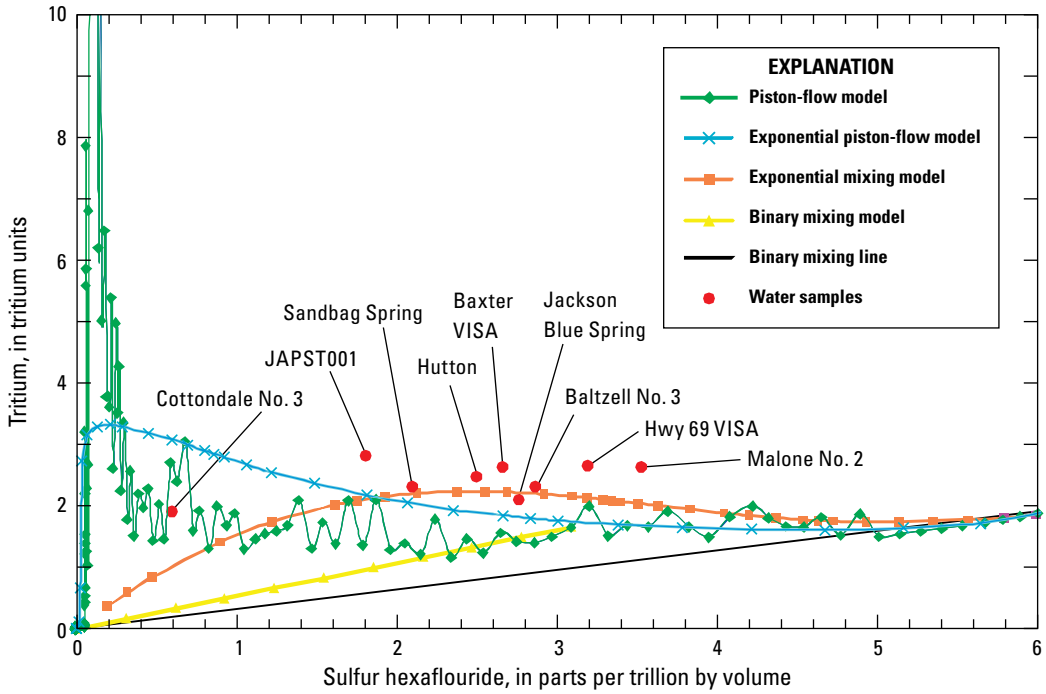

Figure 24. Measured concentrations of tritium and sulfur hexafluoride in groundwater from wells, and lumped-parameter model curves for groundwater-age distributions in the study area.

Table 3. Summary of average apparent ages of water derived from CFC-11, CFC-12, CFC-113, SF_6, and $^3H/^3He$ measurements, and the estimated date of recharge.

[CFC, chlorofluorocarbon; SF_6, sulfur hexafluoride; $^3H/^3He$, tritium/tritiogenic helium-3]

Station name (alternate name)	Date	CFC-11 age, in years	CFC-12 age, in years	CFC-113 age, in years	SF_6 age, in years	$^3H/^3He$ age, in years	Average age, in years	Estimated date of recharge
RF-41	8/15/2007		33	31		33	32	mid 1970s
CP-21A	8/16/2007		30	26		30	29	late 1970s; early 1980s
CP-18A	8/15/2007		25	20		25	23	early to mid 1980s
Malone No.2	8/15/2007		15	22	13		17	late 1980s; early 1990s
JAPST001 (McArthur)	8/15/2007	24	18	20	21		21	late 1980s
Baltzell Springs Group	8/15/2007				16		16	early 1990s
Cottondale No.3	8/15/2007	32		25	30		29	early 1980s
Hutton	8/15/2007				17		17	early 1990s
Sandbag Spring	8/15/2007	12		22	19		18	late 1980s
Highway 69 VISA (NWFW-MD-80)	8/15/2007	23	18	20	14		20	late 1980s
Baxter VISA (NWFW-MD-85)	8/15/2007	25	19	20	16		19	late 1980s
Jackson Blue Spring	8/15/2007			21	16		19	late 1980s early 1990s

CFC ratios generally were less useful for determination of apparent ages given the relatively high incidence of CFC-12 contamination (table 3). However, the CFC-113/CFC-11 ratio was useful in estimating average apparent ages for four sites: Cottondale No. 3, Baxter VISA, Hwy 69 VISA, and JAPST001. The average apparent ages generally agreed relatively well with those based on SF_6 concentrations, with the exceptions of water samples from wells Hwy 69 VISA and Baxter VISA where the SF_6 average apparent ages underestimated the CFC-113 ages by 6 and 4 years, respectively. The SF_6 average apparent ages also underestimated the CFC-11 ages at these two wells by 9 years. Unfortunately, no age determinations could be obtained using ^3H and its daughter decay product $^3He_{trit}$ at these sites due to sampling and laboratory problems. However, based on analyses of ^3H alone, the ^3H apparent age at Cottondale No. 3 is consistent with the SF_6 apparent age at that site. Otherwise, the lack of agreement between average apparent ages based on CFC and SF_6 indicate the likelihood of mixtures of waters from different parts of the aquifer.

Model Calibration, Simulated Water Budgets, and Limitations

The regional-scale model was calibrated with 328 observed groundwater level measurements, 68 observed streamflow measurements, and 2 lake measurements, representing conditions during September 19–October 18, 1999. The simulated potentiometric surface of the Upper Floridan aquifer (1980–2005) followed historic measured potentiometric surfaces of the Upper Floridan aquifer (fig. 25); simulated heads matched observed heads reasonably well (fig. 26). Head residuals (observed heads minus simulated heads) ranged from –36.20 to 46.77 ft (fig. 27) with an average residual of –0.14 ft and a median of –1.96 ft. The standard deviation was 13.49 ft. Fifty percent of head residuals were less than 5 ft and 63 percent were less than 10 ft (fig. 28). Simulated heads in the north-central part of the active modeled area are lower than observed heads (fig. 25). Actual (reported) precipitation was

comparatively low in the north-central part of the model area during the calibration period compared to the rest of the model area; therefore, simulated recharge may have been underestimated in this area (fig. 16).

Sixty-eight simulated stream and spring flows were compared to observed flows. The majority of observed streamflows matched simulated streamflows with little or no adjustment to conductances used in the original models; however, a few of the conductances were adjusted during calibration to better match the observed flow. Flow residuals (the difference between observed and simulated flows) were small (fig. 29). The average flow residual was –1.1 ft^3/s. More than 50 percent of simulated flows were within 10 percent of observed flows. The maximum flow residual was 36.5 ft^3/s for an observed flow of 363.4 ft^3/s, and the minimum flow residual was –61.3 ft^3/s for an observed flow of –44.4 ft^3/s (fig. 30). Simulated flow was less than observed flow 20 times, simulated flow exceeded observed flow 28 times, and simulated and observed flows were equal 20 times. The median flow residual was 0.0 ft^3/s. The total of all observed flows was 3,326.5 ft^3/s, and the total of all simulated flows was 3,254 ft^3/s, an error of less than 1 percent of total observed flows. Additionally, simulated lake flows were compared to estimated flows for Lakes Seminole and Blackshear. The estimated flow at Lake Blackshear was –105 ft^3/s (out of the aquifer into Lake Blackshear), and simulated flow was –112 ft^3/s. Estimated flow at Lake Seminole was 125 ft^3/s (from Lake Seminole into the aquifer), and simulated flow was 162.2 ft^3/s.

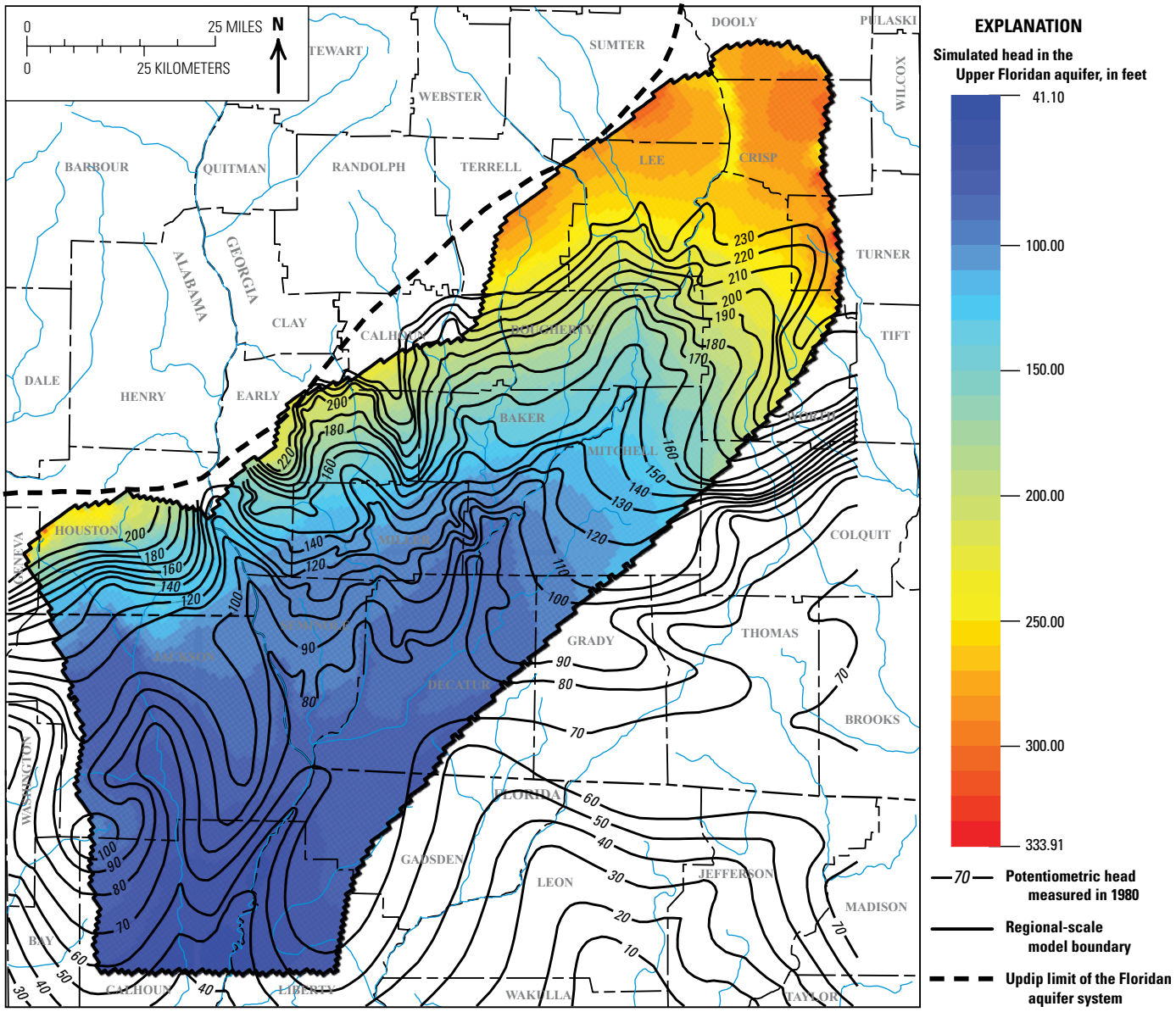

Base from U.S. Geological Survey digital data,1:24,000
Albers Equal-Area Conic Projection

Figure 25. Simulated heads in the Upper Floridan aquifer (October 1999) and potentiometric contours measured in1980.

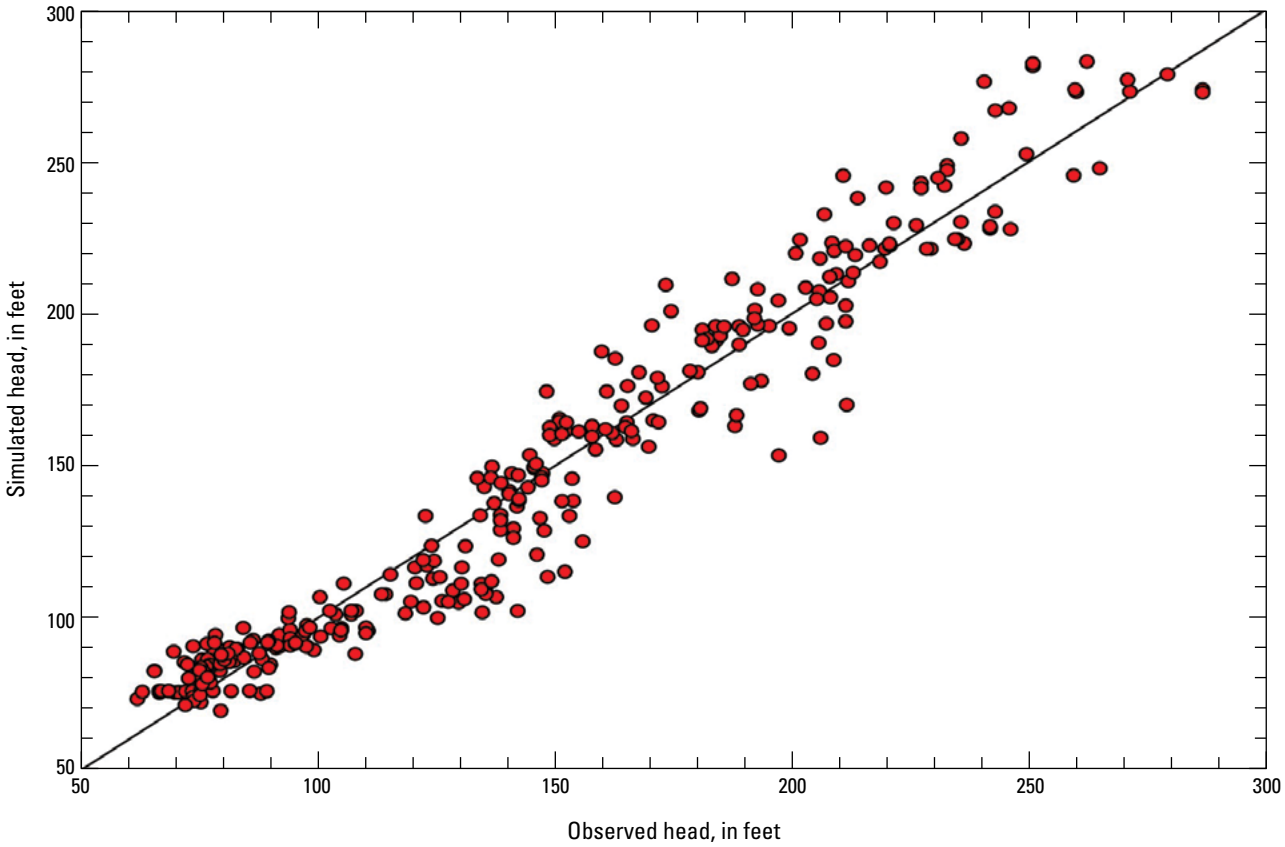

Figure 26. Comparison of observed heads and simulated heads in the regional-scale calibration model.

The final calibrated horizontal and vertical hydraulic conductivities for layers representing the Upper Floridan aquifer were the result of the published hydraulic conductivity values from Jones and Torak (2006) and Torak and others (1996) multiplied by the sinkhole multiplier array and then adjusted in parameter estimation by a scaling variable. The Upper Floridan aquifer is represented in model layers 2 to 4. Model layer 1 has three zones that represent residuum, sand, or the limestone of the Upper Floridan aquifer.

Final calibrated horizontal hydraulic conductivity for layer 1 in the regional-scale model was a constant 5.13 ft/d for model-grid cells zoned as residuum (67.1 percent of the active modeled area; fig. 31). For areas zoned as sand (25.7 percent of the active modeled area) hydraulic conductivity was 163.5 ft/d. Horizontal hydraulic conductivities vary from 28.5 to 45,000 ft/d in areas where layer 1 is zoned as the Upper Floridan aquifer (7.2 percent of the active modeled area—in riverbeds). Horizontal hydraulic conductivities for layer 1 were calibrated using parameter optimization, but the model was relatively insensitive to changes in layer 1 parameters (less than 5 percent of the composite scaled sensitivities).

The calibrated vertical hydraulic conductivity for layer 1 ranged from 0.003 to 40,470 ft/d (fig. 32), with a mean of 118.0 and a median of 7.714×10^{-2} ft/d. The vertical hydraulic conductivity for layer 1 was greatest in river channels and valleys where water has eroded sediments and the units composing the Upper Floridan aquifer are at land surface or exposed in the riverbed. The vertical hydraulic conductivity for layer 1 in model-grid cells categorized as the Upper Floridan aquifer ranged from 40.5 to 40,470 ft/d, and the mean was 1,295.7 ft/d. The vertical hydraulic conductivity for model-grid cells categorized as residuum ranged from 0.003 to 0.17 ft/d, and the mean was 0.05 ft/d. Vertical hydraulic conductivity for sandy materials ranged from 1.9 to 105.2 ft/d, and the mean was 96.6 ft/d.

The calibrated hydraulic horizontal conductivities for layers 2 through 4 of the regional-scale model ranged from 28.53 to 45,000 ft/d (fig. 33). The mean and median were 2,977.5 and 1,741.5 ft/d, respectively. The calibrated vertical hydraulic conductivity of layers 2 through 4 of the regional-scale model ranged from 40.47 to 40,470.0 ft/d (fig. 34); the mean and median vertical hydraulic conductivity were 617.8 and 593.7 ft/d, respectively.

The number and location of observations used in the model calibration affect parameter sensitivities and determine which parameters are sensitive enough to be estimated using optimization techniques (Poeter and others, 2005). The composite scaled sensitivities are calculated as part of the parameter estimation process. The most sensitive parameters are recharge and the horizontal conductivity of the Upper Floridan

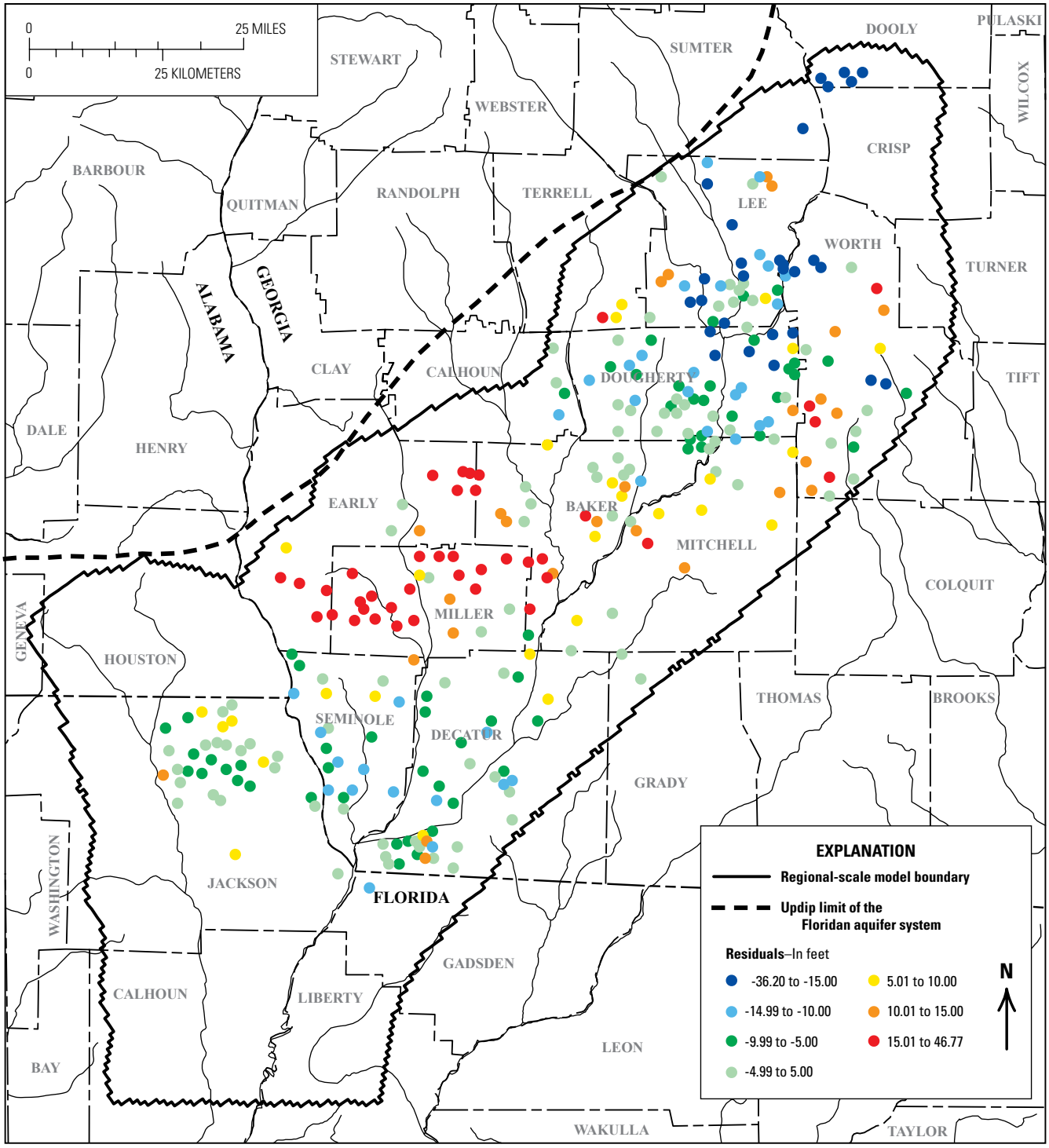

Base from U.S. Geological Survey digital data,1:24,000
Albers Equal-Area Conic Projection

Figure 27. Head residuals in the regional-scale calibration model.

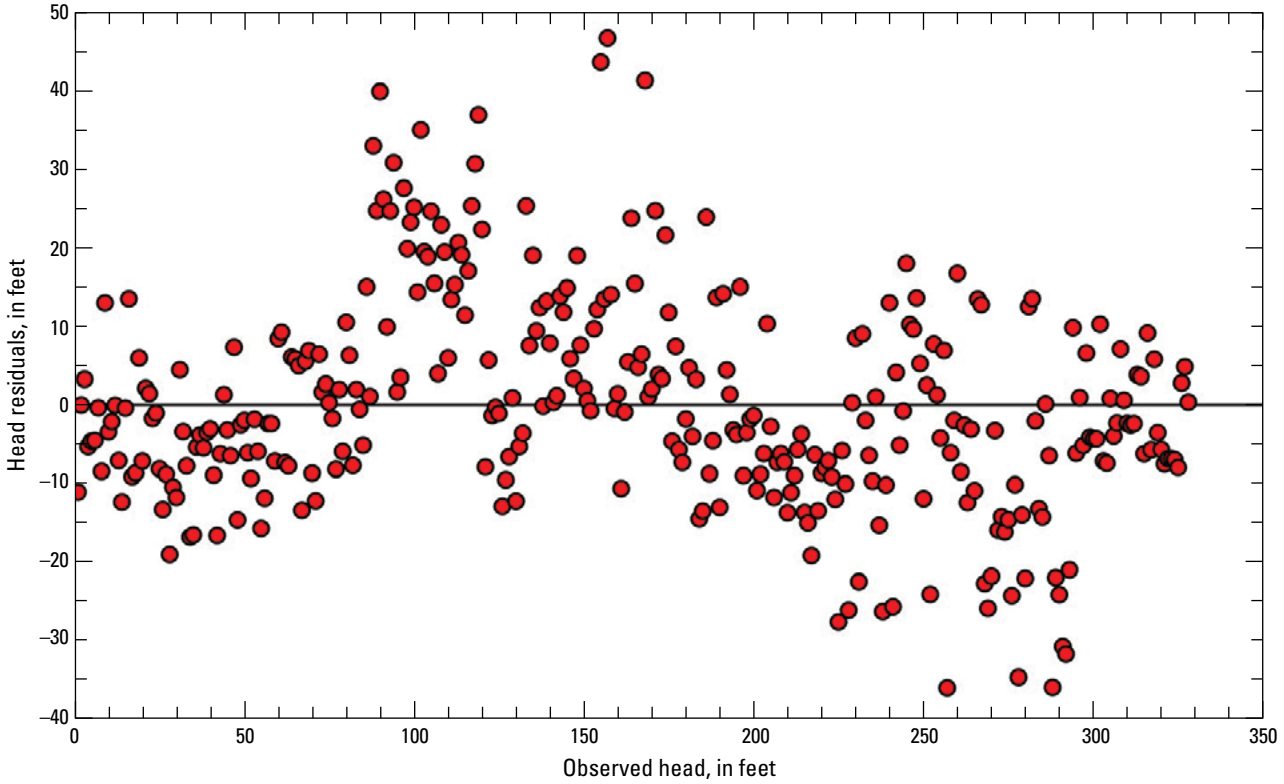

Figure 28. Comparison of observed heads and head residuals in the Upper Floridan aquifer in the regional-scale calibration model.

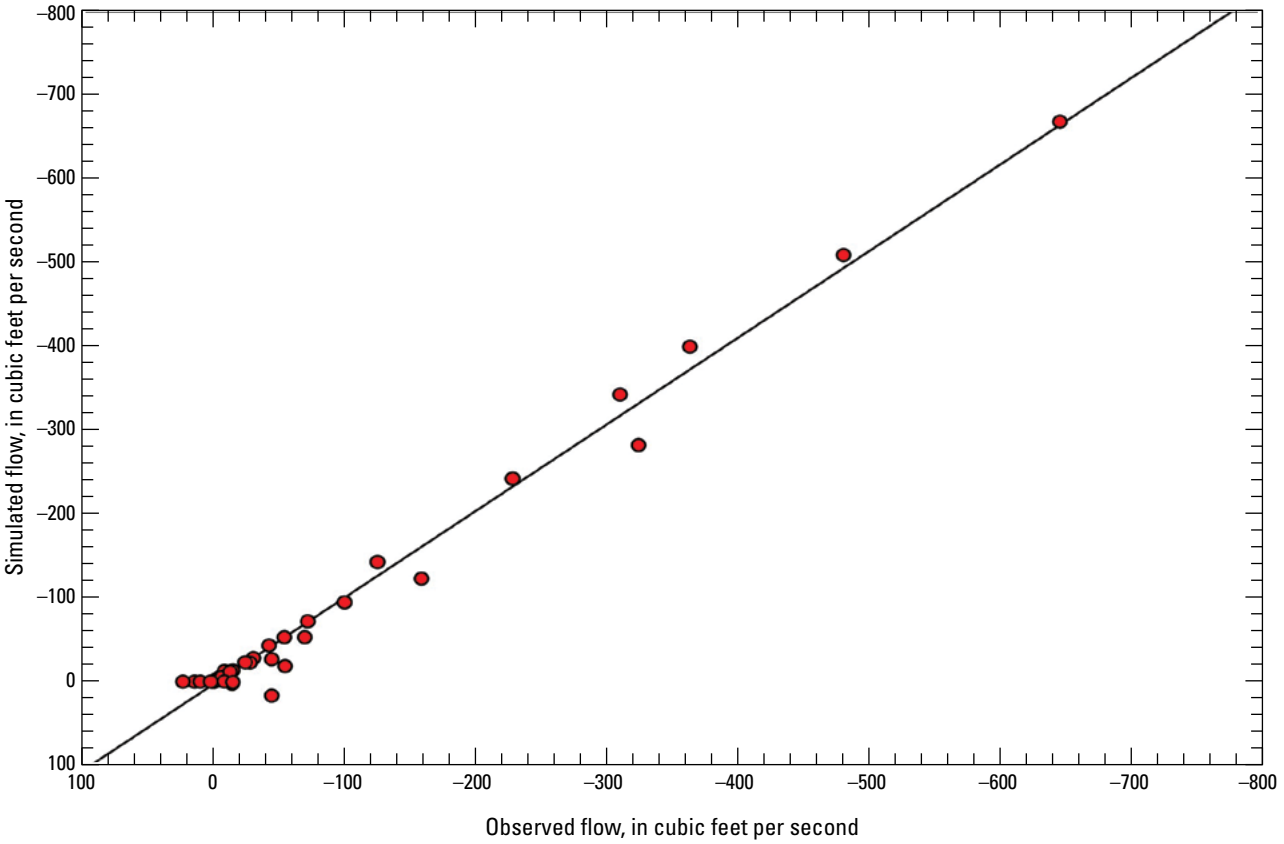

Figure 29. Observed flow and simulated flow (October 1999) in the regional-scale calibration model.

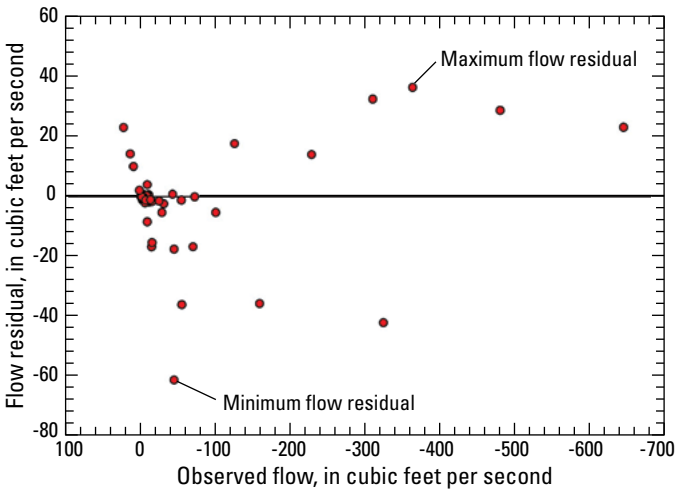

Figure 30. Observed flow and flow residual (October 1999) for the regional-scale calibration model.

aquifer (layers 2–4). Simulated heads and flows respond most to changes in these two parameters. Remaining parameters, including vertical hydraulic conductivity of the residuum, were less sensitive. The sensitivities of the vertical hydraulic conductivity of the Upper Floridan aquifer (layers 2–4) and the horizontal and vertical conductivity of the sand (layer 1) had the lowest composite scaled sensitivity.

Water Budgets from Regional-Scale Groundwater-Flow Simulations

The inflows and outflows in the volumetric water budget for the regional-scale steady-state groundwater calibration model for September–October 1999 were equal (total 5,973 ft^3/s or 3,860 Mgal/d) (table 4). Water levels, flows, recharge rates, potentiometric surface patterns, and water budget components were used in the calibration of the groundwater-flow model. Total inflows and outflows from the constant-head boundary were 991 ft^3/s (640 Mgal/d) and 803 ft^3/s (519 Mgal/d), respectively. Total inflows and total outflows from the head-dependent boundary were 1,457 ft^3/s (942 Mgal/d) and 1,209 ft^3/s (782 Mgal/d). Total discharge/leakage to rivers (perennial streams in this model) was 3,444 ft^3/s (2,226 Mgal/d). Leakage from river cells to the groundwater system was 230 ft^3/s (149 Mgal/d) and occurred mainly upstream from Lake Seminole (fig. 15). Total discharge to springs and non-perennial streams from drains was 290 ft^3/s (187 Mgal/d) (table 4; fig. 15). The total withdrawal from wells (irrigation and public-supply) was 228 ft^3/s (148 Mgal/d) (table 4).

The inflows and outflows in the volumetric water budget for the regional-scale long-term steady-state model also were equal (total 5,735 ft^3/s or 3,705 Mgal/d) (table 4). Total inflows and outflows from the constant-head boundary were 1,022 ft^3/s (660 Mgal/d) and 631 ft^3/s (408 Mgal/d), respectively. Total inflows and total outflows from the head-dependent boundary were 1,531 ft^3/s (990 Mgal/d) and 1,164 ft^3/s (752 Mgal/d), respectively. Total discharge to rivers (perennial streams in this model) was 3,254 ft^3/s (2,103 Mgal/d). Leakage from river cells to the groundwater system was 243 ft^3/s (157 Mgal/d). Total discharge to springs and non-perennial streams from drains was 222 ft^3/s (143 Mgal/d). The total withdrawal from irrigation and public-supply wells was 464 ft^3/s (300 Mgal/d) (table 4).

Chipola Local-Scale Model Water Budget

Total flow in the Chipola Local-Scale Model (CLSM) area was 2,523 ft^3/s (1,631 Mgal/d), and inflows equaled outflows (table 5). The majority of inflows were from recharge (34.3 percent) and from the head-dependent boundary (Lake Seminole, 45.5 percent). Outflow to rivers was overwhelmingly the largest component (80.1 percent) of the flows out of the model (2,022 ft^3/s, or 1,307 Mgal/d). Specified flows on the boundaries totaled 7.7 percent of the total inflows (194 ft^3/s or 125 Mgal/d) and 2.5 percent of the total outflows (64 ft^3/s or 41 Mgal/d) (fig. 35; table 5). Specified flow boundaries were used because the location of water divides in the area is uncertain. Constant heads provided 9.6 percent of the total budget as inflows (241 ft^3/s or 156 Mgal/d) and 6.5 percent

Table 4. Volumetric water budgets for the regional-scale steady-state calibration and long-term models.

[ft^3/s, cubic feet per second]

	Regional-scale steady-state calibration model		Regional-scale steady-state long-term model	
Volumetric water-budget components	Inflows, in ft^3/s	Outflows, in ft^3/s	Inflows, in ft^3/s	Outflows, in ft^3/s
Constant head boundary	991	803	1,022	631
Wells	0	228	0	464
Drains	0	290	0	222
River leakage	230	3,444	243	3,254
Head-dependent boundary	1,457	1,209	1,531	1,164
Recharge	3,295	0	2,939	0
Total	5,973	5,973	5,735	5,735
Areal average recharge, in inches per year	7.44		6.63	

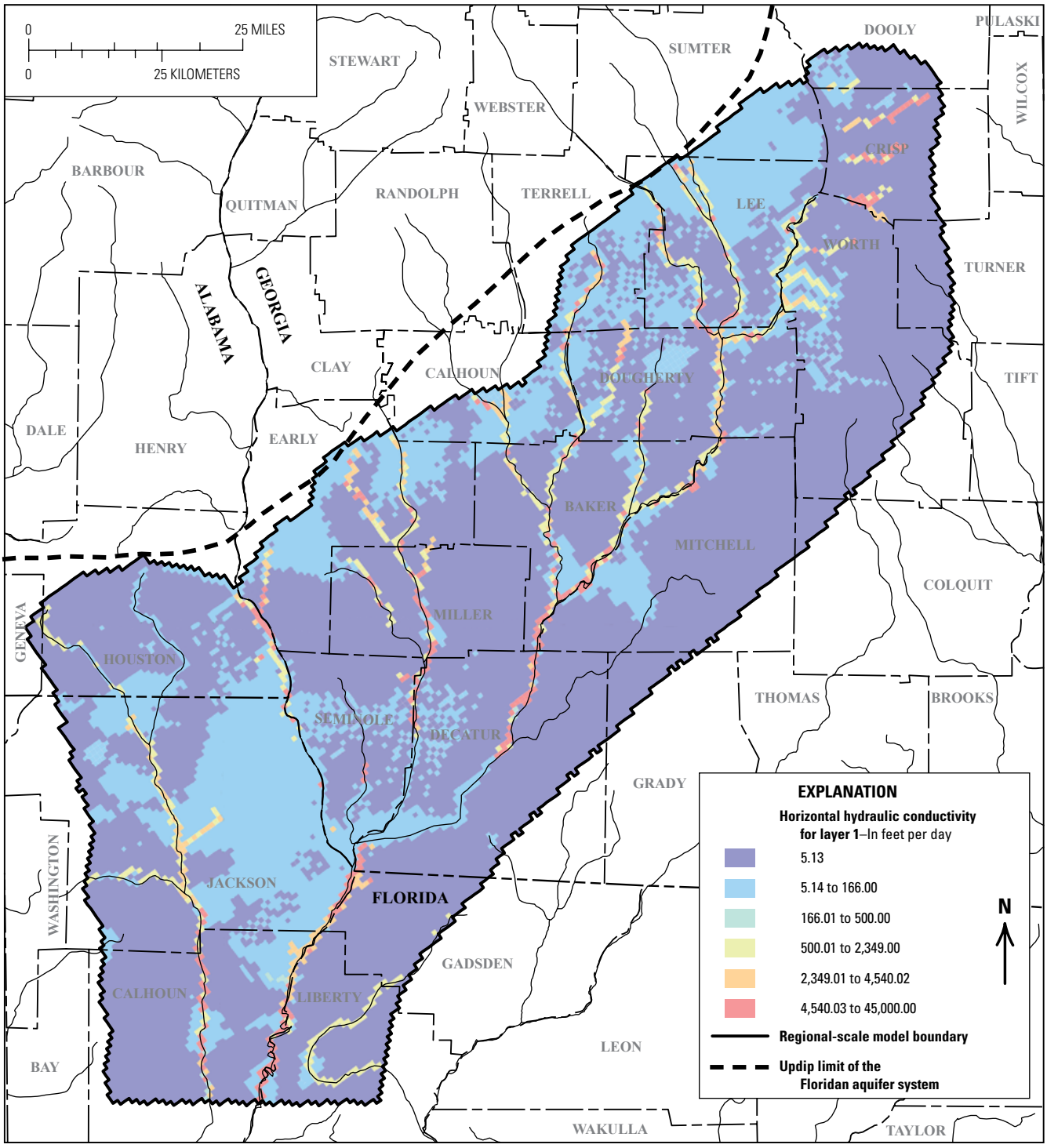

Base from U.S. Geological Survey digital data,1:24,000
Albers Equal-Area Conic Projection

Figure 31. Distribution of horizontal hydraulic conductivity for layer 1 of the regional-scale model.

of the total budget as outflows (163 ft^3/s or 105 Mgal/d). Recharge in the CLSM ranged from 0.34 to 24.6 in/yr in the model area; however, the areal average recharge was 6.61 in/yr. A total of 5 percent of cells had recharge of 10.0 in/yr or more. Rivers in the CLSM lost 76 ft^3/s (49 Mgal/d) to the aquifer and gained 2,022 ft^3/s (1,307 Mgal/d), which included tributaries of the Chattahoochee and Flint Rivers as well as Spring Creek (fig. 35*A*). Drains (springs) received a total of 138 ft^3/s (89 Mgal/d) from the aquifer in the CLSM (table 5). Withdrawals from wells totaled about 53 ft^3/s (34 Mgal/d).

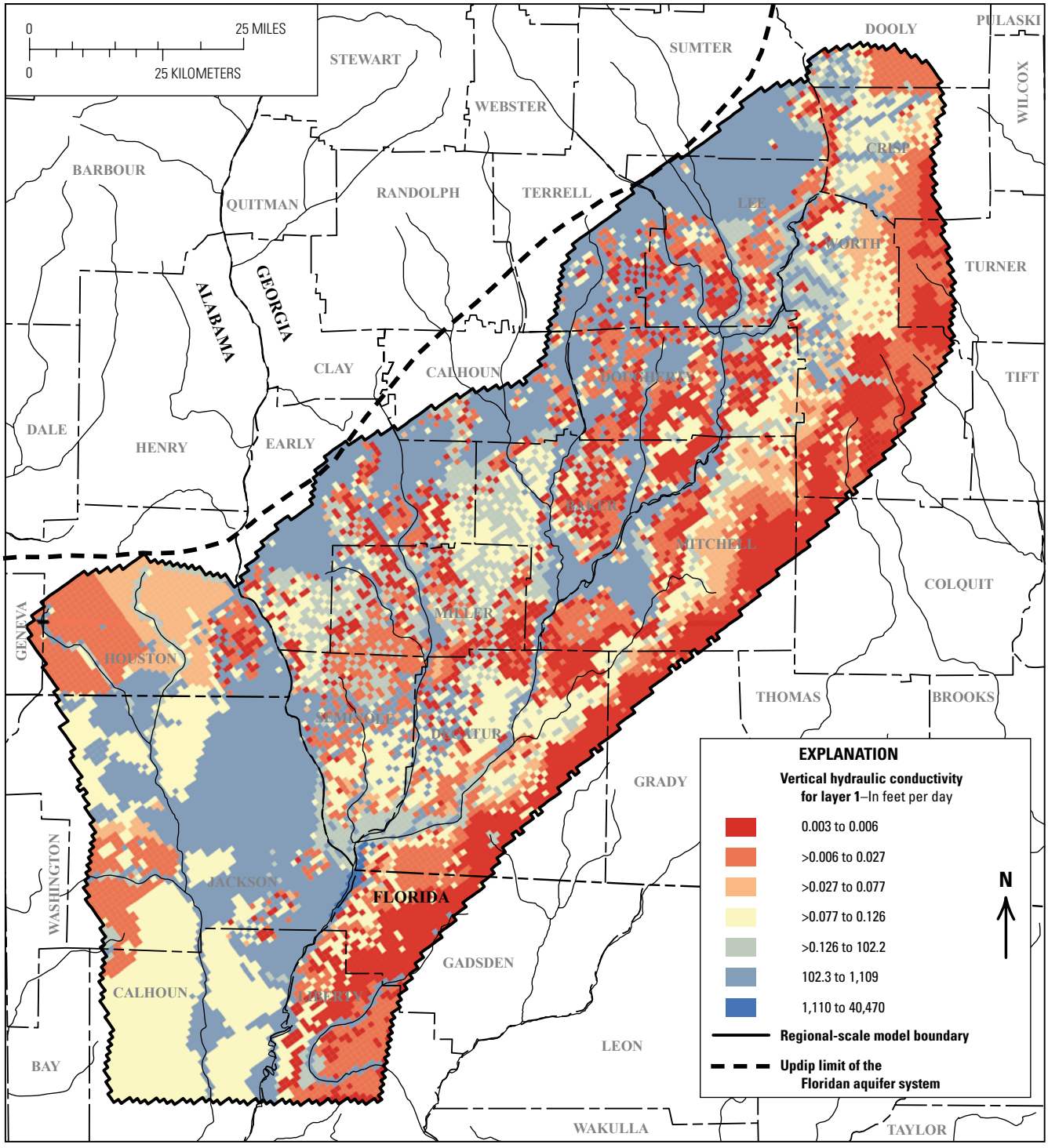

Base from U.S. Geological Survey digital data,1:24,000
Albers Equal-Area Conic Projection

Figure 32. Distribution of vertical hydraulic conductivity for layer 1 of the regional-scale model.

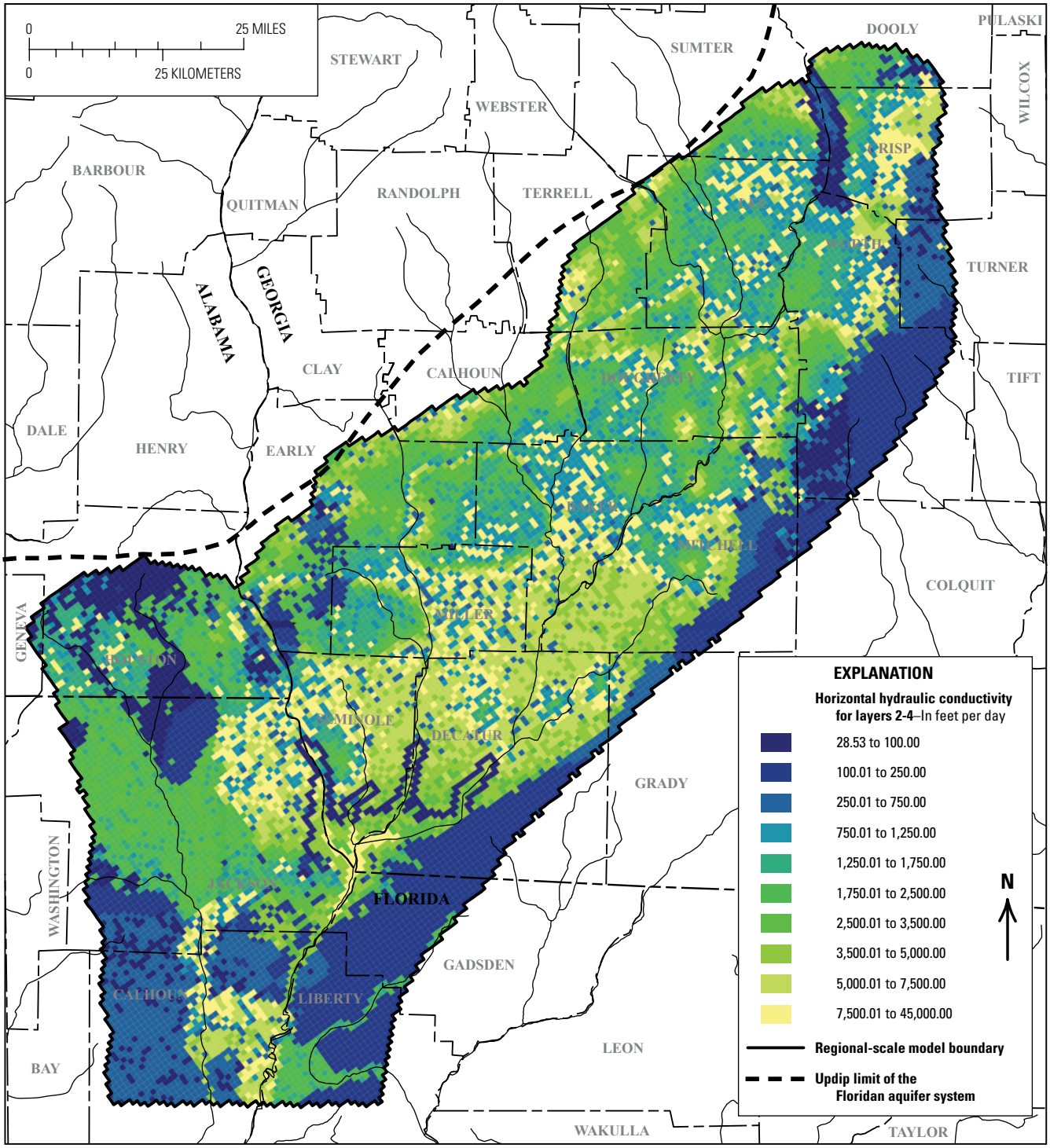

Base from U.S. Geological Survey digital data,1:24,000
Albers Equal-Area Conic Projection

Figure 33. Distribution of horizontal hydraulic conductivity for layers 2–4 of the regional-scale model.

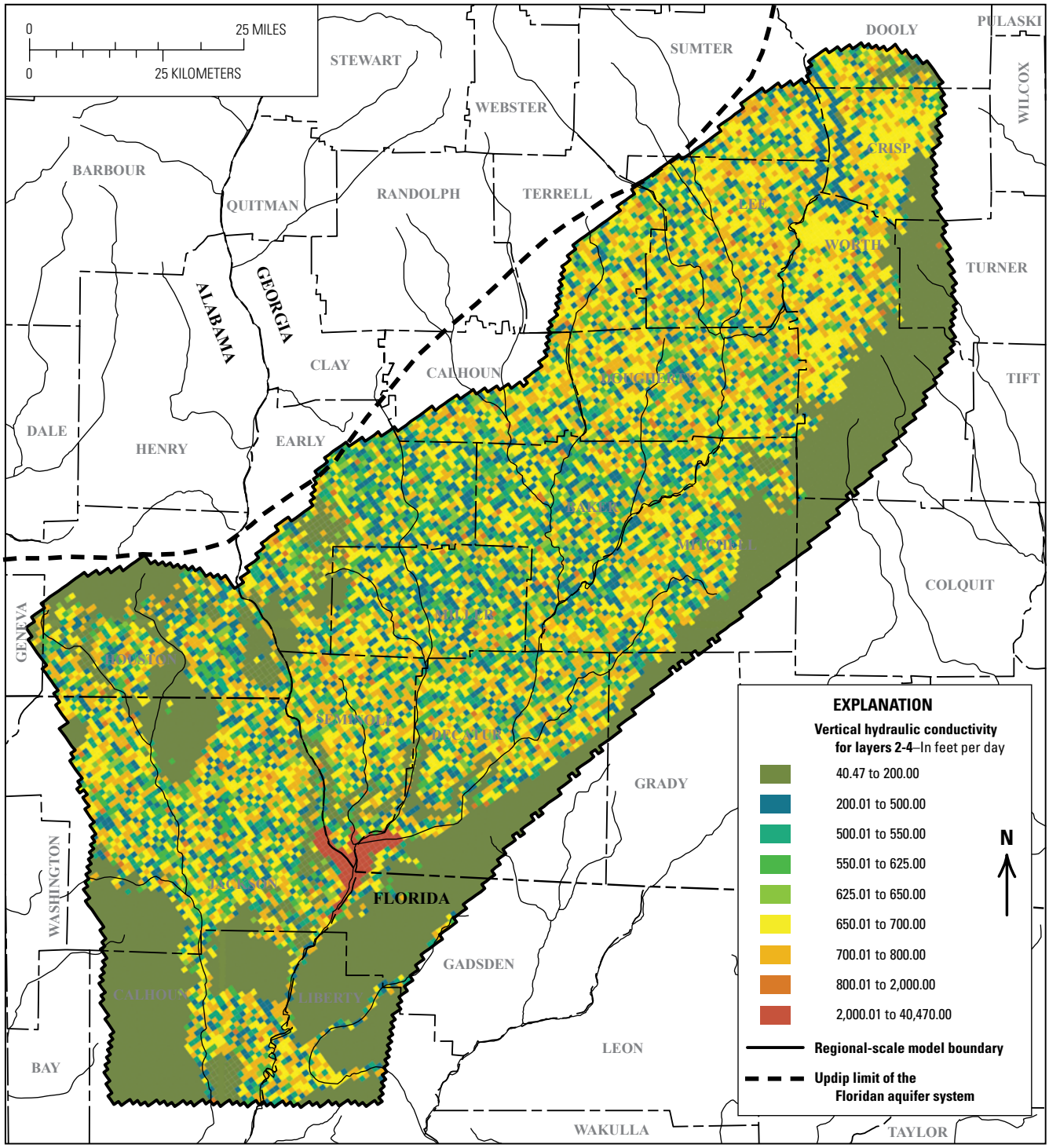

Base from U.S. Geological Survey digital data,1:24,000
Albers Equal-Area Conic Projection

Figure 34. Distribution of vertical hydraulic conductivity for layers 2–4 of the regional-scale model.

Withdrawals, primarily for irrigation, accounted for 2.1 percent of the total outflows in the water budget of the CLSM. A total of 742 cells simulated withdrawals in the CLSM. A part of Lake Seminole was simulated with head-dependent boundary conditions, and flows were 1,149 ft^3/s (742 Mgal/d) into and 84 ft^3/s (54 Mgal/d) out of the aquifer (fig. 35*A*).

Middle Flint Local-Scale Model Water Budget

Total flow in the Middle Flint Local-Scale Model (MFLSM) was 2,671 ft^3/s (1,727 Mgal/d). The greatest components of inflow were recharge (27.1 percent), constant head (20.6 percent), and specified flows (40.7 percent). The greatest components of outflows were constant heads (10.1 percent), river leakage (73.2 percent), and wells (5.7 percent). Specified flows into the modeled area totaled 1,088 ft^3/s (703 Mgal/d) whereas specified flows out of the area were 163 ft^3/s (105 Mgal/d) (fig. 35*B*; table 5). Specified flow boundaries were used because of the uncertainty of the location of water divides in the area. Constant-head boundaries on the northern side provided flow into (549 ft^3/s or 355 Mgal/d) and out of (270 ft^3/s or 174 Mgal/d) the local-scale model (fig. 36; table 5). Areal average recharge was 6.77 in/yr, and recharge ranged from 0.01 to 14.56 in/yr. Leakage from the aquifer to rivers in the MFLSM was 1,954 ft^3/s (1,263 Mgal/d); leakage from the rivers to the aquifer was 309 ft^3/s (200 Mgal/d) (table 5; fig. 35*B*). Drains (springs and non-perennial streams) accounted for 133 ft^3/s (86 Mgal/d) of the total discharge out of the aquifer (table 5). Withdrawals, primarily for irrigation, totaled 151 ft^3/s (98 Mgal/d); the MFLSM has a total of 914 wells. Withdrawals from individual wells in the MFLSM ranged from 0.01 to 26.5 ft^3/s (0.009 to 17.2 Mgal/d), and the average withdrawal was 0.2 ft^3/s (0.11 Mgal/d).

Limitations of the Models

The conceptualization of the groundwater-flow system was based on the work of Torak and others (1993, 1996) and Jones and Torak (2006). Thus, no effort was made in the current study to test how the previously used boundary conditions affected the model results. The model developed for this study is fully three-dimensional in order to more accurately simulate long-term transport of nitrate with particle tracking, whereas the previous models were one-layer two-dimensional models focused on groundwater/surface-water interactions. Additionally, the hydraulic conductivity distribution of the Upper Floridan aquifer was modified in an attempt to incorporate karst features into the flow model. In the current study the upper unit in both local and regional models has a minimum thickness of 10 ft in areas, where the Upper Floridan aquifer is at land surface, and a maximum thickness of more than 600 ft. The upper part of the system represents three distinctive hydrogeologic units—the sandy sediments that form the surficial aquifer system, the residuum, and the Upper Floridan aquifer in the river channels. The incorporation of these details facilitates a more accurate estimation of movement of water from the top of the system through surficial materials and into the Upper Floridan aquifer.

To simulate the long-term transport of nitrate, it was important to incorporate karst features into the model, because these features focus recharge and increase groundwater flow nearby. Most hydraulic conductivity estimates for the Upper Floridan aquifer were derived from kriging of aquifer test data in the Jones and Torak (2006) model or blocky zones in the Torak and others (1996) model. Methods of geospatial analysis were used in conjunction with available DEM data to identify sinkhole densities that impart higher horizontal and vertical hydraulic conductivity and are used to highlight model cells with maximum sinkhole density. However, older DEM data for some of the 1:24,000-scale maps in some areas limit the accuracy of sinkhole density calculations. Improved topographic data acquisition would increase the accuracy of sinkhole density delineation in future studies.

The equivalent porous media approach applied in this and previous models might be improved by explicitly simulating karst features, such as submerged caverns, within the aquifer. Simulating these features with the conduit flow process for MODFLOW (Shoemaker and others, 2008) may be a better method for incorporating conduit or pipe-like features; however, submerged conduits have not been mapped in the ACFB.

Table 5. Volumetric water budgets for the Middle Flint and Chipola Local-Scale Models.

[ft^3/s, cubic feet per second; MFLSM, Middle Flint Local-Scale Model; CLSM, Chipola Local-Scale Model]

Volumetric water-budget components	Flows into the MFLSM, in ft^3/s	Flows out of the MFLSM, in ft^3/s	Flows into the CLSM, in ft^3/s	Flows out of the CLSM, in ft^3/s
Constant-head boundary	549	270	241	163
Wells	0	151	0	53
Drains	0	133	0	138
River leakage	309	1,954	76	2,022
Head-dependent boundaries	0	0	1,149	84
Recharge	725	0	863	0
Specified flows	1,088	163	194	64
Total	2,671	2,671	2,523	2,523
Areal average recharge, in inches per year	6.77		6.61	

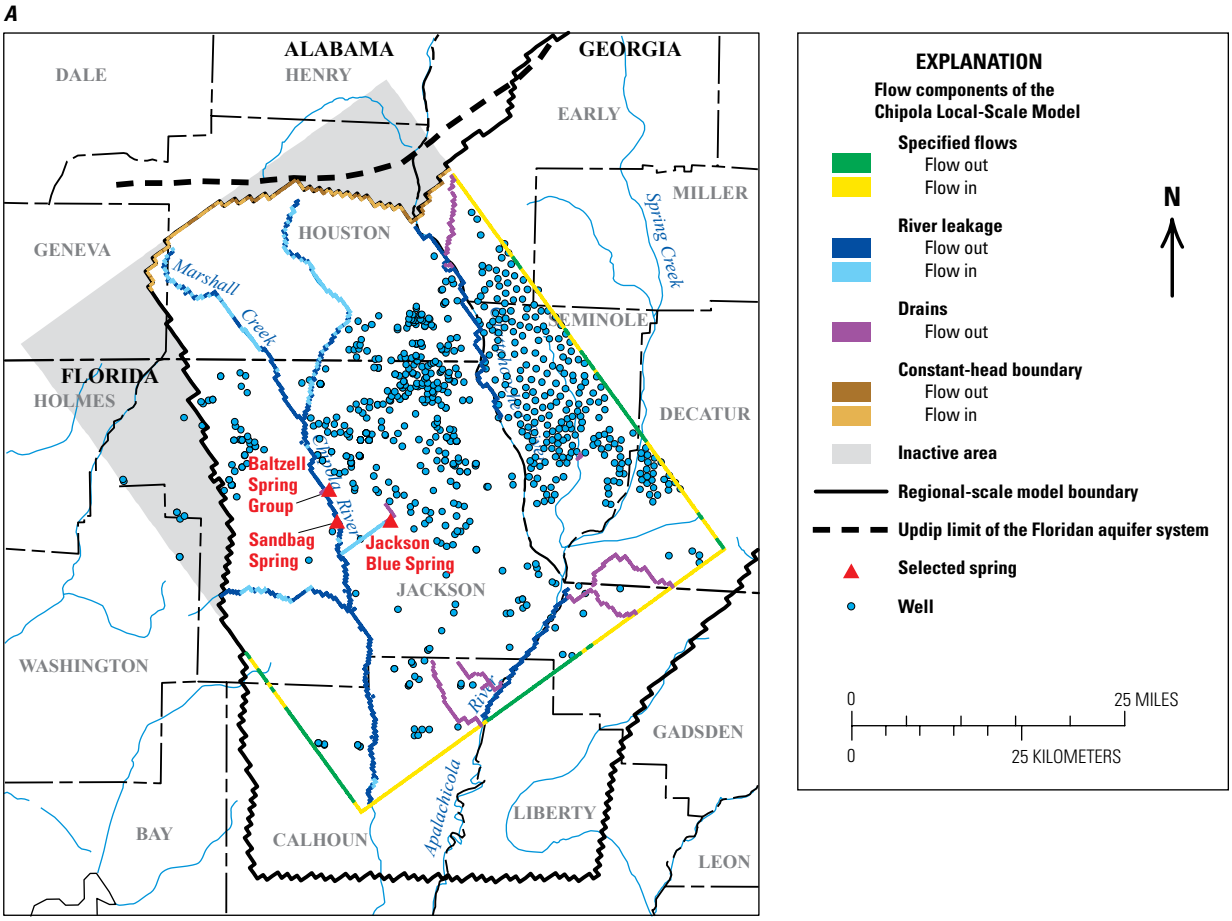

Figure 35. Flow components, including specified and head-dependent boundary fluxes, wells, river leakage, drains, and constant head for (*A*) the Chipola River Basin.

The regional model was recalibrated for a stressed steady-state period (September 19–October 18, 1999) that differed from long-term average conditions for transport; 328 groundwater level measurements and 68 streamflow observations were used for the recalibration. None of the 328 water-level measurements were in the surficial aquifer system (model layer 1); therefore, the hydraulic properties of model layer 1 were mostly insensitive compared to other parameters in the parameter estimation process. The hydraulic properties of the surficial aquifer system cannot be accurately estimated given the calibration data available for the study. Many flow measurements used in the calibration were small or zero, because the period included the end of a long drought. Springs and river-flow observations in the Chipola River Basin were not measured during the period of calibration, and values used were an average of the available measured flows. Since this model was largely based on information from previous models, net recharge estimates are based on the percentage of precipitation. The sensitivity analysis indicated that recharge and hydraulic conductivity of the Upper Floridan aquifer were the most sensitive parameters given the available observation dataset. Additional precipitation observations could refine spatial distribution of recharge and improve calibration and future simulations.

An important simplifying assumption was the use of long-term average (1975–2005) steady-state conditions for particle tracking the transport of nitrate. Inherent in this assumption is the transient seasonal nature of both rainfall and groundwater withdrawals, which were averaged and assumed to provide reasonable estimates of Darcy flux when using particle tracking to define contributing areas to selected springs and wells. The timeframe of the model included a period during which the nitrate was applied (Frick and others, 1996) and another period that included dry, wet, and average years. Ideally, if the observed head and flow data were available for transient calibration of the model for the full period of record, there would be more confidence in the estimates of hydraulic conductivity and recharge. However, the use of steady-state stresses (representing long-term average) has been successful for similar studies in the past and has been used commonly for creating the flow fields used in particle tracking (Pollock, 1994; Eberts and others, 2005; Crandall and others, 2009).

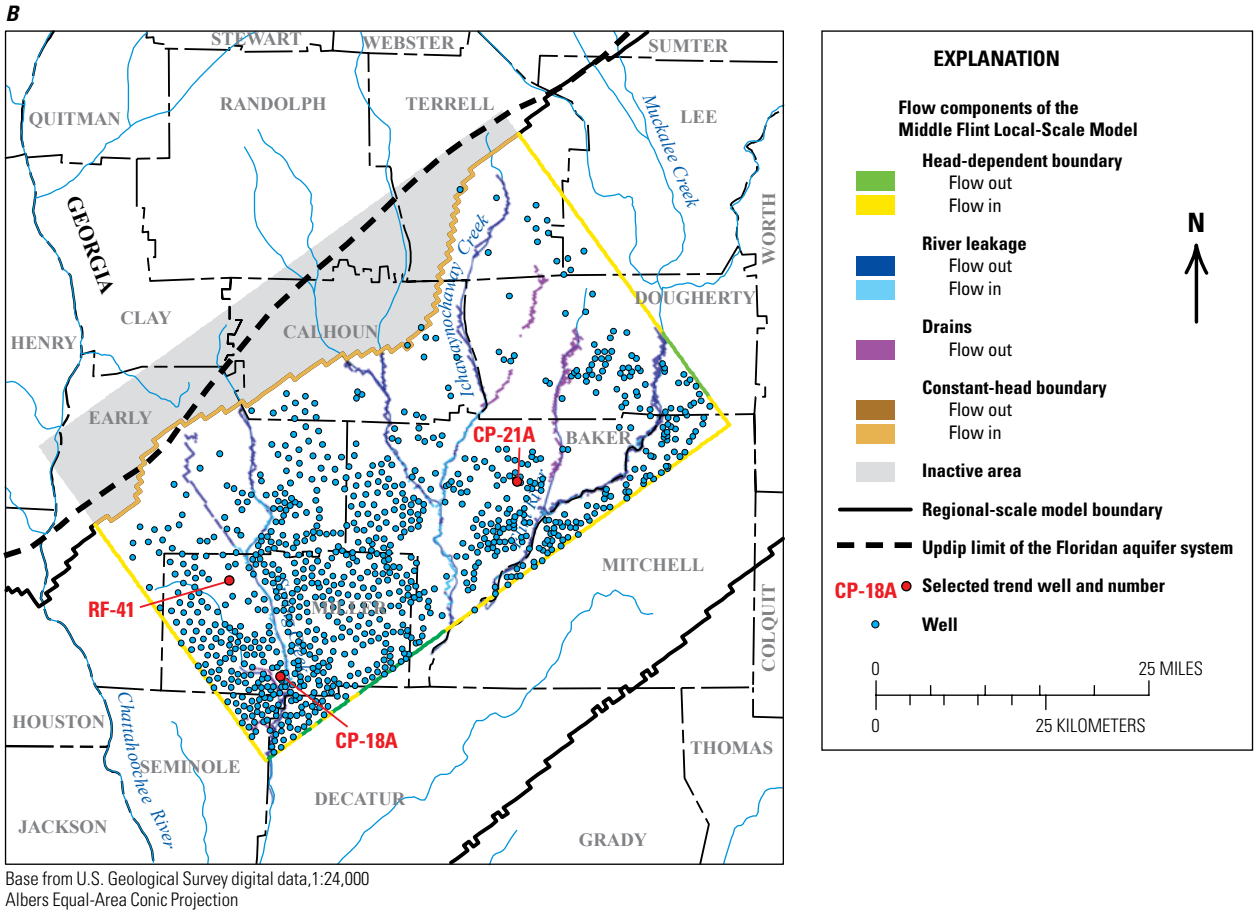

Figure 35. Flow components, including specified and head-dependent boundary fluxes, wells, river leakage, drains, and constant head for (*B*) the middle Flint River Basin. —Continued

In the study by Jones and Torak (2006), hydraulic conductivity was calibrated for the initial conditions; only the storage properties in the transient calibration of 1 year of monthly data required further modification. The Jones and Torak (2006) model, however, was calibrated with a trial-and-error process. Since the current model was calibrated with stressed steady-state simulations, no effort was made to estimate storage properties. If parameter estimation is used in a transient calibration of the regional model, it is possible that the estimates of hydraulic conductivity and net recharge may change.

Simulated Particle Travel Times

The range in simulated particle travel times (a surrogate for age) for recharge waters reaching selected wells or springs cannot be compared directly with the average apparent age of recharge water derived from atmospheric tracers. Atmospheric tracers yield an average apparent age for each well or spring (Katz and others, 2007). Particle tracks yield a distribution of particles, each with an associated travel time (age). The average tracer-derived apparent age of water was compared to the median water particle ages (based on travel times). Particles move through the aquifer on the basis of pore velocity, which equals the Darcy velocity divided by porosity; thus, this comparison was used to calibrate porosities.

Simulated particle travel times (ages) for all sites ranged from less than 1 day to more than 511 years for Jackson Blue Spring (table 6). The range in simulated particle travel times was greater for the springs than it was for the wells. This is consistent with what is known about groundwater discharging to springs from young (conduit flow) and older (porous matrix flow) sources. Simulated particle travel times ranged from about 2 to 153 years for the three selected NAWQA long-term monitor wells RF-41, CP18A, and CP-21A (table 6). The monitor wells are open to the base of the surficial aquifer system and to the top of the Upper Floridan aquifer. Overall, the median travel times were within the same order of magnitude of measured average apparent ages using tracers. Median simulated travel times were slightly older than average apparent travel times. Median particle travel times for wells RF-41, CP-21A, and CP-18A were about 36, 35, and 50 years

(table 6), whereas measured average apparent travel times of the wells were about 32, 29, and 23 years (table 3), respectively. Median particle travel time for groundwater reaching well CP-18A was about 26 years older than the average apparent age determined using tracers. The median particle travel time for groundwater reaching well RF-41, however, was only about 4 years older than the measured average apparent age using tracers. The maximum particle travel time for all wells (about 153 years) was computed for well RF-41; about 70 percent of the particle travel times for all three wells was 70 years or less (fig. 36).

The median travel times of simulated particles reaching Jackson Blue Spring, Baltzell Springs Group, and Sandbag Spring were about 30, 62, and 38 years, respectively (table 6). The distribution of particle travel times (ages) for the three springs was bi-modal (fig. 36) with more than 50 percent of the particles having travel times of 50 years or less and the remaining particle travel times ranging from about 51 to 512 years. A bi-modal distribution is expected for travel times in karst areas where conduit flow paths are relatively rapid, and flow through the matrix is much slower. The measured average apparent ages from tracers were about 19, 16, and 18 years for Jackson Blue Spring, the Baltzell Springs Group, and Sandbag Spring, respectively (table 3). The oldest median particle travel time (age) occurred for Baltzell Springs Group (about 62 years). Baltzell Springs Group is a series of five or more springs (average flow approximately 30 ft^3/s) with a short spring run flowing into the Chipola River. Jackson Blue Spring is a first-order magnitude spring (flows greater than 100 ft^3/s) that has many large conduits contributing flow from several directions. The relatively short simulated travel times of water discharging at springs indicate their possible occurrence within a stratigraphic layer having a higher frequency of larger interconnected voids or conduits. Anecdotal evidence indicates that many conduits are visible along the bed and bank of the Chipola River for most of the upper and middle reaches. The median particle travel time to these springs was less than about 60 years, indicating fairly young recharge to the springs.

Predicting Future Nitrate Concentrations at Selected Sites

Nitrate concentrations in groundwater were estimated for six sites in the lower ACFB for the period 2002–50. Irrigated agriculture land-use practices are extensive in the study area and will likely continue for the foreseeable future. Travel times were estimated along flow paths reaching selected wells and springs to examine temporal changes in nitrate concentration within the aquifer. Fertilizer sales data and temporal atmospheric deposition totals were used to predict future nitrate concentrations. County-level nitrogen fertilizer sales and atmospheric deposition totals were developed for each county where selected sites were located and were used as a proxy for nitrate input to groundwater for the period 1945–2001. These input functions were used with particle travel times and recharge rates to predict nitrate concentrations in selected sites from 2002–50 under three different nitrogen management scenarios. The first scenario simulated nitrate input fixed at 2001 levels for the period 2002–50. The second scenario simulated a 4 percent per year reduction (from each previous year) in nitrate input to groundwater for 2002–50. The third scenario eliminated the input of nitrogen to the groundwater system after 2001 for the 2002–50 simulation period.

Areas Contributing Recharge

Areas contributing recharge (ACR) to selected discharge sites were identified using particle-tracking methods, and historic and current land-use practices were assessed with respect to their effects on water quality. Recent land use/land cover in the contributing areas include row-crop agriculture, wetlands, and forested areas, but nutrient sources mainly occurred in populated and agricultural land-use areas (Frick and others, 1996). Forward particle tracks from land surface usually terminate at discharge points, such as springs and streams; however, the quality of groundwater from a monitor well or spring may reflect the mixing of water from local and intermediate flow

Table 6. Summary statistics for particle ages for selected wells and springs.

[<, less than]

Percentile of flow	Age of particles, in years					
	Jackson Blue Spring	Baltzell Springs Group	Sandbag Spring	Well RF-41	Well CP-21A	Well CP-18A
Minimum	< 1 day	1	< 1 day	21	2	35
Median	30	62	38	36	35	50
Average	43	166	23	48	32	56
Maximum	512	339	39	153	87	99
Number of particles	16,845	2,133	1,015	999	999	999

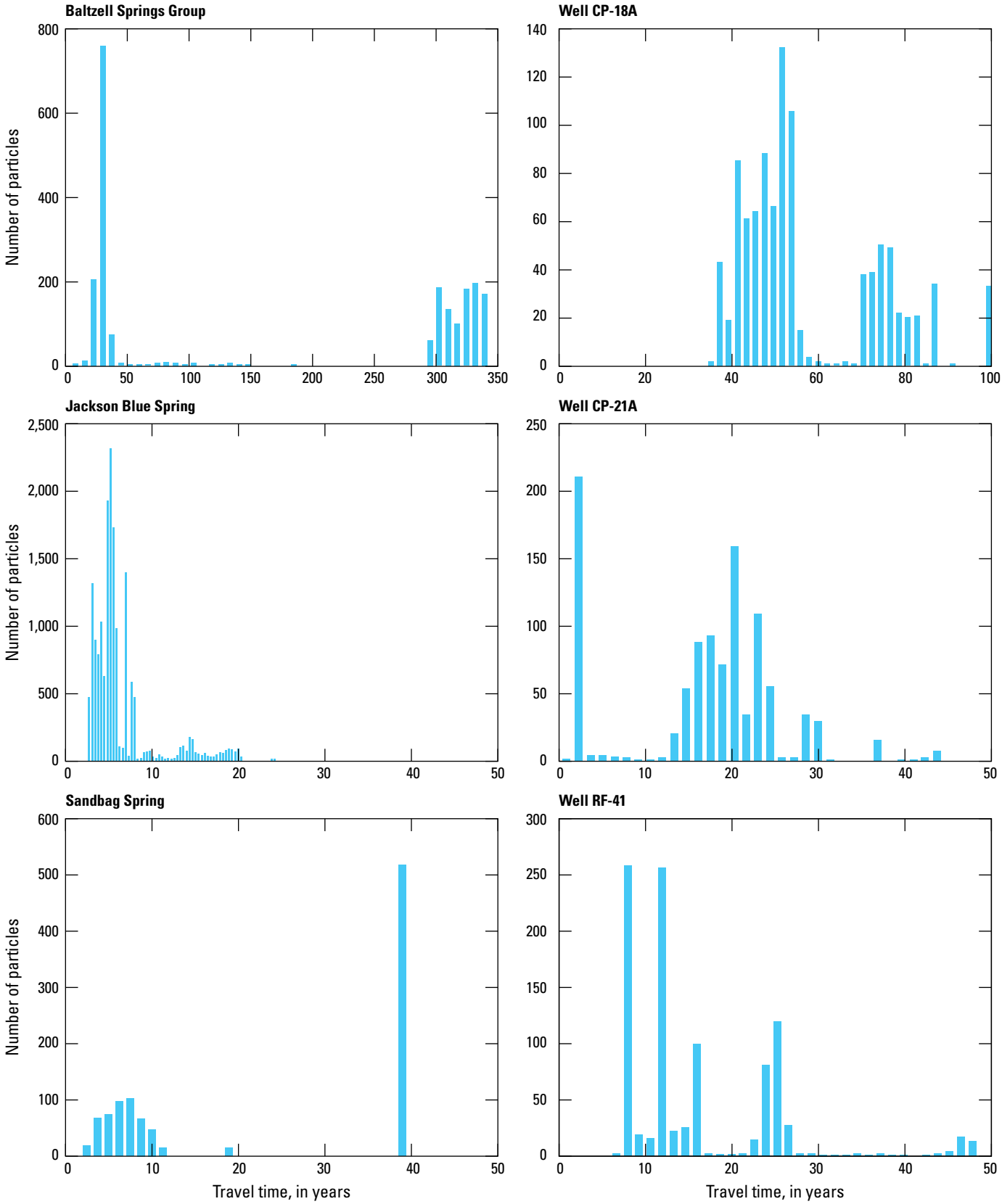

Figure 36. Simulated travel time for particles in the Chipola and Middle Flint Local-Scale Models.

paths within the aquifer near the wells. Simulated ACR extend north and northwest from the springs or well head (figs. 37 and 38). Irrigated row-crop agriculture predominates in the ACR for wells CP-21A, Jackson Blue Spring, and Baltzell Springs Group; the ACR for Sandbag Spring and wells RF-41 and CP-18A also includes wetlands and forested areas.

Estimation of Nitrate Concentrations

Nitrate concentrations were estimated on the basis of nitrogen fertilizer sales data obtained from the U.S. Department of Agriculture Bureau of Agricultural Statistics (1945–2001) and nitrogen deposition from atmospheric sources obtained from the National Atmospheric Deposition Program (NADP). The data were compiled by county as part of the nationwide NAWQA Program (Alexander and Smith, 1990; Battaglin and Goolsby, 1994; Ruddy and others, 2006; fig. 11). Potential data uncertainties and constraints include: (1) fertilizer application might not occur in the same year or county in which it was purchased, (2) fertilizer application is not evenly distributed within counties, (3) fertilizer applications cover an unknown fraction of the area contributing recharge, (4) individual States might use different methods to report non-farm sales and total sales of nitrogen fertilizer, (5) variable rainfall recharge affects fertilizer applications, and (6) the depth to the water table (travel times through the unsaturated zone) is variable. Typically, there is a lag time between fertilizer application at land surface and nitrate arrival at the water table. Travel times in the unsaturated zone vary depending on permeability of soils, irrigation practices, and the presence of sinkholes. Furthermore, geochemical processes, such as dilution and denitrification, may reduce the concentration of nitrate along groundwater flow paths.

Estimates of the nitrate input to the groundwater system were calculated for the period 1945–2050. Simulated nitrate concentrations in the input function were scaled to match observed nitrate concentrations (calibration data) over time in groundwater at each sampling site. Scaling was necessary because the historic fertilizer sales data may not accurately reflect the application amount. Other issues also may contribute to uncertainty, including the units used for the input function, the number of particles used to track the flow paths and travel times to the receptor sites, agricultural practices (crops grown and irrigation and fertilizer usage rates), recharge rates, soil and aquifer properties, the percentage of

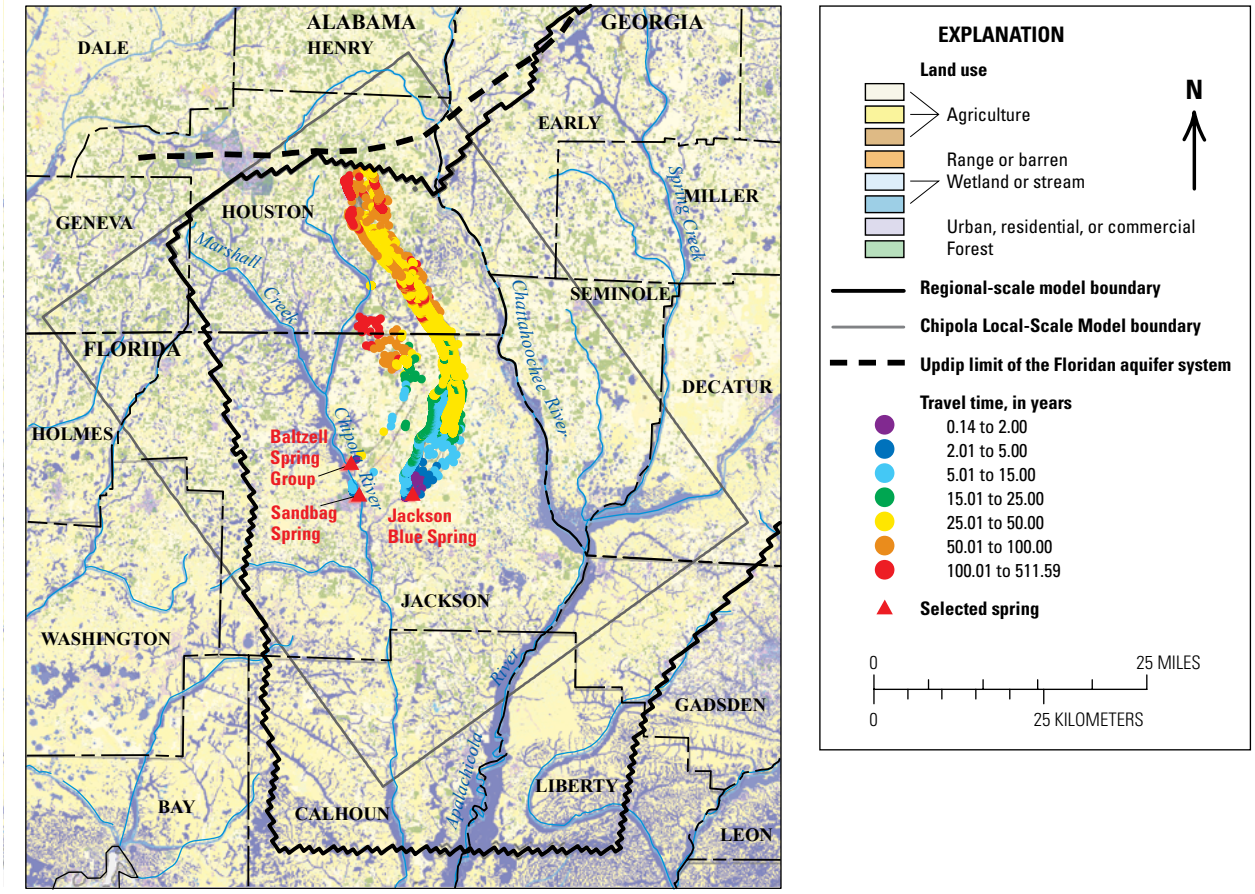

Base from U.S. Geological Survey digital data,1:24,000
Albers Equal-Area Conic Projection

Figure 37. Particle endpoint travel times and land use for Jackson Blue Spring, Baltzell Springs Group, and Sandbag Spring in the Chipola Local-Scale Model.

the area contributing recharge to the selected receptor sites, the percentage of fertilizer bought that was used during the year, and the size of the agricultural land area contributing recharge to the aquifer. The scaling factors were as follows: 0.0029 for Jackson Blue Spring (16,845 particles were used for 11 drain cells); 0.03 for Baltzell Springs Group (2,133 particles used for 2 cells); 4.5 for Sandbag Spring (1,015 particle used for 1 cell); 1.0 for well CP-18A; 0.5 for well CP-21A; and 0.09 for well RF-41 (999 particles for each well cell). Additionally, particle-simulated ages were an overestimate in well CP-18A, whereas the five other sites used in the calibration of porosity had close age matches. To account for the poor fit at well CP-18A, nitrate applications were shifted 21 years ahead in the input function to provide a closer match to the observed concentrations. Nitrate groundwater concentrations were within the anticipated range for this site, but travel times were overestimated as compared to tracer-derived estimates. Simulated travel time is within the same order of magnitude as tracer-derived ages at all sites.

Nitrate concentrations in each well or spring were determined by summing the total recharge-weighted nitrate concentration assigned to each water particle recharged during a specific year for each well. During a given year, the nitrate concentration for each traced water particle is a function of the applied nitrogen fertilizer plus the atmospheric deposition during the year of recharge for the appropriate year and county. Nitrate concentrations for wells and springs were calculated for three management scenarios during the period 1945–2050. Calculated nitrate concentrations for the period 1945–2007, however, were used only for calibration purposes and compared to measured nitrate concentrations. Nitrate concentrations were estimated for 2002–50 using model simulation. Nitrate concentrations from groundwater samples collected during 1993–2007 were used to calibrate the transport aspect of the model. Simulated nitrate concentrations were compared to observed concentrations (fig. 39); the relation had a coefficient of regression (r^2) of 0.90.

Estimated nitrate concentrations were close to the observed nitrate concentrations in groundwater samples from most wells and springs, although travel times to well CP-18A and Baltzell Springs Group were somewhat longer, causing the simulated nitrate to have a later arrival time than the observed values. Simulated nitrate concentrations in Baltzell Springs Group, however, matched fairly closely even though simulated travel times for water particles tend to exceed the apparent tracer-derived age.

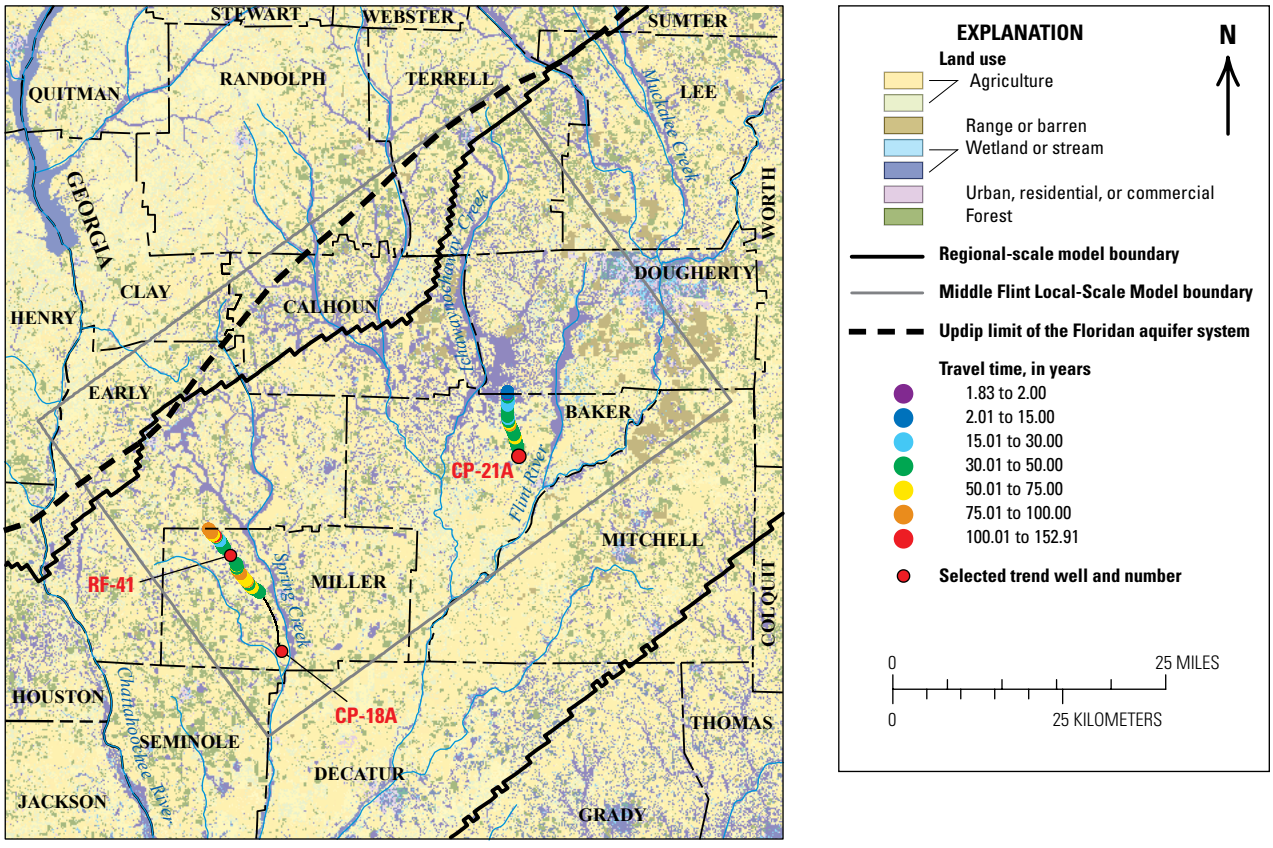

Base from U.S. Geological Survey digital data,1:24,000
Albers Equal-Area Conic Projection

Figure 38. Particle endpoint travel times and land use for wells CP-18A, CP-21A, and RF-41 in the Middle Flint Local-Scale Model.

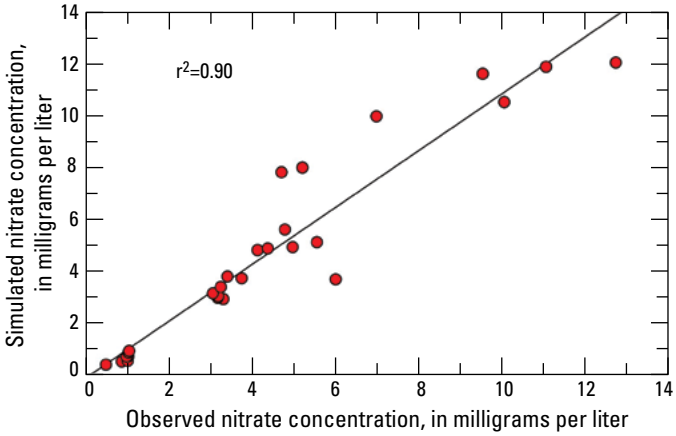

Figure 39. Comparison of observed and simulated nitrate concentrations in wells and springs, 1993–2007.

Simulated Nitrate Concentrations Under Three Nitrate Fertilizer Management Scenarios

Nitrate concentrations were simulated during 2002–50 in wells RF-41, CP-21A, and CP-18A, and in Baltzell Springs Group, Jackson Blue Spring, and Sandbag Spring under three different nitrate fertilizer management scenarios. In scenario 1, nitrate inputs were fixed at 2001 levels for the period 2002–50. Scenario 2 simulated a gradual (4 percent per year) reduction in nitrate input to groundwater for the period 2002–50. Scenario 3 eliminated all nitrate input to the groundwater system after 2001.

A comparison of the three management scenarios indicates that simulated nitrate concentrations in wells (fig. 40) would peak up to 40–50 years after fertilizer sales and atmospheric deposition totals reached their maximum levels. Nitrogen fertilizer sales and atmospheric deposition totals for Jackson County, Florida, peaked in 1979–82; nitrogen inputs declined in 1984 and then remained relatively constant through 2010 (fig. 11). Nitrate concentrations had exceeded 3.00 mg/L in wells CP-18A and CP-21A in 1978 and 1984, respectively. Simulated nitrate concentrations in CP-18A were projected to reach 12.82 mg/L in 2012, and are projected to peak at 13.76 mg/L in 2026 under management scenario 1. Nitrate concentrations are projected to remain above 3.00 mg/L in well CP-18A through the end of the simulation period 2002–50 under all management scenarios. Simulated nitrate concentrations in well CP-21A exceeded 5 mg/L by 2012 and were projected to peak at 7.82 mg/L in 2030, under management scenario 1 (fig. 40). Projected nitrate concentrations in CP-21A will decrease slowly under management scenarios 1 and 2 by 2050, but concentrations will remain relatively high by the end of the simulation period under scenarios 1 and 2 (6.84 mg/L and 4.0 mg/L, respectively). After 2030, nitrate concentrations will decrease steadily under management scenario 3 (nitrate input set at zero), to less than 3.00 mg/L by 2042 and to slightly less than 1.0 mg/L by 2050. Simulated nitrate concentrations in well RF-41 are projected to peak in 2020 at 1.10 mg/L for all scenarios; concentrations are projected to remain at 1.10 mg/L by 2050 under scenario 1, and to decrease to 0.77 and 0.25 mg/L under management scenarios 2 and 3, respectively (fig. 40).

Simulated nitrate concentrations will peak between 2006 and 2018 in the springs under the three management scenarios, which is approximately 30–40 years after maximum fertilizer sales and atmospheric deposition totals. The peak nitrate concentrations occur 10–20 years earlier in the springs than in the wells. Simulated nitrate concentrations were highest in scenario 1, when nitrate input was fixed at 2001 levels (the most likely management scenario), and lowest in management scenario 3 when nitrate input ceased in 2001 (fig. 40).

Simulated nitrate concentrations in the Baltzell Springs Group began to increase in the mid-1960s and peaked in 2006 at 3.77 mg/L for all three nitrogen management scenarios (fig. 40). Simulated concentrations are projected to drop below 3.00 mg/L by 2012 under all management scenarios. Simulated nitrate concentrations in groundwater from Baltzell Springs Group will drop below the minimum detection level (0.10 mg/L) by 2033 under scenario 3 (nitrate input eliminated after 2001). Nitrate concentrations are projected to drop to 1.57 and 0.65 mg/L for scenarios 1 and 2, respectively, by 2050.

Simulated nitrate concentrations for Jackson Blue Spring peaked in 2011 at 3.51 mg/L under management scenarios 1 and 2 (fig. 40). Simulated nitrate concentrations decrease to less than 3.0 mg/L by 2020 in scenario 1 (fixed at 2001 levels) and by 2013 in scenario 3 (nitrate input eliminated after 2001). Simulated concentrations will continue to decrease by 2050 to 2.28, 1.22, and 0.50 mg/L for management scenarios 1, 2, and 3, respectively, but will not reach background levels of less than 0.10 mg/L by the end of the simulation period under all management scenarios (fig. 40).

Simulated nitrate concentrations in Sandbag Spring are not projected to exceed 1.0 mg/L; concentrations are projected to peak in 2018 at 0.81 mg/L for all three nitrogen management scenarios (fig. 40). Nitrate concentrations will decrease and stabilize at 0.29 mg/L by 2040 under management scenario 1 (input fixed at 2001 levels). Under management scenario 2 (a gradual reduction), nitrate concentrations will decrease to 0.2 mg/L by 2050. Under management scenario 3 (nitrate input eliminated after 2001), nitrate concentrations decrease to background levels (less than 0.10 mg/L) by 2041.

Limitations of Particle Tracking and Estimation of Nitrate Concentrations

Particle tracking uses advective transport only and does not account for adsorption, degradation, dispersion, diffusion, and other processes that may reduce nitrate concentrations in groundwater. Fertilizer sales plus atmospheric deposition totals at the county level are not a refined representation of nitrate input to groundwater over time, although they provided the best approximation available. Ideally, a land-use

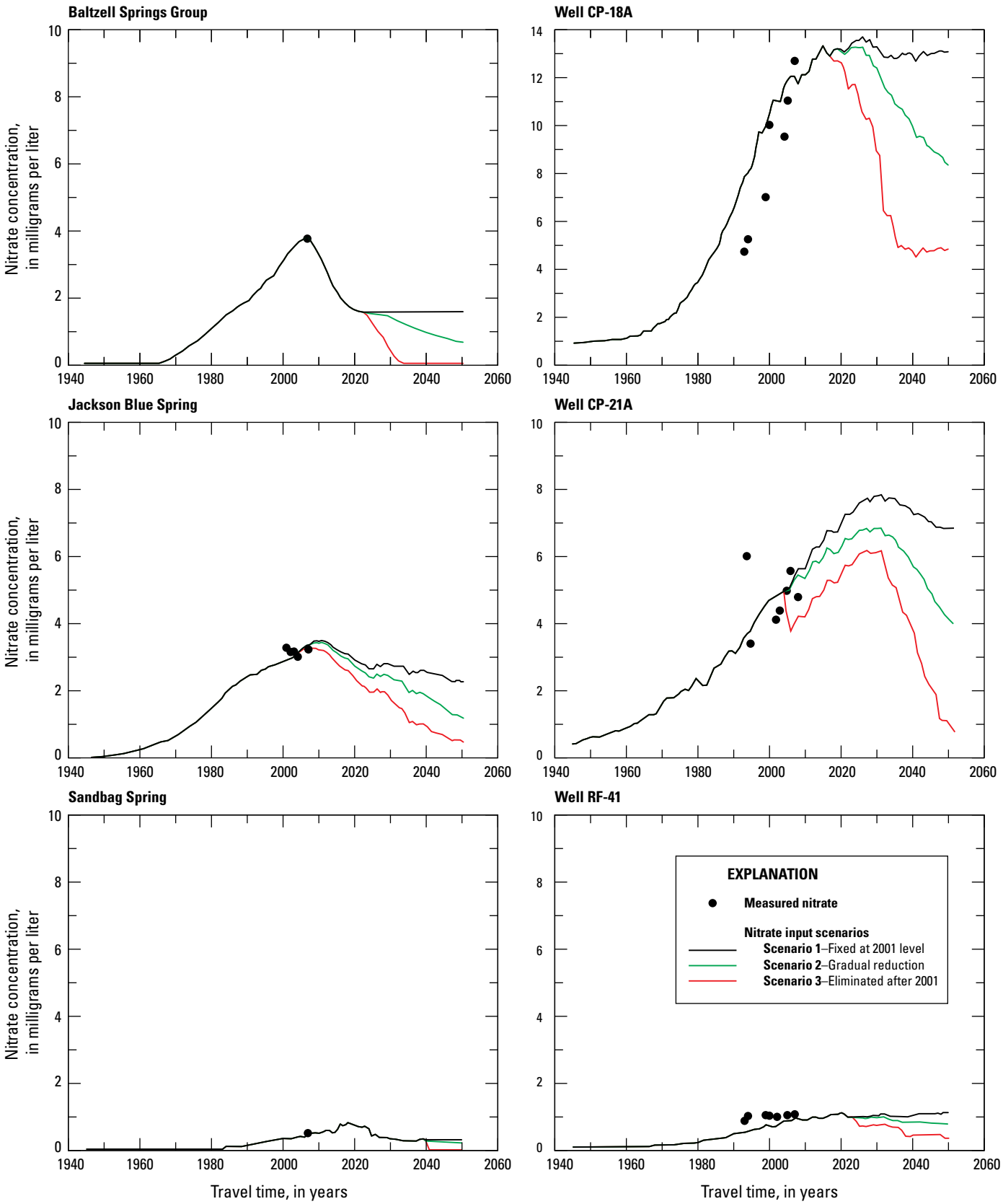

Figure 40. Simulated effects of three nitrate management scenarios on nitrate concentrations in springs and wells, 2001–50.

history for nitrate application would be constructed for each agricultural field in the area contributing recharge, and the exact recharge for each well or spring at the time of sampling would be used to weight the nitrate concentration. Additionally, the areas contributing recharge can change substantially with hydraulic conductivity changes. The robustness of the estimates for hydraulic conductivity and, therefore, the areas contributing recharge would benefit from a probability analysis. Porosities are based on literature values for the appropriate hydrogeologic units. Actual porosities may vary depending on the distribution of surficial sediments and karst features. Estimated contributing areas should be regarded as the most likely areas contributing recharge, travel times, and flow paths to a discharging site (wells, streams, springs), because of the uncertainty associated with karst features and hydraulic conductivity, boundary conditions, withdrawals, flows, and recharge. Additionally, the general nature of the nitrate input function means that simulated nitrate concentrations should be considered the best available estimates in the absence of more data and model simulations.

Summary and Conclusions

The Upper Floridan aquifer supplies irrigation and drinking water in the lower Apalachicola–Chattahoochee–Flint River Basin. Agriculture is the major land use in the lower part of this basin, and withdrawals from the Upper Floridan aquifer, in decreasing order of volumetric consumption, are for agriculture, industry, and domestic and public supply. The aquifer also supplies base flow to streams and provides spring discharge. Much of the groundwater-flow system has relatively short flow paths, high recharge rates (approximately 5 to 25 in/yr), and large discharge features (springs) that provide base flow to streams. Hydrogeology and land uses in the area combine to render the Upper Floridan aquifer system highly vulnerable to nitrate contamination.

Nitrate concentrations in groundwater of the Upper Floridan aquifer in the lower ACFB are higher than in other areas of the Upper Floridan aquifer, and concentrations occasionally exceed the USEPA maximum contaminant level of 10.0 mg/L as nitrogen (U.S. Environmental Protection Agency, 2012). Elevated nitrate concentrations in drinking water are a concern because infants under 6 months of age who drink water containing nitrate concentrations above the USEPA maximum contaminant level of 10 mg/L as nitrogen can become seriously ill with blue baby syndrome (U.S. Environmental Protection Agency, 2012). The maximum concentration of nitrate found during 1993–2007 in the study area was 12.73 mg/L, measured in a water sample from a shallow monitor well. The maximum concentration of nitrate in groundwater from wells or springs discharging to the Chipola River was 6.43 mg/L.

Synoptic sampling of 33 springs and 17 surface-water sites on the Chipola River or its major tributaries was completed during the spring and early summer of 2007. A review of the synoptic data from the springs and surface-water sites was used in conjunction with historical water-quality data to select three springs and two companion flow-path wells for each spring in the Chipola River Basin and three long-term monitor wells in the Flint River Basin for further study. Wells upgradient from the springs were selected on the basis of their locations in the areas contributing recharge to the selected springs. These three springs and their upgradient flow-path wells were sampled late in the summer of 2007 to identify water-quality and geochemical conditions and determine the age of water.

A regional-scale, steady-state, groundwater-flow model was developed and calibrated in MODFLOW 2000 for September–October 1999 conditions, using data collected from previous models for calibration and initial conditions. Parameter estimation was used to calibrate new hydraulic parameters and recharge properties. The regional-scale model was calibrated against 328 measured groundwater levels and 68 flows between reaches. The regional-scale model was then used with long-term average (1975–2005) recharge and withdrawal conditions to generate flow boundaries for two local-scale models. The two local-scale groundwater flow models were used to generate particle-tracking models (MODPATH) and to delineate areas contributing recharge and travel times (particle age distributions) to six sites (three wells and three springs). Average apparent ages of water, obtained from the age tracers tritium-helium, CFC, and SF_6, were used to calibrate porosities.

Particle travel times (a surrogate for age) in wells ranged from a minimum of about 2 years (CP-21A) to a maximum of about 153 years (RF-41). The median particle travel times for the selected monitor wells RF-41, CP-18A, and CP-21A, were about 36, 50, and 35 years, respectively. The average apparent ages of water derived from tracer data were about 32, 23, and 29 years, respectively. Overall, particle travel times were within an order of magnitude and in some cases were quite close to the mean apparent ages determined from age tracer models for two of the three wells. Particle travel times in well CP-18A were older than travel times in the other two wells. About 70 percent of the weighted particle travel times were less than 50 years in wells CP-18A and RF-41. About 70 percent of particle travel times were less than 40 years in well CP-21A.

Particle travel times for the three springs ranged from approximately 1 day to 512 years. The median particle travel times for Jackson Blue Spring, Baltzell Springs Group, and Sandbag Spring were about 30, 62, and 38 years, respectively; The oldest and youngest water particle travel times were simulated for the Jackson Blue Spring and were consistent with processes recharging major springs. The average apparent age of groundwater from tracers for Jackson Blue Spring,

Baltzell Springs Group, and Sandbag Spring was about 19, 16, and 18 years, respectively. About 50 percent of the simulated particle travel times were less than about 66 years for Baltzell Springs Group. Eighty percent of particle travel times for Jackson Blue Spring were less than 50 years.

Nitrate concentrations in the selected wells and springs were estimated using scaled fertilizer sales and atmospheric deposition totals. Particle travel times were derived from the two local-scale groundwater-flow and particle-tracking models. Annual fertilizer sales and atmospheric totals were compiled by county for 1945 to 2001 and were scaled to use as a proxy for nitrogen input to the groundwater-flow system. A nitrate concentration input history was developed for each well or spring on the basis of the county where the well or spring is located. Scaling was used to improve the overall match between simulated and measured nitrate concentrations and to account for uncertainties.

The potential effects of three different nitrogen fertilizer management scenarios on nitrate concentrations in groundwater were assessed by simulating nitrate concentrations in groundwater from 2002 to 2050, using the three nitrogen management scenarios and groundwater particle travel times or apparent ages of water obtained from the groundwater-flow and particle-tracking models. In scenario 1, the nitrate input concentration was fixed at the 2001 level for the 2002 to 2050 simulation period. In scenario 2, the nitrate input concentration was reduced by 4 percent per year for the simulation period. In scenario 3, the nitrate input was set at zero for the 2002 to 2050 simulation period.

Groundwater-flow and particle-tracking models and simulated nitrogen management scenarios indicate that it would take decades for nitrate concentrations in groundwater to decrease below background concentrations even if nitrogen fertilizer use was discontinued completely. Under nitrogen management scenario 3 (nitrate input eliminated after 2001), simulated nitrate concentrations in groundwater at Baltzell Springs Group and Sandbag Spring did not decrease below the background concentration of 0.10 mg/L until 2033 and 2041, respectively. Under management scenario 3, simulated nitrate concentrations in Jackson Blue Spring did not decrease to the background concentration during the simulation period. Under nitrogen management scenarios 1 (nitrate input fixed at 2001 levels) and 2 (a 4 percent reduction per year in nitrate input from 2002 to 2050), simulated nitrate concentrations in all wells and springs remained above the background concentration of 0.10 mg/L in 2050. Nitrate concentrations in groundwater from wells CP-18A and CP-21A remained above 3.0 mg/L through 2050 under nitrogen management scenarios 1 and 2.

References Cited

Albertson, P.N., and Torak, L.J., 2002, Simulated effects of ground-water pumpage on stream-aquifer flow in the vicinity of federally protected species of freshwater mussels in the lower Apalachicola–Chattahoochee–Flint River Basin (Subarea 4), southeastern Alabama, northwestern Florida, and southwestern Georgia: U.S. Geological Survey Water-Resources Investigations Report 02–4016, 53 p.

Alexander, R.B., and Smith, R.A., 1990, County-level estimates of nitrogen and phosphorus fertilizer use in the United States, 1945 to 1985: U.S. Geological Survey Open-File Report 90–130, 12 p. (Also available at http://pubs.usgs.gov/of/ofr90130/.)

Anderson, M.P., and Woessner, W.W., 1992, Applied groundwater modeling: San Diego, Academic Press, 381 p.

Barrios, Kris, and Chellette, Angela, 2004, Chipola River Springs Inventory: Havana, Fla., Northwest Florida Water Management District, Water Resources Special Report 04–01, 49 p.

Battaglin, W.A., and Goolsby, D.A., 1995, Spatial data in geographic information system format on agricultural chemical use, land use, and cropping practices in the United States: U.S. Geological Survey Water-Resources Investigations Report 94–4176, 87 p.

Berndt, M.P., and Crandall, C.A., 2009, Factors affecting water quality in domestic wells in the Upper Floridan aquifer, Southeastern United States, 1998–2005: U.S. Geological Survey Scientific Investigations Report 2009–5147, 39 p.

Berndt, M.P., Katz, B.G., Lindsey, B.D., Ardis, A.F., and Skach, K.A., 2005, Comparison of water chemistry in spring and well samples from selected carbonate aquifers in the United States, *in* Kuniansky, E.L., ed., U.S. Geological Survey Karst Interest Group Proceedings, Rapid City, S.D., September 12–15, 2005: U.S. Geological Survey Scientific Investigations Report 2005–5160, p. 74–81.

Böhlke, J.K., 2006, Tracermodel1, Excel workbook for calculation and presentation of environmental tracer data for simple groundwater mixtures, *in* Use of chlorofluorocarbons in hydrology—A guidebook: Vienna, International Atomic Energy Agency, STI/PUB/1238, Section III.10.3, p. 239–243.

Busenberg E., and Plummer, L.N., 2000, Dating young groundwater with sulfur hexafluoride: Natural and anthropogenic sources of sulfur hexafluoride: Water Resources Research, v. 36, no. 10, p. 3011–3030.

Busenberg, Eurybiades, Plummer, L.N., Bartholomay, R.C., and Wayland, J.E., 1998, Chlorofluorocarbons, sulfur hexafluoride, and dissolved permanent gases in ground water from selected sites in and near the Idaho National Engineering and Environmental Laboratory, Idaho, 1994–97: U.S. Geological Survey Open-File Report 98–274, 72 p.

Busenberg, Eurybiades, Weeks, E.P., Plummer, L.N., and Bartholomay, R.C., 1993, Age dating ground water by use of chlorofluorocarbons (CCl_3F and CCl_2F_2), and distribution of chlorofluorocarbons in the unsaturated zone, Snake River Plain aquifer, Idaho National Engineering Laboratory, Idaho: U.S. Geological Survey Water-Resources Investigations Report 93–4054, 47 p.

Camp, Dresser & McKee Inc., 2001, Final project design report for the Georgia Department of Natural Resources Environmental Protection Division Implementation of the Regional Water Development and Conservation Plan for the Lower Flint River Conservation Reserve Area: Atlanta, Ga., Camp, Dresser & McKee Inc., 99 p.

Cherkauer, D.S., Taylor, R.W., and Bradbury, K.R., 1987, Relation of lake bed leakance to geoelectrical properties: Ground Water, v. 25, p. 135–140.

Cooley, R.L., 1992, A modular finite-element model (MODFE) for areal and axisymmetric ground-water-flow problems, Part 2: Derivation of finite-element equations and comparisons with analytical solutions: U.S. Geological Survey Techniques of Water-Resources Investigations, book 6, chap. A4, 108 p.

Cook P.G., and Böhlke, J.K., 1999, Determining timescales for groundwater flow and solute transport, *in* Cook, P.G., and Herczeg, A.L., eds., Environmental tracers in subsurface hydrology: Boston, Kluwer Academic Publishers, p. 1–30.

Cook, P.G., and Solomon, D.K., 1997, Recent advances in dating young groundwater: Chlorofluorocarbons, $^3H/^3He$, and ^{85}Kr: Journal of Hydrology, v. 191, p. 245–265.

Cook, P.G., Solomon, D.K., Plummer, L.N., Busenberg, E., and Schiff, S.L., 1995, Chlorofluorocarbons as tracers of groundwater transport processes in a shallow, silty sand aquifer: Water Resources Research, v. 31, p. 425–434.

Cooke, C.W., 1939, Scenery of Florida interpreted by a geologist: Florida Geological Survey Bulletin 17, 118 p.

Couch, C.A., Hopkins, E.H., and Hardy, P.S., 1996, Influences of environmental settings on aquatic ecosystems in the Apalachicola–Chattahoochee–Flint River Basin: U.S. Geological Survey Water-Resources Investigations Report 95–4278, 58 p.

Crandall, C.A., 2007, Hydrogeologic setting and ground-water flow simulations of the Northern Tampa Bay Regional Study Area, Florida, Section 5, *in* Paschke, S.S., ed., Hydrogeologic settings and ground-water flow simulations for regional studies of the transport of anthropogenic and natural contaminants to public-supply wells—Studies begin in 2001: U.S. Geological Survey Professional Paper 1737–A, p. 5–1—5–29. (Also available at http://pubs.usgs.gov/pp/2007/1737a/.)

Crandall, C.A., Kauffman, L.J., Katz, B.G., Metz, P.A., McBride, W.S., and Berndt, M.P., 2009, Simulations of groundwater flow and particle tracking analysis in the area contributing recharge to a public-supply well near Tampa, Florida, 2002–05: U.S. Geological Survey Scientific Investigations Report 2008–5231, 53 p.

Culbreath, M.A, 1988, Geophysical investigation of lineaments in South Florida: Tampa, Fla., University of South Florida, Department of Geology, Master's thesis, 97 p.

Dalton, M.S., and Frick, E.A., 2008, Fate and transport of pesticides in the ground water systems of southwest Georgia, 1993–2005: Journal of Environmental Quality, v. 37, p. S264–272.

Domenico, P.A., and Schwartz, F.W., 1990, Physical and chemical hydrogeology: New York, John Wiley and Sons, Inc., 824 p.

Eberts, S.M., Erwin, M.L., and Hamilton, P.A., 2005, Assessing the vulnerability of public-supply wells to contamination from urban, agricultural, and natural sources: U.S. Geological Survey Fact Sheet 2005–3022, 4 p.

Elder, J.F., Flagg, S.D., and Mattraw, H.C., Jr., 1988, Hydrology and ecology of the Apalachicola River, Florida: A summary of the river quality assessment: U.S. Geological Survey Water-Supply Paper 2196–D, 46 p.

Fenneman, N.M., 1938, Physiography of the eastern United States: New York, McGraw-Hill, Inc., 714 p.

Florida Geological Survey, 1986, Hydrogeological units of Florida, compiled by the Southeastern Geological Society Ad Hoc Committee on Florida Hydrostratigraphic Unit Definition: Florida Geological Society Special Publication 28, 9 p.

Focazio, M.J., Reilly, T.E., Rupert, M.G., and Helsel, D.R., 2002, Assessing ground-water vulnerability to contamination: Providing scientifically defensible information for decision makers: U.S. Geological Survey Circular 1224, 33 p.

Franklin, M.A., and Meadows, P.E., 1999, Water resources data, Florida, Water year 1998, Volume 4, Northwest Florida: U.S. Geological Survey Water-Data Report FL–98–4, 169 p.

Frick, E.A., Buell, G.R., and Hopkins, E.H., 1996, Nutrient sources and analysis of nutrient water-quality data, Apalachicola–Chattahoochee–Flint River Basin, Georgia, Alabama, Florida, 1972–90: U.S. Geological Survey Water-Resources Investigations Report 96–4101, 120 p.

Frick, E.A., and Dalton, M.S., 2007, Alachlor and two degradates of Alachlor in ground and surface water, southwestern Georgia and adjacent parts of Alabama and Florida, 1993–2005, in Proceedings of the 2007 Georgia Water Resources Conference, March 27–29, 2007: Athens, Ga., The University of Georgia, 6 p.

Frick, E.A., Hippe, D.J., Buell, G.R., Couch, C.A., Hopkins, E.H., Wangsness, D.J., and Garrett, J.W., 1998, Water quality in the Apalachicola–Chattahoochee–Flint River Basin, Georgia, Alabama, and Florida, 1992–95: U.S. Geological Survey Circular 1164, 38 p.

Gesch, Dean, Evans, Gayla, Mauck, James, Hutchinson, John, Carswell, W.J., Jr., 2009, The National Map—Elevation: U.S. Geological Survey Fact Sheet 2009–3053, 4 p. (Also available at http://ned.usgs.gov/.)

Gesch, D.B., 2007, Chapter 4—The national elevation dataset, *in* Maune, D.F., ed., Digital elevation model technologies and applications: The DEM User's Manual (2d ed.): Bethesda, Md., American Society for Photogrammetry and Remote Sensing, p. 99–118.

Gianessi, L.P., and Reigner, N., 2006, Pesticide use in U.S. crop production: 2002 with comparisons to 1992 & 1997: Fungicides and herbicides: Washington, D.C., CropLife Foundation, unpaginated, accessed May 20, 2006, at http://www.croplifefoundation.org/Documents/ PUD/NPUD%20 2002/Fung%20&%20Herb%202002% 20Data%20Report.pdf.

Hach Company, 1992, DR/2000 Spectrophotometer procedures manual: Loveland, Colo., Hach Company, 554 p.

Harbaugh, A.W., Banta, E.R., Hill, M.C., and McDonald, M.G., 2000, MODFLOW-2000, The U.S. Geological Survey modular ground-water model—User guide to modularization concepts and the ground-water flow process: U.S. Geological Survey Open-File Report 00–92, 121 p.

Hayes, L.R., Maslia, M.L., and Meeks, W.C., 1983, Hydrology and model evaluation of the principal artesian aquifer, Dougherty Plain, Southwest Georgia: Georgia Geologic Survey Bulletin 97, 93 p.

Hazlett, R.C., 1989, A study of lineaments and fracture traces mapped on the Crescent City Ridge, Putnam and Volusia Counties, Florida: University of Florida, Master's thesis, 97 p.

Heaton, T.H.E., and Vogel, J.C., 1981, Excess air in groundwater: Journal of Hydrology, v. 50, p. 201–216.

Herrick, S.M., and LeGrand, H.E., 1964, Solution subsidence of a limestone terrain in southwest Georgia: International Association of Scientific Hydrology, v. 9, no. 2, p. 25–36.

Hicks, D.W., Gill, H.E., and Longsworth, S.A., 1987, Hydrogeology, chemical quality, and availability of ground water in the Upper Floridan aquifer, Albany area, Georgia: U.S. Geological Survey Water-Resources Investigations Report 87–4145, 52 p.

Hill, M.C., and Tiedeman, C.R., 2007, Effective groundwater model calibration: With analysis of data, sensitivities, predictions, and uncertainty: New York, Wiley and Sons, 464 p.

Hook, J.E., Hoogenboom, G., Paz, J., Mullen, J., Bergstrom, J., and Risse, M., 2010, Agricultural irrigation water demand, Georgia's major and minor crops 2011 through 2050, revised April 30, 2010, Water use projections with details of irrigated acres, water sources, irrigation depths, and projected crops for each county in the Lower Flint–Ochlockonee Water Planning Region: University of Georgia under contract with the Georgia Environmental Protection Division and the Georgia Environmental Facilities Authorities (038952–01 and 038950–01), 57 p.

IDEXX Corporation, 2006, IDEXX Colilert® Test method for the simultaneous detection of total coliforms and *E. coli* in water: IDEXX Colilert® package insert from IDEXX, accessed October 3, 2012, at http://www.idexx.com/view/xhtml/en_us/water/colilert.jsf?selectedTab=Overview.

Jones, L.E., and Torak, L.J., 2004, Simulated effects of impoundment of Lake Seminole on ground-water flow in the Upper Floridan aquifer in southwestern Georgia and adjacent parts of Alabama and Florida: U.S. Geological Survey Scientific Investigations Report 2004–5077, 18 p.

Jones, L.E., and Torak, L.J., 2006, Simulated effects of seasonal ground-water pumpage for irrigation on hydrologic conditions in the lower Apalachicola–Chattahoochee–Flint River Basin, southwestern Georgia and parts of Alabama and Florida, 1999–2002: U.S. Geological Survey Scientific Investigations Report 2006–5234, 83 p. (Also available at http://pubs.usgs.gov/sir/2006/5234/.)

Katz, B.G., 2004, Sources of nitrate contamination and age of water in large karstic springs of Florida: Environmental Geology, v. 46, p. 689–706.

Katz, B.G., Böhlke, J.K., and Hornsby, H.D., 2001, Timescales for nitrate contamination of spring waters, northern Florida, U.S.A.: Chemical Geology, v. 179, p. 167–186.

Katz, B.G., Crandall, C.A., Metz, P.A., McBride, W.S., and Berndt, M.P., 2007, Chemical characteristics, water sources and pathways, and age distribution of ground water in the contributing recharge area of a public-supply well near Tampa, Florida, 2002–05: U.S. Geological Survey Scientific Investigations Report 2007–5139, 85 p.

Kauffman, L.J., Baehr, A.L., Ayers, M.A., and Stackelberg, P.E., 2001, Effects of land use and travel time on the distribution of nitrate in the Kirkwood-Cohansey aquifer system in southern New Jersey: U.S. Geological Survey Water-Resources Investigations Report 01–4117, 49 p.

Knochenmus, L.A., and Robinson, J.L., 1996, Descriptions of anisotropy and heterogeneity and their effect on groundwater flow and areas of contribution to public-supply wells in a karst carbonate aquifer system: U.S. Geological Survey Water-Supply Paper 2475, 43 p.

Koterba, M.T., Wilde, F.D., and Lapham, W.W., 1995, Ground-water data-collection protocols and procedures for the National Water-Quality Assessment Program: Collection and documentation of water-quality samples and related data: U.S. Geological Survey Open-File Report 95–399, 113 p.

Kwader, Thomas, and Schmidt, Walter, 1978, Top of the Floridan aquifer of northwest Florida: Northwest Florida Water Management District in cooperation with the Florida Bureau of Geology, Map Series 86, 1 sheet, scale 1:500,000.

Langevin, C.D., 1998, Stochastic methods for evaluating the potential for wetland rehydration in covered-karst terrains: Tampa, University of South Florida, Ph.D. dissertation, 133 p.

LeGrand, H.E., and Stringfield, V.T., 1966, Development of permeability and storage in the Tertiary limestones of the southeastern states, U.S.A.: International Association of Scientific Hydrology Bulletin, v. 11, p. 61–73.

Lindsey, B.D., Katz, B.G., Berndt, M.P., Ardis, A.F., and Skach, K.A., 2010, Relations between sinkhole density and anthropogenic contaminants in selected carbonate aquifers in the eastern United States: Environmental Earth Sciences, v. 60, no. 5, p. 1073–1090.

Longwell, C.R., Flint, R.F., and Sanders, J.E., 1969, Physical geology: New York, John Wiley and Sons, Inc., 685 p.

Ludin, A., Weppernig, R., Bonisch, G., and Schlosser, P., 1998, Mass spectrometric measurement of helium isotopes and tritium: Palisades, N.Y., Lamont-Doherty Earth Observatory, Columbia University, Technical Report 98–06.

Maloszewski, P., and Zuber, A., 1996, Lumped parameter models for the interpretation of environmental tracer data, *in* Manual on mathematical models in isotope hydrology: Vienna, International Atomic Energy Agency, IAEA-TEC-DOC 910, p. 9–50.

Miller, J.A., 1986, Hydrogeologic framework of the Floridan aquifer system in Florida and parts of Georgia, Alabama, and South Carolina: U.S. Geological Survey Professional Paper 1403–B, 91 p.

Moore, W.E., 1955, Geology of Jackson County, Florida: Florida Geological Survey Bulletin 37, 101 p.

Mosner, M.S., 2002, Stream-aquifer relations and the potentiometric surface of the Upper Floridan aquifer in the lower Apalachicola–Chattahoochee–Flint River Basin in parts of Georgia, Florida, and Alabama, 1999–2000: U.S. Geological Survey Water-Resources Investigations Report 02–4244, 45 p.

National Oceanic and Atmospheric Administration, 2003, Climatological data annual summary, 2002: National Oceanic and Atmospheric Administration, v. 106, no. 13, 28 p.

Ozyurt, N.N., and Bayari, C.S., 2003, LUMPED: A Visual Basic code of lumped parameter models for mean residence time analyses of groundwater systems: Computers and Geosciences, v. 29, p. 79–90.

Plummer, L.N., and Busenberg, Eurybiades, 1999, Chlorofluorocarbons, *in* Cook, P.G., and Herczeg, A., eds., 1999, Environmental tracers in subsurface hydrology: Boston, Mass., Kluwer Academic Press, chap. 15, p. 441–478.

Plummer, L.N., Busenberg, E., Drenkard, S., Schlosser, P., Ekwurzel, B., Weppernig, R., McConnell, J.B., and Michel, R.L., 1998, Flow of river water into a karstic limestone aquifer—2. Dating the young fraction in groundwater mixtures in the Upper Floridan aquifer near Valdosta, Georgia: Applied Geochemistry, v. 13, p. 1017–1043.

Poeter, E.E., Hill, M.C., Banta, E.R., Mehl, Steffen, and Christensen, Steen, 2005, UCODE_2005 and six other computer codes for universal sensitivity analysis, calibration, and uncertainty evaluation: U.S. Geological Survey Techniques and Methods, book 6, chap. 11, sec. A, p. 283.

Pollock, D.W., 1994, User's guide for MODPATH/MODPATH-PLOT, version 3: A particle tracking post-processing package for MODFLOW, the U.S. Geological Survey finite-difference ground-water flow model: U.S. Geological Survey Open-File Report 94–464 [variously paged].

Pratt, T.R., Richards, C.J., Milla, K.A., Wagner, J.R., Johnson, J.L., and Curry, R.J., 1996, Hydrogeology of the Northwest Florida Water Management District: Northwest Florida Water Management District Water Resources Special Report 96–4, 98 p.

Reilly, T.E., Plummer, L.N., Phillips, P.J., and Busenberg, Eurybiades, 1994, The use of simulation and multiple environmental tracers to quantify groundwater flow in a shallow aquifer: Water Resources Research, no. 30, p. 421–433.

Reves, W.D., 1961, The limestone resources of Washington, Holmes, and Jackson Counties, Florida: Florida Geological Survey Bulletin 42, 121 p.

Ruddy, B.C., Lorenz, D.L., and Mueller, D.K., 2006, County-level estimates of nutrient inputs to the land surface of the conterminous United States, 1982–2001: U.S. Geological Survey Scientific Investigations Report 2006–5012. (Also available at http://pubs.usgs.gov/sir/2006/5012/.)

Schlosser, P., Stute, M., Dorr, H., Sonntag, C., and Munnich, K.O., 1988, Tritium/^{3}He dating of shallow groundwater: Earth Planetary Science Letters, v. 89, p. 353–362.

Schlosser P., Stute, M., Sonntag, C., and Munnich, K.O., 1989, Tritiogenic ^{3}He in shallow groundwater: Earth Planetary Science Letters, v. 94, p. 245–256.

Schmidt, Walter, and Coe, Curtis, 1978, Regional structure and stratigraphy of the limestone outcrop belt in the Florida panhandle: Florida Department of Natural Resources, Bureau of Geology Report of Investigation, no. 86, 25 p.

Scott, T.M., 1992, A geological overview of Florida: Florida Geological Survey Open-File Report 50, 78 p.

Sever, C.W., 1965a, Ground-water resources and geology of Seminole, Decatur and Grady Counties, Georgia: U.S. Geological Survey Water-Supply Paper 1809–Q, 30 p.

Sever, C.W., 1965b, Groundwater resources of Bainbridge, Georgia: Georgia Geological Survey Information Circular 32, 10 p.

Shoemaker, W.B., Kuniansky, E.L., Birk, Steffen, Bauer, Sebastian, and Swain, E.D., 2008, Documentation of a Conduit Flow Process (CFP) for MODFLOW-2005: U.S. Geological Survey Techniques and Methods, book 6, chap. A24, 50 p.

Solomon, D.K., and Sudicky, E.A., 1991, Tritium and helium-3 isotope ratios for direct estimation of spatial variations in groundwater recharge: Water Resources Research, v. 27, no. 9, p. 2309–2319.

Spitz, F.J., 2001, Method and computer programs to improve pathline resolution near weak sinks representing wells in MODFLOW and MODPATH ground-water-flow simulations: U.S. Geological Survey Open-File Report 00–392, 41 p.

Taylor, R.W., and Cherkauer, D.S., 1984, The application of combined seismic and electrical measurements to the determination of the hydraulic conductivity of a lake bed: Ground Water Monitoring & Remediation, v. 4, p. 78–85, doi: 10.1111/j.1745-6592.1984.tb00897.x.

Torak, L.J., 1993, A Modular Finite-Element model (MODFE) for areal and axisymmetric ground-water-flow problems, Part 1: Model description and users manual: U.S. Geological Survey Open-File Report 90–194, 153 p.

Torak, L.J., Crilley, D.M., and Painter, J.A., 2006, Physical and hydrochemical evidence of lake leakage near Jim Woodruff Lock and Dam and of ground-water inflow to Lake Seminole, and an assessment of karst features in and near the lake, southwestern Georgia and northwestern Florida: U.S. Geological Survey Scientific Investigations Report 2005–5084, 90 p.

Torak, L.J., Davis, G.S., Strain, G.A., and Herndon, J.G., 1993, Geohydrology and evaluation of water-resource potential of the Upper Floridan aquifer in the Albany area, southwestern Georgia: U.S. Geological Survey Water-Supply Paper 2391, 59 p.

Torak, L.J., Davis, G.S., Strain, G.A., and Herndon, J.G., 1996, Geohydrology and evaluation of stream-aquifer relations in the Apalachicola–Chattahoochee–Flint River Basin, southeastern Alabama, northwestern Florida, and southwestern Georgia: U.S. Geological Survey Water-Supply Paper 2460, 94 p.

Torak, L.J., and McDowell, R.J., 1996, Ground-water resources of the lower Apalachicola–Chattahoochee–Flint River Basin in parts of Alabama, Florida, and Georgia—Subarea 4 of the Apalachicola–Chattahoochee–Flint and Alabama–Coosa–Tallapoosa River Basins: U.S. Geological Survey Open-File Report 95–321, 145 p.

Torak, L.J., and Painter, J.A., 2006, Geohydrology of the lower Apalachicola–Chattahoochee–Flint River Basin, southwestern Georgia, northwestern Florida, and southeastern Alabama: U.S. Geological Survey Scientific Investigations Report 2006–5070, 80 p.

Torgersen, T., Clarke, W.B., and Jenkins, W.J., 1979, The tritium/helium-3 method in hydrology, in Proceedings of an International Symposium on Isotope hydrology, v. II, June 19–23, 1978, Vienna: International Atomic Energy Agency, p. 917–929.

U.S. Army Corps of Engineers, 1948, Definite project report on Jim Woodruff Dam (formerly Junction Project), Apalachicola River, Florida: U.S. Army Corps of Engineers, Mobile District, Mobile, Ala., v. II, apps. II and III, 63 p.

U.S. Army Corps of Engineers, 1973, Survey report on Apalachicola, Chattahoochee, and Flint Rivers, Alabama, Florida, and Georgia: U.S. Army Corps of Engineers, Mobile District, 44 p.

U.S. Army Corps of Engineers, 2004, Lineament analysis South Florida Region, Aquifer storage and recovery regional study, Draft Technical Memorandum, Central and South Florida Project Comprehensive Everglades Restoration Plan: U.S. Army Corps of Engineers, Jacksonville District, 55 p.

U.S. Environmental Protection Agency, 2012, Basic information about nitrate in drinking water, accessed October 3, 2012, at http://water.epa.gov/drink/contaminants/basicinformation/nitrate.cfm.

U.S. Geological Survey, 2009, National Elevation Dataset (NED): U.S. Geological Survey database, accessed October 3, 2012, at http://ned.usgs.gov/Ned/about.asp.

Vernon, R.O., 1951, Geology of Citrus and Levy Counties: Florida Geological Society, Geology Bulletin No. 33, 256 p.

Wagner, J.R., and Allen, T.W., 1984, Ground water section, *in* 1984 water assessment for the Apalachicola–Chattahoochee–Flint River Basin water management study: U.S. Army Corps of Engineers, and States of Alabama, Florida, and Georgia, v. 3, app. III, sec. 3, 129 p.

Watson, T.W., 1981, Geohydrology of the Dougherty Plain and adjacent area, southwestern Georgia: Georgia Geologic Survey Hydrologic Atlas 5, 4 pls.

Williams, S.R., 1985, Relationship of groundwater chemistry to photolineaments in a karst aquifer: Tampa, University of South Florida, Geology Department, Master's thesis.

Zuber, A., 1986, Mathematical models for the interpretation of environmental radioisotopes in groundwater systems, *in* Fritz, P., and Fontes, J.-Ch., eds., Handbook of environmental isotope geochemistry: Amsterdam, Elsevier, p. 1–59.

Appendix

Appendix. Measured field properties, nitrate, and bacteria in synoptic field reconnaissance samples, 2007.

[No., number; <, less than; >, greater than; CR, county road; Hwy, Highway]

Local site name (and USGS site number, if available)	Date sampled	Water temperature, in degrees Celsius	Specific conductance, in microsiemens per centimeter	Dissolved oxygen, in milligrams per liter	pH, standard units	Nitrate as Nitrogen, in milligrams per liter	Total coliform, colonies per 100 milliliters	*Escherichia coli*, colonies per 100 milliliters	Discharge, in cubic feet per second
Baltzell No.1	4/16/2007	20.45		5.9	7.39	4.4	186	4	
Baltzell No.1	4/23/2007	20.52	323	8.8	7.42	5.5	345	1	
Baltzell No.2	4/16/2007	20.51		5.4	7.38	3.9	649	4	
Baltzell No.2	4/23/2007	20.58	323	9	7.5	3.6	980	1	
Baltzell No.3	4/16/2007	20.55		5.7	7.31	5.6	172	4	
Baltzell No.3	4/23/2007	20.54	322	8.8	7.43	3	210	<1	
Baltzell No.4	4/16/2007	20.31		5.8	7.42	3.3	328	<1	
Baltzell No.4	4/23/2007	20.28	316	7.2	7.46				
Baltzell No.5	4/16/2007	20.05		6.8	7.47	2.8	236	5	
Baltzell No.5	4/23/2007	20.5	321	8.7	7.43	3.2	86	1	
Baltzell Spring Run	4/16/2007								30.5
Blue Hole	4/17/2007	19.28	313	7.9	7.46	0.2	225	4	6.8
Crack-in-the-Woods Spring	4/16/2007	18.02		6.6	7.51	3.6	201	6	
Crack-in-the-Woods Spring	4/23/2007	20.62	316	9.3	7.43	2.9	158	<1	
Daniel Spring Creek Below Small Tributary	5/17/2007	21.41	242	6	7.59	1.3	>2,420	54	
Daniel Spring (the 2 most upstream springs)	5/17/2007	20.17	2,370	5.2	7.87	1.5	>2,420	4	
Grotto Spring	5/15/2007	20.4	268	2.4	7.59	1.1	111	<1	
Hays Spring Run	6/28/2007	25.38	259	7.7	7.99	2	>2,420	36	
Heidi Hole	6/13/2007	20.63	351	6.4	7.33	2.8	>2,420	<1	
Hole in the Wall	6/13/2007	20.07	307	7.5	7.39	1.6	>2,420	<1	
Indian Washtub Spring	6/13/2007	20.86	284	12.5	7.53	2.7	>2,420	<1	
Jackson Blue	4/17/2007	20.56	268	11.1	7.64	3.3	35	<1	
Leaf Spring	4/16/2007	20.57		6.2	7.43	3.6	517	1	
Leaf Spring	4/23/2007	20.39	317	9.1	7.41	3	308	8	

Appendix. Measured field properties, nitrate, and bacteria in synoptic field reconnaissance samples, 2007.—Continued

[No., number; <, less than; >, greater than; CR, county road; Hwy, Highway]

Local site name (and USGS site number, if available)	Date sampled	Water temperature, in degrees Celsius	Specific conductance, in microsiemens per centimeter	Dissolved oxygen, in milligrams per liter	pH, standard units	Nitrate as Nitrogen, in milligrams per liter	Total coliform, colonies per 100 milliliters	*Escherichia coli*, colonies per 100 milliliters	Discharge, in cubic feet per second
McRae Spring Resurgence on Chipola River	5/15/2007	20.8	186	4.2	8	0.1	228	10	
Peacock Spring	5/15/2007	21	176	3.6	7.92	0.2	73	<1	
Sally Spring	5/15/2007	20.9	260	1.5	7.75	0.2	3	<1	
Sandbag Spring	4/17/2007	20.22	356	6.8	7.32	0.1	980	39	
School Bus Spring	5/16/2007	20.63	234	3.1	7.37	5.3	1414	9	
Shangri-La Spring	6/13/2007	20.52	256	9.6	7.55	2.6	>2,420	<1	
Simms Spring	5/16/2007	26.24	255	9.2	8.65	<0.1	>2,420	1	
Unnamed spring at CR 280A bridge	5/16/2007	21.41	305	1.5	7.51	2.4	31	<1	
Twin Caves Spring	6/13/2007	20.31	313	10.5	7.45	1.5	1,553	1	
Unnamed spring (down stream of boat ramp at CR 280A on right bank at Waypoint No.19	5/16/2007	19.73	289	3.3	7.49	2.7	548	<1	
Unnamed spring on right bank of Chipola River at Waypoint No.16	5/15/2007	20.8	227	3.5	7.67	0.2	11	<1	
Window Spring	5/15/2007	20.8	231	5	7.6	0.4	199	<1	
Big Creek at CR 55, Alabama	6/21/2007	23.8	173	7.1	7.53	2.4	>2,420	84	
Chipola River at Altha, FL (02359000)	4/17/2007								663
Chipola River at Altha, FL (02359000)	6/28/2007	26.37	235	8	8.14	0.9	1,986	8	
Chipola River at CR 280A bridge	5/16/2007	24.69	275	7.6	8.01	1.8	>2,420	15	

Appendix. Measured field properties, nitrate, and bacteria in synoptic field reconnaissance samples, 2007.—Continued

[No., number; <, less than; >, greater than; CR, county road; Hwy, Highway]

Local site name (and USGS site number, if available)	Date sampled	Water temperature, in degrees Celsius	Specific conductance, in microsiemens per centimeter	Dissolved oxygen, in milligrams per liter	pH, standard units	Nitrate as Nitrogen, in milligrams per liter	Total coliform, colonies per 100 milliliters	*Escherichia coli*, colonies per 100 milliliters	Discharge, in cubic feet per second
Chipola River at Hwy 162	6/21/2007	25.85	237	7.7	7.98	1.4	>2,420	16	
Chipola River at Marianna, FL (02358789)	4/18/2007	17.3	244	7.6	7.57	<0.1	1,733	21	339
Chipola River at Peacock Bridge	6/28/2007	26.76	247	7.9	8.1	1.4	>2,420	26	
Chipola River above CR 166 bridge	4/17/2007	17.63	241		7.69	1.1	980	24	
Chipola River above Baltzell Springs	4/16/2007	16.31	376	8	7.63	2	921	33	
Chipola River below Waddells Mill Creek	6/21/2007	26.07	242	7.2	7.88	0.8	>2,420	26	
Cowarts Creek at CR 53, Alabama	6/21/2007	23.15	168	6.7	7.7	1.8	>2,420	71	
Cowarts Creek at CR 55, Alabama	6/21/2007	23.54	245	6.5	7.78	0.1	>2,420	101	
Cowarts Creek at Hwy 2 (02358772)	4/18/2007	16.8	202	6.7	7.42	<0.1	1,414	141	54.6
Dry Creek at Hwy 73 bridge	6/28/2007	22.76	229	7.9	7.93	0.2	1,986	32	
Limestone Creek at Hwy 109, Alabama	6/21/2007	23.12	197	6.9	7.34	4.1	>2,420	83	
Marshall Creek (02358760)	4/18/2007	16.1	124	6.9	7.01	0.1	>2,420	21	159

Appendix. Measured field properties, nitrate, and bacteria in synoptic field reconnaissance samples, 2007.—Continued

[No., number; <, less than; >, greater than; CR, county road; Hwy, Highway]

Local site name (and USGS site number, if available)	Date sampled	Water temperature, in degrees Celsius	Specific conductance, in microsiemens per centimeter	Dissolved oxygen, in milligrams per liter	pH, standard units	Nitrate as Nitrogen, in milligrams per liter	Total coliform, colonies per 100 milliliters	*Escherichia coli*, colonies per 100 milliliters	Discharge, in cubic feet per second
Mill Creek at Lucy Grade Road, Alabama	6/21/2007	23.09	250	2.6	7.06	0	>2,420	67	
Rocky Creek (upstream of Hogpen Spring) at Waypoint No.18	5/16/2007	20.91	247	9.7	4.99	0.9	>2,420	105	
Waddells Mill Creek	6/21/2007	26.89	264	6.2	7.78	0.3	>2,420	33	

Prepared by:
USGS Science Publishing Network
Raleigh Publishing Service Center
3916 Sunset Ridge Road
Raleigh, NC 27607

For additional information regarding this publication contact:
Director
USGS Florida Water Science Center
Suite 108
4446 Pet Lane
Lutz, FL 33559-6302
(813) 498-5000

Or visit the USGS Florida Water Science Center Web site at:
http://fl.water.usgs.gov